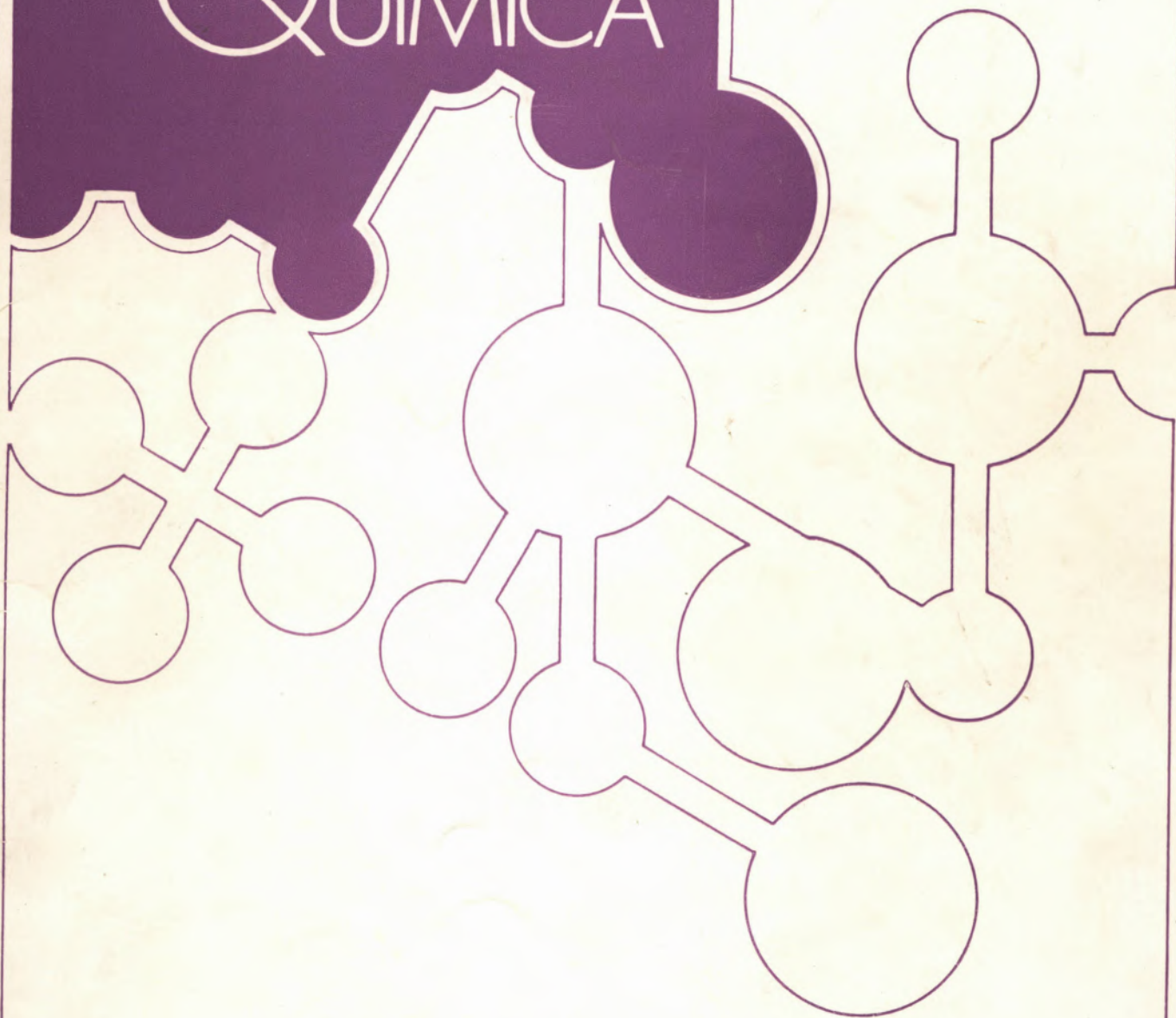
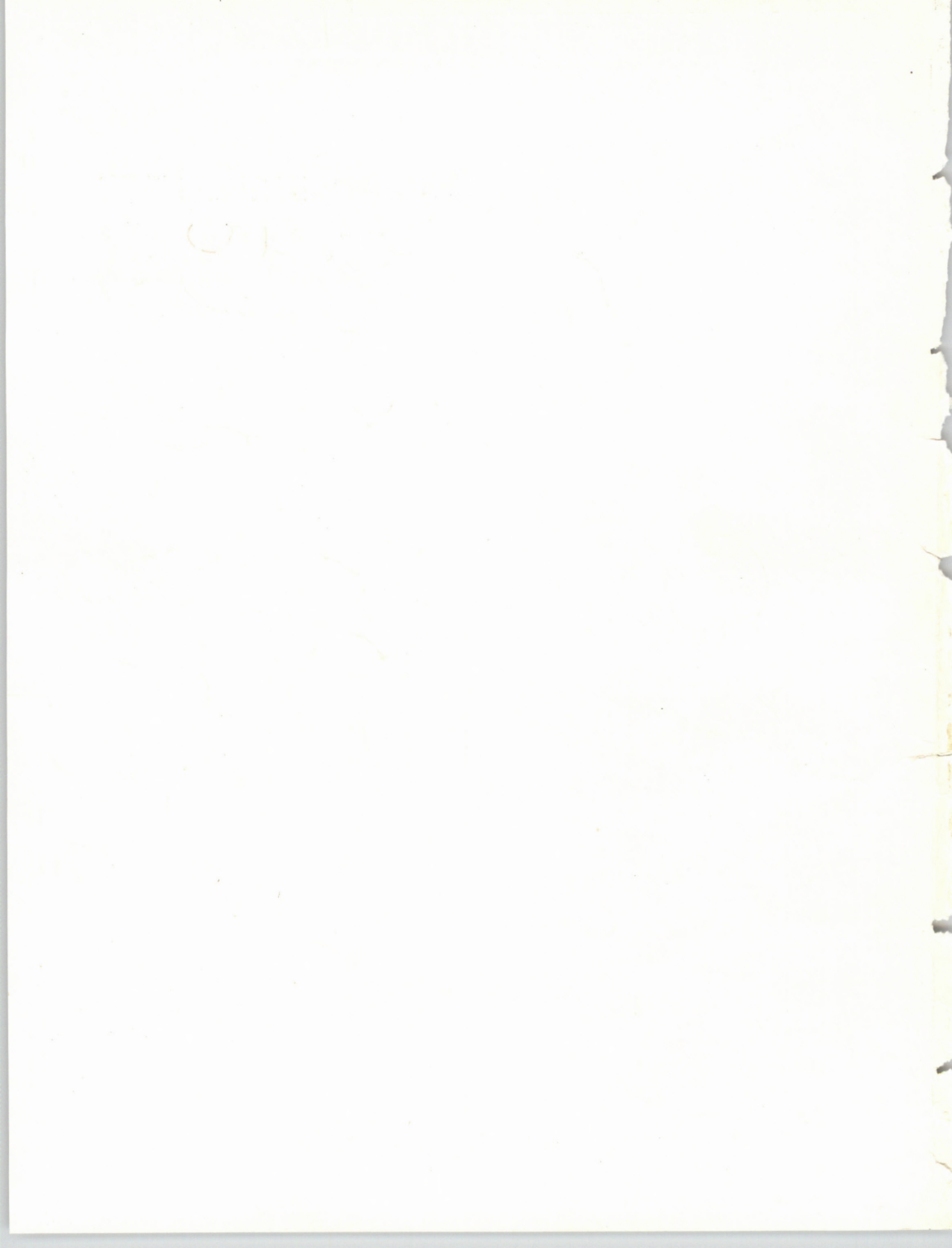


# REVISTA PORTUGUESA DE QUÍMICA



RPTQAT 27(3/4) 427-523 (1985)  
ISSN 0035-0419





Rev. Port. Quím., Vol. 27, N.º 3, 4  
Pp. 427-523 — Porto, 1985

# REVISTA PORTUGUESA DE QUÍMICA

Propriedade e edição da  
SOCIEDADE PORTUGUESA DE QUÍMICA  
em continuação da  
REVISTA DE QUÍMICA PURA E APLICADA  
fundada em 1905 por  
Ferreira da Silva.  
Subsidiada pelo  
INSTITUTO NACIONAL DE INVESTIGAÇÃO CIENTÍFICA

---

Director

A. HERCULANO DE CARVALHO

---

**Editores** M. A. V. RIBEIRO DA SILVA  
Departamento de Química, Faculdade de Ciências,  
Universidade do Porto, 4000 Porto

A. J. C. VARANDAS  
Departamento de Química, Universidade de Coimbra,  
3049 Coimbra Codex

---

Comissão redactorial

LUÍS ALCÁCER  
ALBERTO AMARAL  
J. M. PEIXOTO CABRAL  
JOÃO OLIVEIRA CABRAL  
JORGE C. G. CALADO  
R. A. GUEDES DE CARVALHO  
FERNANDA MADALENA A. COSTA  
A. ROMÃO DIAS  
JOSÉ TEIXEIRA DIAS  
SEBASTIÃO J. FORMOSINHO  
BERNARDO HEROLD  
VICTOR GIL  
SUNDARESAN PRABHAKAR  
JOSÉ SIMÕES REDINHA  
JOAQUIM J. B. ROMERO  
MANUEL ALVES DA SILVA  
J. J. R. FRAUSTO DA SILVA  
CÉSAR A. N. VIANA  
ANTÓNIO V. XAVIER

---

Os artigos publicados são de exclusiva responsabilidade dos seus autores

---

Redacção e administração

Departamento de Química-Faculdade de Ciências-Porto

Composição, impressão  
e acabamento

Imprensa Portuguesa  
Rua Formosa, 108-116 - Porto

Capa

Luís Filipe de Abreu

---

Publicação trimestral. Número avulso: 500\$00. Assinatura (quatro números), Portugal 1600\$00,  
outros países: U.S. \$12 por número, \$40 por assinatura





---

## índice

---

SEBASTIÃO J. FORMOSINHO	427	MOLECULAR STRUCTURE AND CHEMICAL REACTIVITY. THE ROLE OF THE ACTIVATION ENERGY
R. D. GILLARD	443	PSEUDO-BASE MECHANISMS IN ORGANIC, COORDINATION AND BIOCHEMISTRY
DEREK PLETCHER	449	RECENT DEVELOPMENTS IN ORGANIC ELECTROSYNTHESIS
NOSRAT M. ABED NADIA S. IBRAHIM SUZAN I. AZIZ	459	NITRILES IN HETEROCYCLIC SYNTHESIS: A ROUTE FOR SYNTHESIS OF FUNCTIONALLY SUBSTITUTED THIAZINONES
MARIA CONCEIÇÃO PEDROSO DE LIMA CARLOS A. S. PALITEIRO	463	NÚMEROS DE TRANSFERÊNCIA DO SULFATO DE ZINCO EM ÁGUA A 25° C
HIGUINALDO J. CHAVES DAS NEVES HARTMUT FRANK	474	ANÁLISE DE MONOSSACARIDOS POR CROMATOGRAFIA GÁS-LÍQUIDO: CGL E CGL/EM DE N,O-TRIMETILSILIL AMINODEOXIALDITÓIS
ARMANDO J. L. POMBEIRO	483	STUDIES ON THE OXIDATION REACTIONS OF THE DINITROGEN COMPLEX <i>trans</i> -[ReCl(N <sub>2</sub> )(Ph <sub>2</sub> PCH <sub>2</sub> CH <sub>2</sub> PPh <sub>2</sub> ) <sub>2</sub> ]
ANA M. LOBO SUNDARESAN PRABHAKAR M. AMÉLIA SANTOS HENRY S. RZEPA	492	MAGNETIC NON-EQUIVALENCE IN THE LOW-TEMPERATURE NUCLEAR MAGNETIC RESONANCE SPECTRA OF N-BENZYL-N-METHYLHYDROXYLAMINE AND ITS ANION — COMPARISON WITH SCF — MO CALCULATIONS
ABDOU O. ABDELHAMID NOSRAT M. ABED	500	SYNTHESIS OF PYRIDAZINE, PYRIDAZIN-3-ONE, 2-AMINO PYRROLE AND 2,5-DIAMINO-PYRIDINE DERIVATIVES FROM PROPANEDINITRILE
MARIA MANUELA GONÇALVES MOTTA C. FERREIRA DE MIRANDA	505	ADSORPTION OF MOLYBDATE BY CLAY MINERALS I — KAOLINITE
ROSA A. LORENZO FERREIRA M. <sup>a</sup> DEL CARMEN CASAIS LAIÑO F. BERMEJO MARTINEZ	511	SPECTROPHOTOMETRIC DETERMINATION OF VANADIUM(IV) WITH ETHYLENEDIAMINE-N,N' DIPROPIONIC ACID (EDDPA)
ADELA BERMEJO BARRERA M. <sup>a</sup> CARMEN LUACES PAZOS F. BERMEJO MARTINEZ	516	SPECTROPHOTOMETRIC DETERMINATION OF PALLADIUM(II) WITH BUTYLENEDIAMINETETRAMETHYLENEDIPHOSPHONIC ACID (BDTMPA)
S. J. FORMOSINHO	521	ON THE VALIDITY OF LINEAR FREE ENERGY RELATIONSHIPS IN CHEMICAL KINETICS

---

SEBASTIÃO J. FORMOSINHO

Departamento de Química,  
Universidade de Coimbra,  
3049 Coimbra, Portugal



---

## MOLECULAR STRUCTURE AND CHEMICAL REACTIVITY. THE ROLE OF THE ACTIVATION ENERGY \*

*A semi-empirical intersecting-state-model allows the calculation of the energy barrier of elementary reactions in terms of the reaction energy, the force constants and the sum of the bond length of the reactive bonds, the bond order at the transition state and the so called «mixing entropy». Some of these parameters provide new mechanistic insights on gas phase reactions of hydrides and nonhydrides, and on electron transfer and nucleophilic substitution reactions in liquid solutions. The model is compared with current approaches which relate activation energies with molecular structure, namely linear free energy relationships, Marcus and BEBO theories, and Woodward-Hoffmann rules.*

\* Ferreira da Silva Lecture delivered in portuguese, at Braga, during the 8<sup>th</sup> Annual Meeting of the Sociedade Portuguesa de Química, April 1985.

Ferreira da Silva, one of the most eminent portuguese analytical chemists of all times, and the founder of the Sociedade Portuguesa de Química was born in 1853. Chemical kinetics had just started, with the measurement of the rate of inversion of sucrose by Wilhemy [1] in 1850. Ferreira da Silva was thus able to follow the first developments of this discipline which stands, together with thermodynamics, as the most significant quantitative criterium for chemical reactivity. In 1889 Arrhenius [2] explained the effect of temperature on reaction rates, which was probably the most important advance in the understanding of chemical kinetics during the lifetime of Ferreira da Silva. According to Arrhenius, in a reacting system an equilibrium exists between ordinary and «active» molecules, and only the latter ones are rich enough energetically to undergo chemical reaction. The apparent activation energy is the difference between the average energy of the active molecules and the average energy of all the molecules. It is precisely the relationship between molecular structure and activation energy which is the topic of this lecture. It is thus my pleasure to bring here two eminent chemists whose lifes ran in parallel: Ferreira da Silva 1853-1923 and Arrhenius 1859-1927.

### STRUCTURE — REACTIVITY RELATIONSHIPS: AN HISTORICAL VIEW

The theoretical calculation of the absolute rates of chemical reactions is one of the most important, and at the same time one of the most difficult problems in chemistry today. The problem is particularly crucial with respect to prediction of the activation energy. It was first pointed out by Marcelin [3] in 1915, that the activation energy is conveniently treated from the point of view of the passage of a system over a potential energy surface. London [4] was the first to suggest, in 1928, that the properties of the activated complexes can be calculated by quantum mechanics, using the same methods that are used for

calculating the energies of stable molecules. Although a considerable progress has been made on the methods for the calculations of potential energy surfaces [5], the problem can only consider to be solved for the most simple chemical reactions. Furthermore the potential energy surfaces provide mainly a synthetic view of the role of the different molecular factors on the activation energy, in spite of some general qualitative insights, which have been provided for the topography of these surfaces [6]. Thus, it is no surprise that simpler methods, based on chemical analogies, have enjoyed a wide success in predicting reaction rates for the less simple chemical reactions.

Taylor in 1914 [7] was the first person to seek for a correlation between rate constants,  $k$ , and thermodynamic parameters (equilibrium constants  $K$ ), a suggestion which was developed in 1924 by Brönsted [8] for acid-base catalysis:  $k = GK^\alpha$  ( $G$  and  $\alpha$  are constants). The influence of substituents on the rates of organic reactions has been interpreted in terms of electrical effects by Robinson and Ingold and many other [9]. However probably the most successful approach was the one of Hammett [10], in 1940, based also on linear free-energy relationships.

The relation between the structure of the activated complexes and those of reactants and products was considered explicitly by Leffler in 1953 [11], by postulating that the slope of a rate-equilibrium relationship ( $(\partial \log k / \partial \log K) = \gamma$ ) (measures the position of the transition state along the reaction coordinate).

About the same time Hammond also considered this problem [12] by postulating that the position of the transition state is displaced toward the reactants as the reaction becomes more exergonic.

Explicit relationships between molecular parameters and activation energies,  $E_a$ , have also been studied. In 1938 Evans and Polanyi [13] found an empirical linear relationship between  $E_a$  and the enthalpies of several elementary reactions in the vapour

phase. In 1956 Marcus [14], based on an intersecting harmonic potential energy curve model, related the activation free energy,  $\Delta G^\ddagger$ , with the free energy of the reaction,  $\Delta G^\circ$

$$\Delta G^\ddagger = \Delta G^\ddagger(o) \left( 1 + \frac{\Delta G^\circ}{4\Delta G^\ddagger(o)} \right)^2$$

where  $\Delta G^\ddagger(o)$  is the activation free energy for the thermoneutral reaction. This theory, which was initially developed for outer sphere electron transfers, has been extended to other kinds of reactions [15]. Other energy barriers rather than the parabolic ones have been considered by Johnston and coworkers [16] and by Agmon and Levine [17], all of which include Leffler's interpretation of the transition state configuration [18]. The most famous method is that developed during the early sixties by Johnston: the BEBO method (bond-energy-bond-order) which was designed for hydrogen-atom transfer reactions. This method is based on the empirical rule of Pauling between bond length,  $R$ , and bond order,  $n$ ,

$$R - R_e = 0.26 \ln n$$

and on a relationship between energy and bond order

$$E = D_e n^p$$

where  $R_e$  is the bond length for a bond order of unity,  $p$  is the energy coefficient and  $D_e$  the dissociation energy. Furthermore the model assumes that the bond being formed is continuously replaced by the old one such as  $n_1 + n_2 = 1$ , for single chemical bonds. The influence of substituents on the rates of organic reactions has been interpreted in terms of electronic theories since very early times [9] and these ideas have been extended to the influence of substituents on the energy of activation (19,20). However such effects are mainly viewed as a perturbation on the reference reaction. In fact, most of

the models which we have considered so far only provide relationships between thermodynamic and kinetic parameters. The BEBO model is virtually the only case where the role of electronic factors is explicitly assumed via the bond order  $n$ . Woodward and Hoffmann [21], in 1965, have provided an important insight on the relationship between electronic structure and activation energy by proposing that during a concerted reaction molecular orbital symmetry is conserved. The application of this principle has revealed the existence of chemical processes where the bond order at the transition state is zero, the so called forbidden reactions, and which have very high activation energies. Since then the potentialities of molecular orbital methods to the study of the dynamic properties of the chemical systems has been extensively explored [22].

#### A GENERAL INTERSECTING STATE MODEL FOR THE ACTIVATION ENERGY

##### QUALITATIVE PREDICTIONS

It is well established that reactions of the type  $A + BC \rightarrow AB + C$  can be interpreted in terms of independent bond-forming and bond-breaking process [16]. The course of such reactions can be represented by plotting the energy for bond-breaking of BC or bond-forming of AB against a common reaction coordinate. The point where the states of BC and AB cross corresponds to the transition state. As Figure 1 shows the energy of the transition state relative to reactants (BC) is dependent on three parameters:

- I — the energy of the reaction,  $\Delta E$  ( $\Delta H$ ) or equivalent parameters such as  $\Delta G$ , if potential free energy curves are considered.
- II — The characteristics of the potential energy curves for the reactive bonds, BC and AB. For harmonic oscillators such curves are characterized

by their force constants,  $f$ , but for more realistic curves, e.g. Morse oscillators, the potential energy curves can be characterized in terms of force constants and dissociation energies,  $D_e$ .

- III — the distance,  $d$ , between the minima of the two potential energy curves in the nuclear configuration diagram of Figure 1.

Since  $\Delta E$ ,  $f$  and  $D_e$  can be obtained, in principle, from thermodynamic and spectroscopic data, the development of a general model for the calculation of  $E_a$  requires the establishment of relationships between  $d$  and molecular structure.

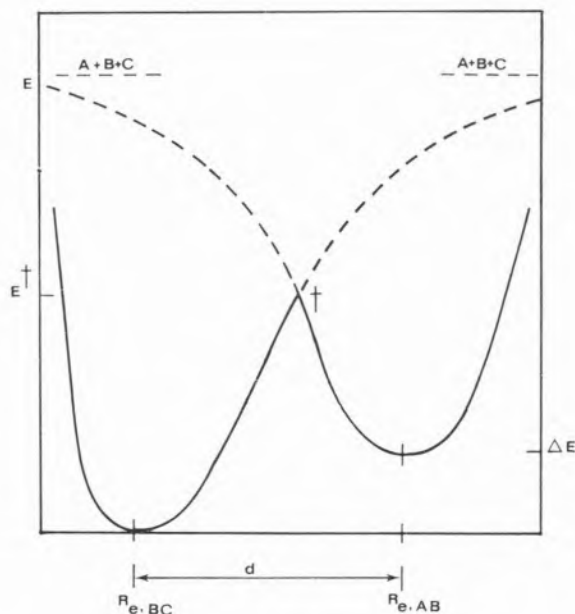


Fig. 1

Intersecting Morse energy curve representation for the reaction  $A + BC \rightarrow AB + C$ .

As Figure 1 reveals the horizontal displacement of the two oscillators,  $d$ , corresponds to the sum of the bond distensions of reactants and products at the transition state. Relationships between  $d$  and molecular structure have to be sought on such bond distensions.



If the equilibrium bond length  $R_{e,BC}$  of the reactant BC is small its distension at the transition state is also expected to be small. However if  $R_{e,BC}$  is large such a distension can also be large. The same is also valid for the product bond length  $R_{e,AB}$  and because  $d$  is the sum of the two bond distensions, we can predict that  $d$  is proportional to  $R_{e,AB} + R_{e,BC}$ .

At the transition state the energy of the reaction,  $\Delta E$ , has to be accommodated as internal energy of the activated complexes. This implies that a further distension of the bonds AB and BC will occur, and, consequently,  $d$  should also depend on  $\Delta E$ .

In addition to the dependence of  $d$  on geometric ( $R_{e,AB} + R_{e,BC}$ ) and thermodynamic ( $\Delta E$ ) parameters,  $d$  should be dependent on electronic parameters. According to the BEBO model during the whole course of the reaction the overall bond order is unity,  $n_{AB} + n_{BC} = 1$ . This is certainly true if in the reactants and products there are only occupied bonding molecular orbitals. However if in the reactants and/or products there are occupied nonbonding or antibonding orbitals which acquire a bonding character at the transition state, the overall bond order of the activated complexes can be higher than 1,  $n_{AB} + n_{BC} = m$  ( $m > 1$ ). This siphoning of electron density into the activated complexes would decrease its bond distensions. Consequently,  $d$  should depend also on the bond order,  $n^\ddagger$ , at the transition state.

### QUANTITATIVE MODEL

A quantitative model which introduces the concept of *variable bond order* along the reaction coordinate was developed recently in collaboration with Professor Varandas [23]. The model is based on the Pauling relationship [24] between bond length and bond order

$$R - R_e = a \ln n$$

where  $a$  is a constant, and on the concept of «entropy of mixing»,  $M$ , introduced by Agmon and Levine [17],

$$M = -n_{AB} \ln n_{AB} - n_{BC} \ln n_{BC}$$

The model defines the energy along the reaction coordinate as

$$E = n \Delta E - \lambda M$$

where  $n = n_{AB}$  is the variable for the reaction progress and  $\lambda$  a parameter which has the dimensions of energy. At the transition state  $E$  has a maximum, and we have shown [23] that

$$d = \frac{2a \ln 2}{m} + \frac{a}{2\lambda^2} \Delta E^2$$

However  $d$  should also depend on  $R_{e,AB} + R_{e,BC}$ . To have a normalized bond distension we have considered this in the Pauling relationship

$$a = a' (R_{e,AB} + R_{e,BC})$$

where  $a'$  is considered to be an universal parameter. The normalized bond distension is defined as

$$\eta = \frac{d}{R_{e,AB} + R_{e,BC}} \quad (1)$$

and consequently

$$\eta = \frac{a' \ln 2}{n^\ddagger} + \frac{a'}{2\lambda^2} \Delta E^2 \quad (2)$$

where  $n^\ddagger$  is the order of each bond at the transition state,  $n^\ddagger = m/2$ . Equation [2] is the expression which allows the establishment of a quantitative relationship between activation energy and molecular structure.

### CROSSING OF THE POTENTIAL ENERGY CURVES

In the crossing of the potential energy curves at the transition state we have so far



neglected any interaction between the electronic states which leads to a resonance splitting,  $\varepsilon$ , of the curves. As Figure 2 shows

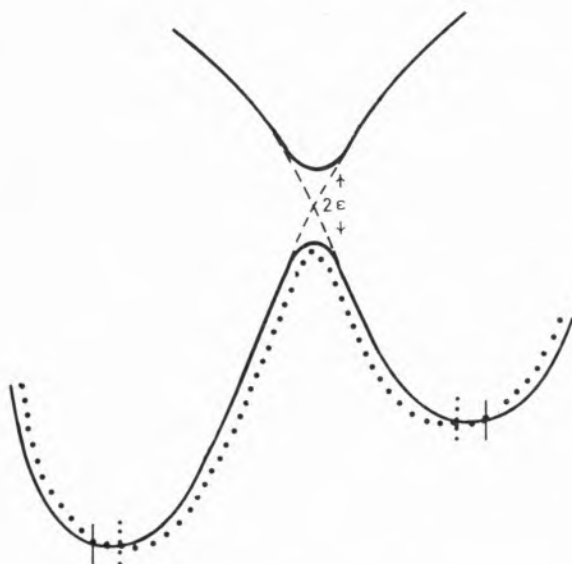


Fig. 2

Effect of the interaction energy on the parameter  $d$ .

the model can take care of such effect through a decrease in  $d$ , a decrease which is large if the resonance splitting is also large. However, in general,  $\varepsilon \ll E_a$  and the resonance splitting does not affect  $d$  in any significant manner. Its main effect is on the transmission coefficient of the rate constant, a factor which takes into account the fact that not every activated complex is converted into products [25].

## EXPERIMENTAL TESTS OF THE THEORY

The model has been tested with several reactions in the vapour phase [23] and in liquid solutions [26,27]. Here we will review briefly some of the most significant aspects of such studies, with the purpose of illustrating the role played by the different molecular parameters.

## GAS PHASE REACTIONS

### Hydrides

If the potential energy curves BC and AB are represented by Morse oscillators, the sum of bond extensions at the transition state is given by [23]

$$d = -\frac{1}{\beta_{AB}} \ln \left\{ 1 - \left( \frac{E^\ddagger - \Delta E}{D_{e,AB}} \right)^{1/2} \right\} - \frac{1}{\beta_{BC}} \ln \left\{ 1 - \left( \frac{E^\ddagger}{D_{e,BC}} \right)^{1/2} \right\} \quad (3)$$

where  $\beta$  are the Morse parameters and  $D_e$  the dissociation energies.  $E^\ddagger$  is the energy of the crossing point of the potential energy curves, considered to be equal to the activation energy. Equation [3] allows the evaluation of  $d$  for several elementary reactions of known activation energies [28]; spectroscopic data were taken from ref. [29]. The reduced bond distension  $\eta$  is calculated through eq. [1].

Figure 3 illustrates the test of eq. [2] for a selection of the reactions already studied [23]. A series of linear correlations of  $\eta$  and  $\Delta E^2$  is found. The slopes appear to be essentially of two types  $3.7 \times 10^{-6} \text{ kJ}^{-2} \text{ mol}^2$  and  $1.3 \times 10^{-5} \text{ kJ}^{-2} \text{ mol}^2$ . The intercepts obey the simple progression 1:1/2:1/3 (0.218; 0.108; 0.072). According to eq. [2] the slopes of the plots of Figure 3,  $a'/2\lambda^2$ , are related to the configurational entropy  $\lambda$ . For elementary gas phase reactions there appear to be essentially two types of slopes corresponding to  $|\lambda| = 77 \text{ kJ mol}^{-1}$  and  $|\lambda| = 145 \text{ kJ mol}^{-1}$ . The lowest entropy  $|\lambda|$  is found in cases where a light atom lies between two dynamically heavy atoms, and the highest entropy when there is no light atom in the middle. When we compare the two kinds of activated complexes  $\text{HHL}^\ddagger$  and  $\text{HLH}^\ddagger$  (H heavy and L light atoms) the first is the one with the highest stretching frequencies. If the entropy

associated with vibration is significant compared with that of rotation we can predict that  $S(HHL^\ddagger) > S(HLH^\ddagger)$ .

The more disordered the activated complexes are, the more states exist to accommodate the energy of the reaction without large bond distensions. Consequently the higher is  $\lambda$  the less is the effect of  $\Delta E^\ddagger$  on  $d$ .

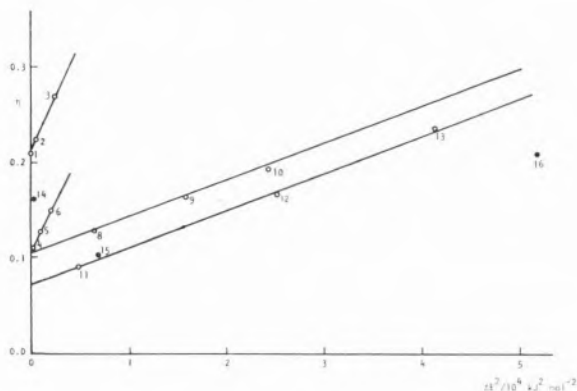


Fig. 3

Plot of the reduced bond distension  $\eta$  as a function of  $\Delta E^\ddagger$ , for elementary gas phase reactions.

○ reactions with hydrides: 1  $H + H_2 \rightarrow H_2 + H$ ; 2  $CH_3 + C_2H_6 \rightarrow CH_4 + C_2H_5$ ; 3  $H + C_2H_6 \rightarrow H_2 + C_2H_5$ ; 4  $Cl + CH_4 \rightarrow HCl + CH_3$ ; 5  $Cl + CH_2Cl_2 \rightarrow HCl + CHCl_2$ ; 6  $CH + CHCl_3 \rightarrow HCl + CCl_3$ ; 7  $Br + CH_4 \rightarrow HBr + CH_3$ ; 8  $Br + H_2 \rightarrow HBr + H$ ; 9  $I + CH_4 \rightarrow HI + CH_3$ ; 10  $F + CH_3 \rightarrow HF + CH_3$ ; 11  $I + C_2H_5I \rightarrow I_2 + C_2H_5$ ; 12  $H + I_2 \rightarrow HI + I$ ; 13  $H + Cl_2 \rightarrow HCl + Cl$  (data selected from ref. 23); ● reactions with nonhydrides; 14  $2NOCl \rightarrow 2NO + Cl_2$ ; 15  $NO + Cl_2 \rightarrow NOCl + Cl$ ; 16  $CO + NO_2 \rightarrow CO_2 + NO$ .

Equation [2] predicts the existence of distinct intercepts, depending on the bond order at the transition state,  $n^\ddagger$ . The intercepts,  $\eta^0$ , should have a reciprocal dependence on  $n^\ddagger$  and this is observed with the following bond orders:  $n^\ddagger = 1/2$ ,  $\eta^0 = 0.218$ ;  $n^\ddagger = 1$ ;  $\eta^0 = 0.108$ ;  $n^\ddagger = 3/2$ ,  $\eta^0 = 0.072$ . The constant  $a'$  is found to be  $a' = 0.156$ , and

$$\eta^0 n^\ddagger = 0.108 \quad (4)$$

The bond order  $n^\ddagger = 1/2$  corresponds to the situation considered in the BEBO model,

$n_{AB} + n_{BC} = 1$ . For a thermoneutral reaction, at the transition state,  $n_{AB} = n_{BC} = n^\ddagger$ ; and consequently  $n^\ddagger = 1/2$ . An example of such type of transition states is provided by reaction  $H + H_2 \rightarrow$  where there are no non-bonding or antibonding electrons in the reactants or the products. Figure 4 illustrates in qualitative terms an energy diagram for the three-center molecular orbitals of the linear activated complex  $H_3^\ddagger$ : The electron distribution leads to a total bond order of unity,  $m = 1$ , and for each of the Hbonds,  $n^\ddagger = 1/2$ .

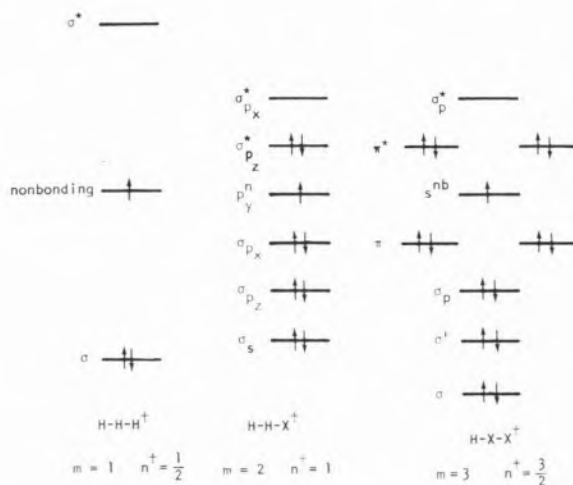


Fig. 4

Molecular orbital energy diagram for triatomic activated complexes ( $X$  is a halogen atom).

A representative reaction of the transition states  $n^\ddagger = 1$  is  $Br + H_2 \rightarrow HBr + H$ . Here there are nonbonding electrons in the bromide atom. If a pair of such electrons acquire a bonding character at the transition state, the overall bond order increases by 1, and, therefore,  $m = 2$ . Figure 4 illustrates the molecular energy diagram [30] for the angular activated complexes  $H_2Br^\ddagger$ , which has  $m = 2$  and average bond orders  $n^\ddagger = 1$ ; for a linear activated complex the maximum bond order would be  $m = 3/2$  and  $n^\ddagger = 3/4$ . This activated complex has features of an electronically excited molecule,

Table 1  
Reduced Oscillators displacement for Elementary Vapour Phase Reactions of Nonhydrides

Reaction	$E_a$ /kJ mol <sup>-1 a)</sup>	$\Delta H$ /kJ mol <sup>-1</sup>	$f/10^3$ kJ mol <sup>-1</sup> A <sup>0-2</sup>	$(R_{e,AB} + R_{e,BC})/A^\circ$	$d/A^\circ$	$\eta$	$\eta_0$	$n^\ddagger$
NO + Cl <sub>2</sub> → NOCl + Cl	96.	83.5	1.95 (Cl—Cl)	2.3 (N—Cl)	0.415	0.105	≈ 0.072	$\frac{3}{2}$
2NOCl → 2NO + Cl <sub>2</sub>	98.6	- 14.8	2.3 (Cl—N)	1.95 (Cl—Cl)	0.634	0.160	0.160	$\frac{2}{3}$
CO + NO <sub>2</sub> → CO <sub>2</sub> + NO	132	- 226	9.15 (C=O)	6.8 (N—O)	0.495	0.211	≈ 0.062	1.75

a) Data collected in K. J. Laidler, «Chemical Kinetics», McGraw-Hill, London, 2<sup>nd</sup> ed., 1965, p. 125.

because the electrons are not occupying all the lowest energy molecular orbitals.

The transition state  $n^\ddagger=3/2$  is illustrated by the reaction  $H + I_2 \rightarrow HI + I$  where a pair of the antibonding electrons of I<sub>2</sub> acquire a bonding character at the transition state. Figure 4 illustrates the corresponding molecular energy diagram which leads to an overall bond order  $m = 3$ .

### Nonhydrides

A few elementary reactions between nonhydride species can also be studied (see Table 1).

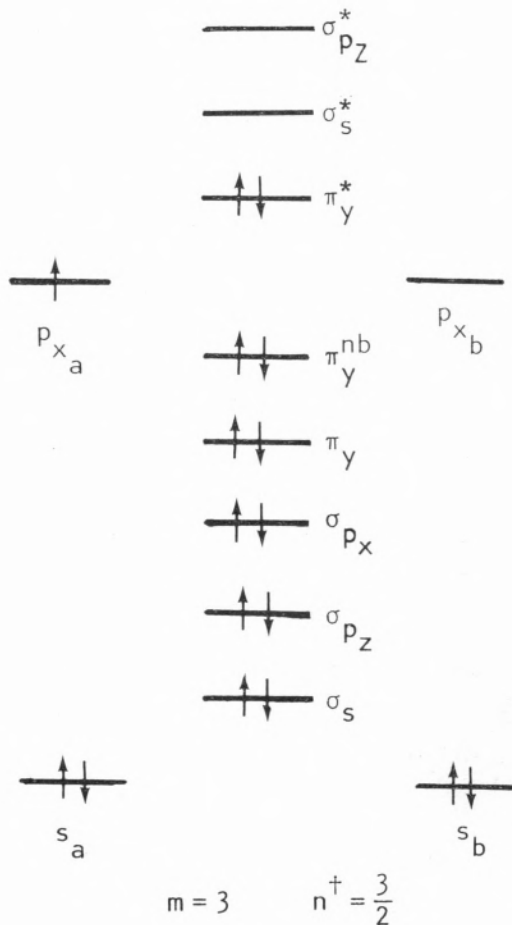


Fig. 5

Molecular orbital energy diagram for an angular  $XY_2^\ddagger$  activated complex

Here, for reasons of simplicity we have considered the reactive bonds as harmonic oscillators. The present data conform with the previous findings, but illustrate other type of transition states.

The reaction  $\text{NO} + \text{Cl}_2 \rightarrow \text{NOCl} + \text{Cl}$  has an intercept close to 0.072, which corresponds to  $n^\ddagger = 3/2$ . Figure 5 illustrates the molecular energy diagram for an angular species  $\text{XY}_2$ , which for this reaction has 17 electrons (14 of  $\text{Cl}_2$  and 3 from O) in the transition state; the bond order at the transition state is  $n^\ddagger = 3/2$ .

For the reaction  $\text{CO} + \text{NO}_2 \rightarrow \text{CO}_2 + \text{NO}$  the number of electrons to be considered is 11 ( $2\text{C} + 6\text{O} + 3\text{N}$ ) which leads to  $m = 3.5$  and consequently to  $n^\ddagger = 1.75$ . With this bond order eq. [14] allows the estimation of  $\eta^\circ = 0.062$ ; eq. [2] then gives  $|\lambda| = 163 \text{ kJ mol}^{-1}$  a value which compares well with  $145 \text{ kJ mol}^{-1}$  found for several other hydride reactions.

Finally the transition state of the reaction  $2\text{NOCl} \rightarrow 2\text{NO} + \text{Cl}_2$  can be understood in terms of an energy diagram for a tetratomic species  $\text{HAAH}$  (Figure 6) with the 14 electrons of the Cl atoms and more 2 electrons, one of each of the terminal atoms. In fact the diagrams of Figure 4 reveal that the conversion of a  $\text{X}_q$  system into  $\text{X}_{q-1}\text{H}$  can be obtained by subtracting 2 electrons to the total number of electrons of  $\text{X}_q$ ; Since this transition state has 20 electrons ( $14 \text{ Cl} + 3\text{O} + 3\text{O}$ ) it is equivalent to 16 electrons in a  $\text{A}_2\text{H}_2$  diagram. As Figure 6 shows the total bond order is  $m = 2$  and since there are 3 bonds, the order per chemical bond is  $n^\ddagger = 2/3$ . Such a value corresponds to  $\eta^\circ = 0.162$  a value in very good agreement with the experimental value (0.160).

These simple considerations on the electronic structure of the activated complexes allow one to interpret the observed bond

orders  $n^\ddagger$  for hydride and nonhydride molecules.

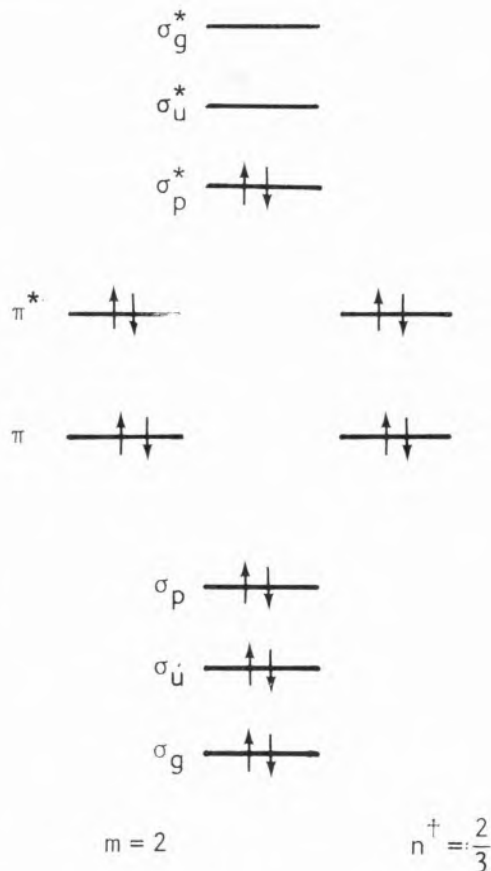


Fig. 6

Molecular orbital energy diagram for a tetratomic molecular species HAAH.

## ELECTRON TRANSFER REACTIONS

### Outer-sphere reactions

The present model is quite general and can be applied to the study of mechanisms of reactions in solution. Although this intersecting-state-model has been developed for bond-breaking bond-forming processes it encompasses reactions where there is no breaking of chemical bonds such as the outer-sphere electron transfer reactions [26]. The transfer of an electron between two reacting moieties occurs for a common configuration of reactants and products found

at the intersection of two potential free energy curves. Assuming that these curves can be represented by harmonic oscillators

$$\frac{1}{2} f_r x^2 = \frac{1}{2} f_p (d - x)^2 + \Delta G^\circ \quad (5)$$

where  $d$  is the horizontal displacement of the oscillators  $x$  is the bond distension in the reactants and  $\Delta G^\circ$  the free energy of the reaction. The activation energy due to the changes in lengths of the ion-ligand bonds is given by

$$\Delta G^\ddagger = \frac{1}{2} f_r x^2 \quad (6)$$

where  $x$  is estimated through eq. [5].

Instead of two separate potential energy curves for the reactants (or products) it is much more convenient to combine these curves into a single one, by averaging the corresponding force constants  $f_r = (f_r' + f_r'')/2$ . Since for the change in configuration of the coordination shell several ligands contribute through in-and out-phase motions, the force constant for the potential energy curve is  $f_r = \sqrt{m'}$  ( $f_r' + f_r''$ )/2 where  $m'$  is the coordination number of the metal ions [26,31].

Table 2 presents the distensions  $d$  and  $\eta$  which reproduce the experimental activation energies for some electron exchange reactions. The interesting result is that  $\eta^\circ \approx 0.108$ , implying a transition state bond order  $n^\ddagger = 1$ , because the ion-ligand bonds are single bonds and there is no chemical breaking during electron transfer.

Table 2

Bond distensions for Electron exchange Reactions \*

Reactants	$\Delta G^\ddagger / \text{kJ mol}^{-1}$	$\eta^\circ$	$d/\text{nm}$
Fe <sup>2+</sup> /Fe <sup>3+</sup>	70.0	0.104	0.043
Cr <sup>2+</sup> /Cr <sup>3+</sup>	82.0	0.108	0.0464
V <sup>2+</sup> /V <sup>3+</sup>	86.3	0.109	0.0476
Mn <sup>2+</sup> /Mn <sup>3+</sup>	93.0	0.116	0.049

The effect of  $\Delta G^\circ$  on  $\Delta G^\ddagger$  can also be evaluated through eqs. [5] and [6] for exothermic reactions. A linear dependence of  $\eta$  and  $(\Delta G^\circ)^2$  was found for the reactions studied [26]. Here the interesting feature is that the observed parameters for the mixing entropy,  $\lambda$ , correlate very well with the entropy of

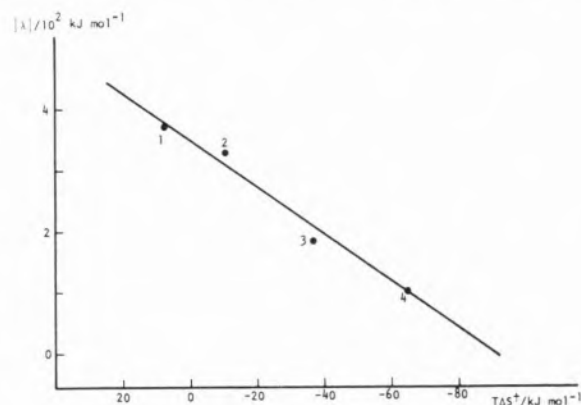


Fig. 7

Correlation of the mixing entropy  $\lambda$  with the entropy of activation ( $T = 298\text{K}$ ) for several outer-sphere electron transfer reactions: 1 Ce<sup>3+</sup>/V<sup>4+</sup>; 2 Cr<sup>2+</sup>/Co<sup>3+</sup>; 3 Eu<sup>2+</sup>/V<sup>3+</sup>; 4 Cr<sup>2+</sup>/Co(NH<sub>3</sub>)<sub>6</sub><sup>3+</sup>; Data selected from ref. 26.

activation,  $\Delta S^\ddagger$  (Figure 7). For  $T = 298\text{ K}$  the observed relationship is

$$|\lambda| / \text{kJ mol}^{-1} = 360 + 4 T\Delta S^\ddagger \quad (7)$$

with  $\Delta S^\ddagger > 0$  there is a small dependence of  $\eta$  on  $(\Delta G^\circ)^2$ ; with  $\Delta S^\ddagger < 0$  there is a large increase of  $\eta$  with an increase in  $|\Delta G^\circ|$ .

#### Inner-sphere reactions

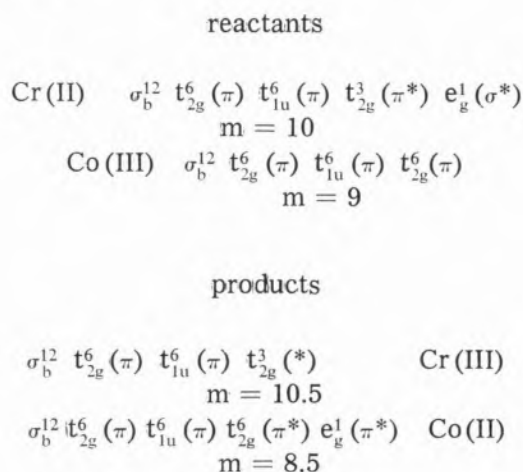
The role of the bond order at the transition state is well illustrated in the case of inner-

\* Data selected from ref. 26.

\*\*  $\lambda(\lambda \ln 2)$  is the intrinsic potential energy barrier of thermoneutral reactions and consequently has enthalpic and entropic contributions. The independent term takes into account the enthalpic contributions together with a term resulting from the conversion of an entropy of mixing in mole fractions into molar concentrations.



sphere reactions where the two reactant species share a common ligand in the activated complexes. Several reactions were studied [26] and all of them have a linear dependence  $\eta$  with  $(\Delta G^\ddagger)^2$  with an intercept  $\eta^\circ \approx 0.068$ . This value is close to the one found for vapour phase reactions with  $n^\ddagger \approx 3/2$ . In order to understand these bond order values let us consider an example of an inner-sphere reaction:  $\text{Cr}^{2+}_{(\text{aq})}/\text{Co}(\text{NH}_3)_5\text{X}^{2+}$ . The most convenient way to interpret these reactions is in terms of the molecular orbital theory. An interaction of  $nd$  ( $t_{2g}$ ) and  $(n+1)$   $p$  orbitals with low-lying nonbonding  $\pi$  ligand orbitals causes changes in the ion coordination shells in the activated complexes and this can lead to electronic configurations such as:



which corresponds to an average total bond order of  $m = 9.5$  and, since there are 6 ion-ligand bonds,  $n^\ddagger = 1.583$ . With this value eq. [4] gives  $\eta^\circ = 0.068$ , as found from the experimental data.

Electron transfer between  $\text{Fe}(\text{CN})_6^{4-}$  and  $\text{Fe}(\text{CN})_6^{3-}$  is an outer-sphere process, because the inner coordination spheres are inert to substitution. However for this reaction  $\eta^\circ = 0.070$ , a value characteristic of an inner-sphere reaction [26]. Because the  $\pi$  orbitals of the  $\text{CN}^-$  ligands can interact with the metal ion orbitals, the metal ligand bonds already have a bond order higher than 1 in reactants and products. The bond order can be

estimated, for example by subtracting the antibonding effect of the  $d$  orbitals from the value of 2 for the metal-ligand bond. Thus, for  $d^5$  and  $d^6$  configurations of the metal ions, the antibonding effect per bond is  $(5+6)/4 \times 6 = 0.46$  and  $n^\ddagger = 1.54$ . With this value the estimated reduced displacement is  $\eta^\circ = 0.070$ .

In 1960 Marcus [32] predicted that for very negative reaction free energies, the rates of electron transfer processes will decrease with a decrease in  $\Delta G^\circ$ . This region, the so called inverted region, has been searched for experimentally in several systems. Examples have been found of the predicted decrease, but

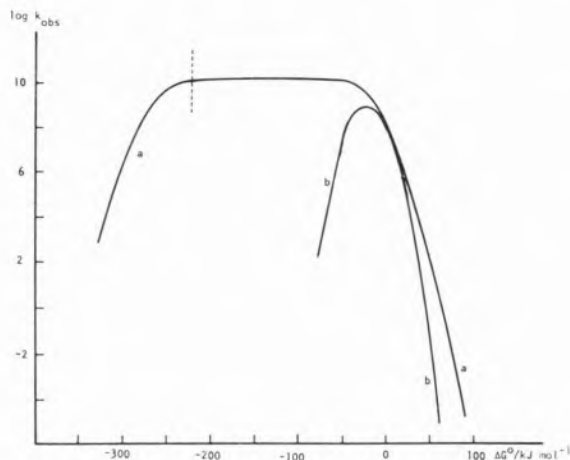


Fig. 8

Calculated rates of electron transfer,  $k_{obs}$ , for inner sphere reactions (--- limit of the region accessible experimentally);  $k_d = 10^{10} \text{ mol}^{-1} \text{ dm}^3 \text{ s}^{-1}$ ;  $k_{-d} = 10^{10} \text{ s}^{-1}$ , frequency factor:  $10^{13} \text{ s}^{-1}$ ,  $\eta^\circ = 0.07$ ,  $f = 3 \times 10^3 \text{ kJ mol}^{-1} \text{ A}^{-2}$ ,  $l = 4 \text{ A}^\circ$ ; a)  $|\lambda| = 290 \text{ kJ mol}^{-1}$ ; b)  $|\lambda| = 90 \text{ kJ mol}^{-1}$ .

for other systems there is no inverted region, because only a diffusion controlled rate plateau has been found [33]. It has been a matter of controversy the kind of parameters which are responsible for the observation or the non-observation of the inverted region. The present model seems to solve such problem in terms of the entropy of mixing.

Figure 8 presents the calculated rates of electron transfer as a function of  $\Delta G^\circ$ , in a system controlled by diffusion, i.e.,

$$k_{\text{obs}} = \frac{k_d k_{\text{et}}}{k_{-d} + k_{\text{et}}}$$

where  $k_d$  is the rate of diffusion,  $k_{-d}$  the rate of separation of the two reacting moieties from the collision complex and  $k_{\text{et}}$  the rate of electron transfer within the collision complex. As the figure shows for a low  $|\lambda|$  the inverted region is observed experimentally, because it occurs at moderately  $\Delta G^\circ$ . However when  $|\lambda|$  is high the inverted region cannot be observed experimentally because it occurs at very negative energies, not experimentally available, even for electrochemically excited states.

## SUBSTITUTION REACTIONS

### Diagnosis of Mechanisms in terms of Bond Order

The molecular parameters of this intersecting-state-model can provide new insights on reaction mechanisms. A good example of this is the diagnosis of the mechanisms of nucleophilic reactions based on the bond order at the transition state [27].

Water exchange reactions of metal ions in aqueous solutions are convenient to illustrate this application because  $\Delta G^\circ = 0$ . The bond order  $n^\ddagger$  is calculated through the procedure already described for the electron transfer reactions. However, since only one bond is stretched along the reacting coordinate, the potential energy curves are calculated with the force constant of a single chemical bond. Two extreme situations can be considered for these reactions: one is an associative mechanism where the rate determining step is the formation of an intermediate of increased coordination number; the other is a dissociative mechanism where in the rate determining step there is the generation an intermediate of reduced coordination num-

ber. For an associative mechanism there is bond-forming and bond-breaking processes and if there is no intervention of nonbonding electrons, the total bond order is conserved and  $n^\ddagger = 1/2$ . For a dissociative mechanism with conservation, of bond order  $n^\ddagger = 1$ .

Table 3 illustrates the calculated  $n^\ddagger$  for several metal ions. The results reveal a continuum of  $n^\ddagger$  values, from 0.5 to values even higher than 1 for cases where some non-

Table 3

Bond Orders at the Transition State for Water Exchange Reactions of Metal Ions <sup>a)</sup>

Ion	$n^\ddagger$	Mechanism <sup>b)</sup>
Cr <sup>3+</sup>	0.51	A
Be <sup>2+</sup>	0.76	I <sub>a</sub>
Fe <sup>2+</sup>	0.85	I <sub>d</sub>
Co <sup>2+</sup>	1.00	D
Gd <sup>3+</sup>	1.30	D <sub>b</sub>

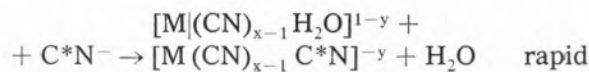
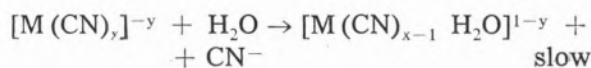
<sup>a)</sup> Data from ref. 27. <sup>b)</sup> A associative; I<sub>a</sub> associative interchange; I<sub>d</sub> dissociative interchange; D dissociative; D<sub>b</sub> dissociative bridging.

bonding electrons of the ligand acquire a bonding character at the transition state. The data reveal that the mechanisms of nucleophilic substitution in fact form a continuum between first and second order processes, where the usual subdivisions are somewhat arbitrary.

### $\Delta G^\circ$ as a driving force for reactions

Marcus has shown very convincingly that for moderately exothermic electron transfer

reactions  $\Delta G^\circ$  acts as a driving force for reactions (14,32,33). However this seems not to be valid for several nucleophilic substitutions. One example is provided by the exchange of cyanide which in fact is rate determined by the aquation process.



According to the present model the activation energy should depend on  $\Delta G^\circ$  of the aquation process, which should also vary with the stability of the cyanide complexes. However, as Table 4 reveals there no corre-

Table 4

Exchange rate and stability of some cyano complexes <sup>a)</sup>

Complex	Dissociation constant	Exchange rate
Fe(CN) <sub>6</sub> <sup>4-</sup>	10 <sup>-37</sup>	very slow
Ni(CN) <sub>4</sub> <sup>2-</sup>	10 <sup>-30</sup>	very fast
Mn(CN) <sub>6</sub> <sup>3-</sup>	10 <sup>-27</sup>	moderate
Ag(CN) <sub>2</sub> <sup>-</sup>	10 <sup>-21</sup>	very fast

<sup>a)</sup> Data from ref. 34

lation between the rates of reaction and the equilibrium constants.

Activation energy depends on several factors and a correlation between  $E_a$  and molecular parameters can only be established when the effect of one of the factors is dominant or when several factors work in the same direction. However when this is not the case, more profound analysis have to be carried out. Table 5 presents the calculated  $\eta^\circ$  for

Table 5

Reduced Displacements for Aquation of Cyanide Metal Complexes

Complexes	$\Delta G^\ddagger / \text{kJ mol}^{-1}$	$f / \text{kJ mol}^{-1} A^{e-2}$ <sup>a)</sup>	$M-C$	$M-O$	$\Delta G^\circ / \text{kJ mol}^{-1}$	$\lambda / \text{kJ mol}^{-1} d$	$d/A^\circ R_{e,AB} + R_{e,BC}/A^\circ$	$\eta^\circ$	Mechanisms					
									Bond order reactant product	Associative	Dissociative			
									$\eta^\circ$	$\eta^\circ$	$\eta^\circ$			
Mn(CN) <sub>6</sub> <sup>3-</sup>	83 <sup>b)</sup>	$2 \times 10^3$	$1.6 \times 10^3$	18	$1.7 \times 10^2 d)$	0.576	4.06	0.141	1.67	1.0	0.667	0.16	1.67	0.065
Fe(CN) <sub>6</sub> <sup>4-</sup>	102 <sup>b)</sup>	$2.8 \times 10^3$	$9.6 \times 10^2$	26	$1.7 \times 10^2 d)$	0.677	4.0	0.168	1.50	1.0	0.625	0.173	1.50	0.072
	130 <sup>c)</sup>				1.1			0.216						
Ag(CN) <sub>2</sub> <sup>-</sup>	74.5	$1.25 \times 10^3$	$4 \times 10^2$	48	$3 \times 10^2 e)$	0.71	5.0	0.140	1.0	1.0	0.5	0.216	1.0	0.108
	60				0.55			0.108						

<sup>a)</sup> J. R. Ferraro «Low Frequency Vibrations of Inorganic and Coordination Compounds». Plenum Press, New York 1971, J. Burgess «Metal ions in Solutions». Wiley, London, 1978, p. 85.<sup>b)</sup> Experimental values of ref. 34<sup>c)</sup> Calculated values; rates compared with the one of Mn(CN)<sub>6</sub><sup>3-</sup>;  $5 \times 10^{-9}$ ;  $30$ ;  $1 \times 10^4 (\text{mol}^{-1} \text{dm}^3 \text{s}^{-1})$ ;<sup>d)</sup>  $T\Delta S^\ddagger = -47 \text{ kJ mol}^{-1}$  | 34 | and eq. (7);<sup>e)</sup>  $T\Delta S^\ddagger = -16 \text{ kJ mol}^{-1}$ .

the aquation processes of  $\text{Mn}(\text{CN})_6^{3-}$  and  $\text{Fe}(\text{CN})_6^{4-}$ , taking into account the endothermicity of the reactions. As the results show the mechanisms are strongly associative. The relative order for the exchange rates is dominated by  $\Delta G^\circ$  and the force constants. Calculations with  $\text{Ag}(\text{CN})_2^-$  seem to show that a very fast exchange can only occur if the mechanism of aquation has a more dissociative character. For this complex the reaction free energy, on its own, would make the exchange process a very slow one.

An even more striking example of the apparent absence of correlation of rate and equilibrium constants has been reported by Taube [35] and concerns substitution reactions of ruthenium ammines complexes. Whereas the equilibrium constants vary ca.  $10^7$  times the rate constants only vary by a factor of 5 (Table 6). Since the rate of complex formation does not reflect the stability of the complex, Taube concluded that there was very little bond formation in the activated complexes.

We have applied our model to calculate  $d$  in order to reproduce  $\Delta G^\ddagger$ . These were estimated from  $k_1$  with a preexponential factor of  $10^{13} \text{ s}^{-1}$ . The force constant Ru-N and Ru-O is  $1.6 \times 10^3 \text{ kJ mol}^{-1} \text{ \AA}^{-2}$  [36] and  $R_{e,AB} + R_{e,BC} = 4.27 \text{ \AA}^\circ$ . Figure 9 presents the plot of  $\eta$  as a function of  $(\Delta G^\circ)^2$ . A good

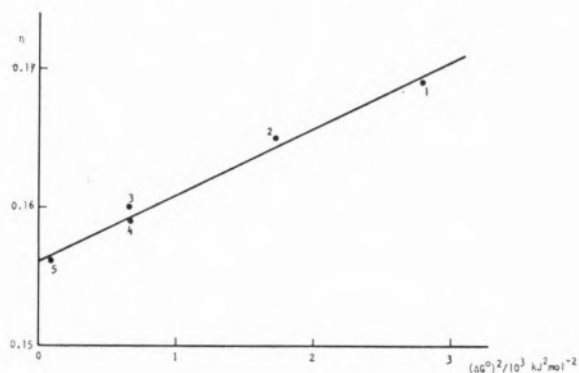
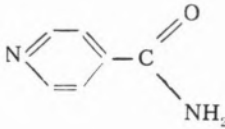
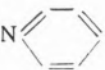


Fig. 9

Reduced displacement  $\eta$  as a function of  $(\Delta G^\circ)^2$  for ruthenium ligand exchange  $[\text{Ru}(\text{NH}_3)_5\text{OH}_2]^{2+} + \text{L} \rightarrow [\text{Ru}(\text{NH}_3)_5\text{L}]^{2+} + \text{H}_2\text{O}$ ; legend for ligands L in Table 6.

Table 6

Specific rates of ligation,  $k_1$ , in  $[\text{Ru}(\text{NH}_3)_5\text{H}_2\text{O}]^{2+}$  as a function of stability <sup>a)</sup>.

	Ligand	$K_{\text{eq}}$	$k_1 / \text{mol}^{-1} \text{ dm}^3 \text{ s}^{-1}$	$-\Delta G^\circ / \text{kJ mol}^{-1}$	$\Delta G^\ddagger / \text{kJ mol}^{-1}$
1		$2 \times 10^9$	0.105	52.8	79.4
2		$2 \times 10^7$	0.093	41.5	79.0
3	$\text{NH}_3$	$3.5 \times 10^4$	0.055	25.8	81.0
4	$\text{N}_2$	$3.3 \times 10^4$	0.073	25.7	80.3
5	$\text{NH}(\text{CH}_3)\text{CH}_2\text{CO}_2\text{Et}$	50	0.021	9.7	83.3

<sup>a)</sup> Data from ref. 35;  $R_{e,AB} + R_{e,BC} = 4.27 \text{ \AA}^\circ$

linear relationship is observed with an intercept  $\eta^0 = 0.156$  and a slope which gives  $|\lambda| = 1.35 \times 10^2 \text{ kJ mol}^{-1}$ .

The first important conclusion is that  $\Delta G^0$  is a driving force for the reaction. However its effect is not significant because there is a considerable entropy of mixing. From eq. [7] an estimation can be made  $\Delta S^\ddagger = -188 \text{ J mol}^{-1} \text{ K}^{-1}$ . The intercept reveals that the mechanism can have a strong associative character,  $I_a$ ; because  $n^\ddagger = 0.69$ . Such conclusion contrast with the conclusion of Taube [35] based only on the apparent lack of correlation between  $k$  and  $\Delta G^0$ .

## EPILOGUE

In contrast with the information provided by potential energy surfaces the present model can assess independently the role of several thermodynamic, geometric and electronic factors on the energy barrier ( $E_a$  or  $\Delta G^\ddagger$ ) of a chemical reaction. The relevant parameters are:

- i — the energy of the reaction,  $\Delta H$  or  $\Delta G$ .
- ii — the force constants,  $f$ , of the reactive bonds or other characteristics of the potential energy curves, such as the dissociation energy.
- iii — the sum of the lengths of the reactive bonds,  $R_{e,AB} + R_{e,BC}$ .
- iv — the bond order at the transition state,  $n^\ddagger$ .
- v — the entropy of mixing,  $\lambda$ , or its equivalent, i.e., the activation entropy,  $\Delta S^\ddagger$ .

This analytic feature of the model is very useful in teaching Chemical Kinetics, because it can help the students to assess, in a qualitative way, the effect of several molecular factors on reaction mechanisms. Within this

kind of model we have already used the parameters  $\Delta H$  ( $\Delta G$ ),  $f$ , and  $R_{e,AB} + R_{e,BC}$  to provide new insights in the teaching of chemical kinetics [37] and molecular reactivity [38]. The discover of the concept of a variable transition state bond order can also be incorporated in the teaching at an university level. The entropy of mixing is probably a more difficult concept to use for qualitative predictions.

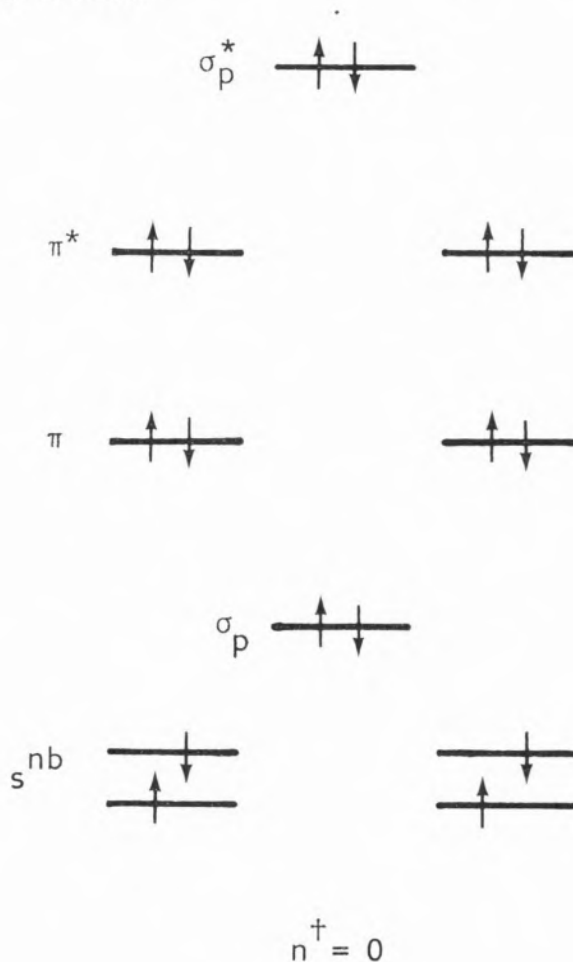


Fig. 10

Molecular orbital energy diagram for the hypothetical cyclic transition state  $H_2I_2^\ddagger$ :

However the scope of the model is considerably broader than the one of its pedagogical value, because it is a quantitative model which generalizes the previous approaches already mentioned including, as parti-



cular cases, the BEBO and Marcus theories. Recently Grunwald [39] has discussed the limitations of the Marcus theory on describing the reaction progress in terms of just one variable. To circumvent this difficulty Grunwald has proposed a new model where two «ad hoc» progress variables are defined. Here the present model virtually adds two independent variables,  $n^\ddagger$  and  $\lambda$ , to the theory of Marcus and is therefore even more flexible than the model of Grunwald.

The role of the electronic factors on the energy barrier for a chemical reaction is a quantification of the Woodward-Hoffmann principles [22]. The conservation of orbital symmetry divides the chemical reactions into allowed and forbidden processes. The latter ones have a bond order at the transition state equal to zero,  $n^\ddagger = 0$ , and therefore have an «infinite» energy barrier, such as the hypothetical elementary reaction  $H_2 + I_2$  (Figure 10). However the allowed processes have different degrees of electronic allowdness which can range from  $n^\ddagger = 1/2$  to  $n^\ddagger = 2$  or even higher values.

In conclusion, we hope to have revealed that the present model can provide new insights on the mechanisms of chemical reactions and can establish a more rigorous framework for the current theories of absolute rates.

On finishing this presentation I would like to refer to the title of Professor Ferreira da Silva lecture for the opening of the academic year at the University of Oporto in November 1911: «A importância e a dignidade da ciência». I and certainly all of you, share that same conviction. This is the best tribute which we can pay to the founder of the Sociedade Portuguesa de Química.

This work was developed through a collaboration of many years with my friend and colleague António Varandas. Our educational and scientific association has influenced in many ways the ideas presented here.

(Received, 20th June 1985)

## REFERENCES

- [1] L. WILHELMY, *Pogg. Ann.*, **81**, 413, 499 (1850).
- [2] S. ARRHENIUS, *Z. Physik Chem.*, **4**, 226 (1889); for the origins of the Arrhenius equation see S.R. Logan, *J. Chem. Educ.*, **59**, 279 (1982); M.C. King, *Ambix*, **28**, 70 (1981), **29**, 49 (1982) and K.J. Laidler, *J. Chem. Educ.*, **61**, 494 (1984).
- [3] A. MARCELIN, *Ann. Phys.*, **3**, 158 (1915).
- [4] F. LONDON, «Probleme der modernen Physik», Sommerfeld Festschrift, 1928, p. 104.
- [5] J.N. MURRELL, S. CARTER, S.C. FARANTOS, P. HUXLEY and A.J.C. VARANDAS «Molecular Potential Energy Functions», Wiley, London, 1984.
- [6] M.H. MOK and J.C. POLANYI, *J. Chem. Phys.*, **51**, 1451 (1969).
- [7] H.S. TAYLOR, *Z. Elektrochem.*, **20**, 201 (1914).
- [8] J.N. BRÖNSTED and K.J. PEDERSON, *Z. Physik. Chem.*, **108**, 185 (1924); J.N. BRÖNSTED, *Chem. Rev.*, **5**, 322 (1928).
- [9] See for example C.K. INGOLD, *Chem. Rev.*, **15**, 225 (1934).
- [10] L.P. HAMMETT, «Physical Organic Chemistry», McGraw-Hill, New York, 1940, pp. 184-199.
- [11] J.E. LEFFLER, *Science*, **117**, 340 (1953); *J. Org. Chem.*, **20**, 1202 (1955).
- [12] G.S. HAMMOND, *J. Am. Chem. Soc.*, **77**, 334 (1955).
- [13] M.G. EVANS and M. POLANYI, *Trans. Faraday Soc.*, **34**, 11 (1938).
- [14] R.A. MARCUS, *J. Chem. Phys.*, **24**, 266 (1956).
- [15] See for example A.J. KRESGE, *Chem. Soc. Rev.*, **2**, 475 (1973); W.J. ALBERY and M.M. KREVOY, *Adv. Phys. Org. Chem.*, **17**, 87 (1978).
- [16] H.S. JOHNSTON, *Adv. Chem. Phys.*, **3**, 13 (1960); H.S. JOHNSTON and P. GOLDFINGER, *J. Chem. Phys.*, **37**, 700 (1962); H.S. JOHNSTON and C. PARR, *J. Am. Chem. Soc.*, **85**, 2544 (1963).
- [17] N. AGMON and R.D. LEVINE, *Chem. Phys. Letters*, **52**, 197 (1977).
- [18] J.L. KURZ, *Chem. Phys. Letters*, **57**, 243 (1978).
- [19] C.N. HINSHELWOOD, K.J. LAIDLER and E.W. TIMM, *J. Chem. Soc.*, 848 (1938).
- [20] R. DAUDEL, «Quantum Theory of Chemical Reactivity», Reidel Publ. Comp., Dordrecht-Holland, 1973.
- [21] R.B. WOODWARD and R. HOFFMANN, *J. Am. Chem. Soc.*, **87**, 395, 2046, 2511 (1965).
- [22] R.B. WOODWARD and R. HOFFMANN, «The Conservation of Orbital Symmetry», Academic Press, 1970; K. Fukui *Acc. Chem. Res.*, **4**, 57 (1971).
- [23] A.J.C. VARANDAS and S.J. FORMOSINHO, *J. Am. Chem. Soc.*, submitted for publication Du 1984.
- [24] L. PAULING, *J. Am. Chem. Soc.*, **69**, 542 (1947).
- [25] See for example K.J. LAIDLER and J.C. POLANYI, *Prog. React. Kinetics*, **3**, 3 (1965).

- [26] S.J. FORMOSINHO, *J. Chem. Soc., Faraday Trans. I*, submitted for publication, Jan. 1985.
- [27] S.J. FORMOSINHO *Inorg. Chem.*, submitted for publication, April 1985.
- [28] G.L. PRATT, «Gas Kinetics», Wiley 1969, p. 158-160.
- [29] B. ROSEN, «Tables de Constants Spectroscopiques. Molecules Diatomiques», International Tables of Selected Constants, 1971, vol. 17.
- [30] See for example, A.D. WALSH, *J. Chem. Soc.*, 2260, 2331 (1953); H.B. GRAY «Electrons and Chemical Bonding», BENJAMIN, New York, 1965.
- [31] S.J. FORMOSINHO, *Mol. Photochem.*, 7, 41 (1976).
- [32] R.A. MARCUS, *Faraday Discuss. Chem. Soc.*, 29, 21 (1960).
- [33] R.A. MARCUS, *Faraday Discuss. Chem. Soc.*, 74, 7 (1982).
- [34] A.W. ADAMSON, J.P. WELKER and W.B. WRIGHT, *J. Am. Chem. Soc.*, 73, 4786 (1951); A.G. MACDIARMID and N.F. HALL, *ibid*, 76, 4222 (1954).
- [35] H. TAUBE, *Comments Inorg. Chem.*, 1, 17 (1981).
- [36] J.R. FERRARO, «Low-Frequency Vibrations of Inorganic and Coordination Compounds», Plenum Press, New York, 1971, p. 192.
- [37] S.J. FORMOSINHO, «Fundamentos de Cinética Química», Fundação Gulbenkian, Lisboa, 1938.
- [38] S.J. FORMOSINHO and A.J.C. VARANDAS, «Estrutura e Reactividade Molecular, Uma Introdu-

ção com base no Modelo da Caixa Potencial», in press.

- [39] E. GRUNWALD, Fundação Gulbenkian, *J. Am. Chem. Soc.*, 107, 125 (1985).

## RESUMO

**Estrutura molecular e reactividade química. A importância da energia de activação.**

*Apresenta-se um modelo semi-empírico de intersecção de curvas de energia potencial para o cálculo de energias de activação. O modelo mostra que a energia de activação depende de factores termodinâmicos e electrónicos: energia de reacção, constantes de força e soma dos comprimentos das ligações químicas reactivas, da ordem de ligação no estado de transição e da chamada «entropia de mistura». Alguns destes parâmetros moleculares são importantes na elucidação do mecanismo de reacções. Ilustra-se este facto com a aplicação do modelo a reacções de hidretos e não-hidretos em fase gasosa, e a reacções de transferência de electrões e substituição nucleofílica em soluções aquosas. Compara-se o modelo com outros formalismos teóricos que procuram relacionar energia de activação e estrutura molecular, nomeadamente as relações lineares de energia livre, as teorias de Marcus e BEBO e as regras de conservação de simetria de Woodward-Hoffmann.*

R.D. GILLARD

Chemistry Department,  
University College,  
P. O. Box 78, Cardiff,  
CF1 1XL, Wales U. K.

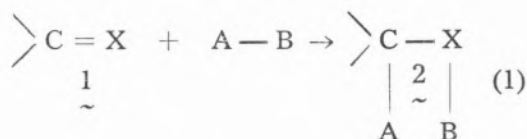


## PSEUDO-BASE MECHANISMS IN ORGANIC, COORDINATION AND BIOCHEMISTRY \*

The comparison between the effect of quaternization (by alkyl and other groups) of N-atoms in imines, including N-heterocycles, and the effect of coordination of the same N-atoms to metal ions is summarized. Mechanisms based on this view of metal ions as quaternizing agents are suggested for organic systems including Sarett's reagent. Similar mechanisms are proposed for metallo-enzymic systems, including coordinated imidazole in xanthine oxidase and in carbonic anhydrase, where the observed  $pK_A$  ( $\sim 7.0$ ) could arise from pseudo-base formations by OH<sup>-</sup> on zinc-bound imidazole rather than H<sup>+</sup> ionization from an acidic group.

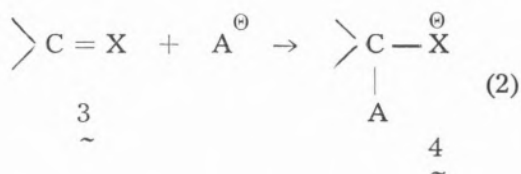
\* Plenary lecture at the 8th Annual Meeting of Portuguese Chemical Society, Braga, April, 1985.

Transformations between double bonds and single bonds, as in [1] where X may be CR<sub>2</sub>, NR, O (or S), and AB may be H-H, HO-OH, HOH, R'RNH,

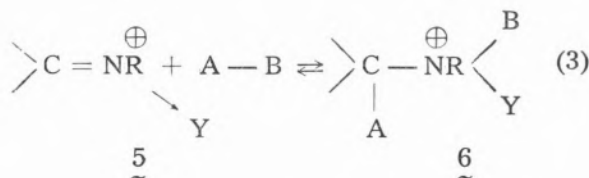


RSH, HCN etc, are always interesting, and often useful, didactically or commercially. The more electronegative (nucleophilic) part of AB attaches to carbon.

Indeed if the acid-base properties of AB are included (for systems where B = H), then the nucleophilic attack may be written as [2]



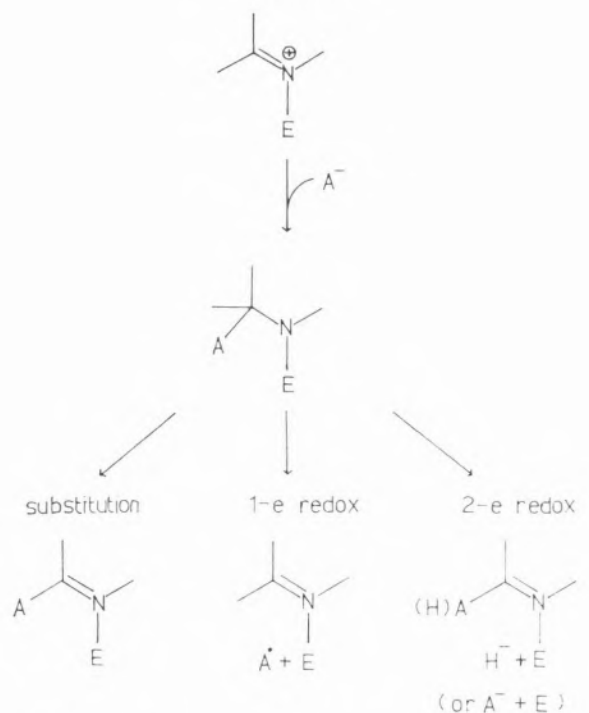
The case where X = NR (for which I use the general name imine) involves a great range of chemistry, including the Schiff bases (where the product of addition of water is the Dimroth base or carbinolamine), oximes, and the many cases where the imine function is part of an aromatic N-heterocyclic ring. It is well known that the equilibrium constant for [3] is larger than that for the parent reaction [1]



That is, by putting a positive charge (Y = =H—protonation, Y = CH<sub>3</sub> etc—alkylation, arylation, N—oxidation, and so forth) on the nitrogen, the neighbouring carbon also becomes more positive (and hence electrophilic). Nucleophiles now add to the unsaturated trigonal carbon better.

The process of adding groups to put a positive charge on the nitrogen of 1 is called quaternization: my theory<sup>1</sup> is that imines (whether N-heterocyclic or not) may be viewed as being quaternized by attachment to metal ions (the process usually thought of as coordination by coordination chemists). Quaternization of the nitrogen of an imine and its coordination to a metal ion lead to similar reactivities (though by virtue of the variable oxidation states accessible to the metal ions, nucleophilic addition to the metal ion complex will give addends which may have redox reactions available which the classical organic systems cannot always imitate). The general situation is shown in Scheme 1. The more polarizing the metal ion, the greater its effect on the reactivity of the ligand.

Scheme 1



e.g. E = carbon  
(in alkyl, aryl etc.)  
CN<sup>-</sup> (Reissert)

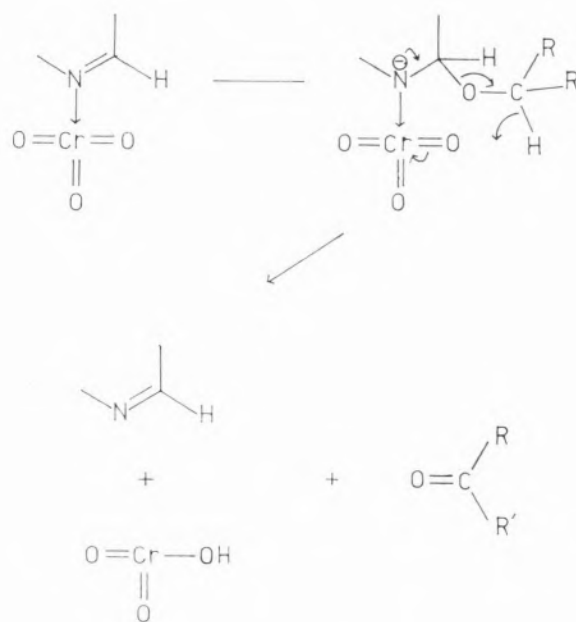
E = metal ion

Na<sup>+</sup>, NH<sub>2</sub><sup>-</sup>, Chichibabin  
K<sup>+</sup>, OH<sup>-</sup>

e.g. E = M<sup>3+</sup>  
A = OH<sup>-</sup>

e.g. E = Rh<sup>3+</sup>  
A =  $\bar{O}CHRR'$   
(alkoxide)

*Organic applications:* To achieve oxidations of organic materials, metal reagents in high oxidation states<sup>2</sup> are commonly employed, like Cr (VI), Mn (VII), or Os (VIII). Occasionally, these metal ions are used in conjunction with an imine when it will form complexes with them and be heavily polarized by them, some carbon atoms becoming electrophilic. Sarett's reagent, and the several modifications of it, involve N-heterocycles and Cr (VI), usually the trioxide or some substance which is in equilibrium with it. These reagents bring about mild (and rather selective) oxidations of primary and secondary alcohols to aldehydes and to ketones respectively. My suggested mechanism is shown:



In this view, the imine is a catalyst. An exactly analogous mechanism applies to the less commonly employed oxidant which uses sulphur trioxide in place of its chromium analogue, and DMSO in place of the organic halo solvent of the Sarett systems. (This pyridine-sulphur trioxide compound is of course better known as a sulphonating agent).

In the Sarett oxidations, the N-heterocycle appears to be mandatory. It is not simply

a matter of Bronsted donor power: non heterocyclic amines with  $pK_b$  equal to that of (say) pyridine do not work<sup>3</sup>.

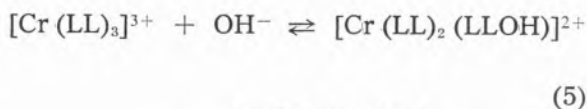
### COORDINATION CHEMISTRY

The «simple» complex ions containing imines, which may be chelating (e.g. bi-imidazole, 1, 10-phenanthroline) have great significance in many such areas as: photolysis of water catalysis of the oxygenation of drying oils, heavy metal analysis, resonance Raman effects (e.g. of pyridine at a silver electrode) and reaction mechanisms. It is as well to understand the species likely to be present in solutions made up from an imine (like 2,2'-bipyridyl) and a metal salt (like chromium (III) perchlorate). There are for such solutions many anomalous dependences on pH of properties, like oxidation potential, rates of solvolysis, electronic and circular dichroism spectra. Significant third order terms in rate equations are common<sup>4</sup>, as in [4].

$$\frac{-d[M(LL)_3]^{3+}}{dt} = [M(LL)_3] (k_1 + k_2 [OH^-] + k_3 [OH^-]^2) \quad (4)$$

How can these arise save through efficient attack of a second hydroxide on a pre-formed 1:1 adduct? Indeed, the dominant term is usually that of  $k_2$ .

This 1:1 adduct [equation 4], which contains a complexed pseudobase has, in my theory, at least one carbon atom with a coordination number 4, (others may possibly be covalently hydrated) and a lifetime more than ephemeral Its spectroscopic properties differ from those of the acid-stable form



$$K = \frac{[Cr(LL)_2(LLOH)]}{[Cr(LL)_3][OH^-]}$$

Equilibrium constants  $K_5$  for [5] are all about  $10^7$ , for  $LL = 2,2'$ -bipyridyl, 1,10-phenan-

throline and complexes of some similar ligands

Understanding in this field has been held back by failure<sup>5</sup> to observe the spectroscopic effects arising from reaction [5]. The reversible colour change between equi-formal solutions at differing pH of these chromium (III) complexes is clear to the naked eye. An entirely typical set<sup>6</sup> of difference spectra obtained using a double beam spectrophotometer, is shown as Figure 1. Con-

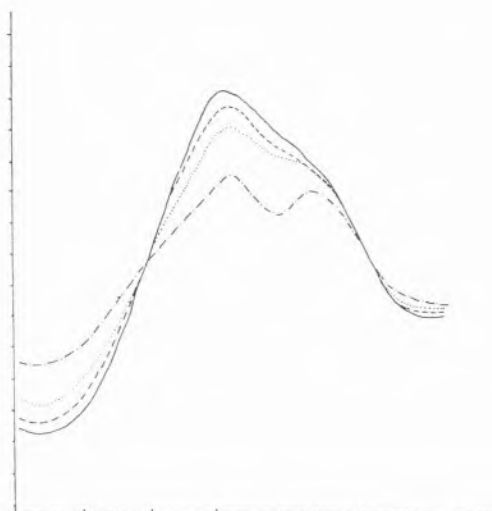


Fig. 1

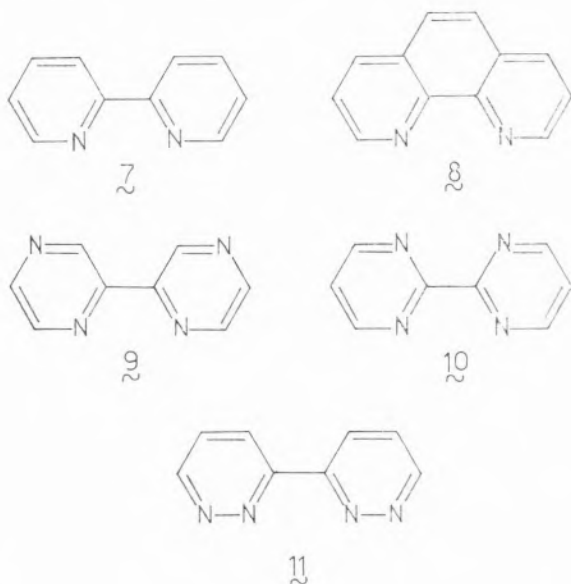
Difference Spectra (270-340 nm) for  $[Cr(2,2'$ -bipyridyl)<sub>3</sub>](ClO<sub>4</sub>)<sub>3</sub>·2H<sub>2</sub>O, in water, 20°C at formal concentration  $3.28 \times 10^{-5}M$ . The reference cell contained the solution at pH 1.65, the sample cell at pH's

—————	11.1
- - - - -	8.9
.....	8.2
- · - · -	6.7

ductances are also informative: these chromium (III) species may be titrated conductimetrically with hydroxide (and behave rather like ethanoic acid). As expected from the increased activity of hydroxide in non-aqueous media, formation of adducts is very obvious<sup>7</sup> in those circumstances. The yellow dilute solution of  $[Cr(LL)_3](ClO_4)_3$  in acetonitrile goes red-brown with a solution of



[NBu<sub>4</sub>]<sup>+</sup>[OH]<sup>-</sup> in methanol/toluene, but, this reverses with acid.



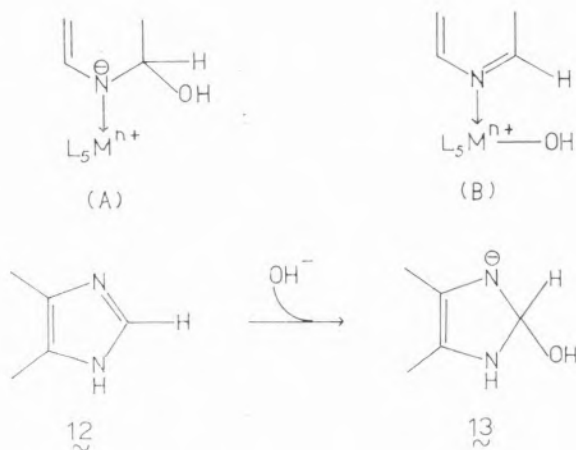
As an aside, the use of iso-electronic series gives an illustrative fact. For the tris-di-imine iron (II) cations where the di-imine is 2,2'-bipyridyl [7] [or 1,10-phenanthroline [8]], the rate constant  $k_2$  of [4] is (in  $\text{dm}^3\text{mol}^{-1}\text{s}^{-1}$ )  $\sim 10^{-3}\text{s}^{-1}$ ; for the isoelectronic cases involving 2,2'-bi-pyrazyl [9] or bipyrimidyl [10] it is (as expected) larger:  $\sim 350$ ; for the bi-pyridazinyl [11] with *no* carbon atom at the kinetically significant position (and no formation of pseudo-base capable of intramolecular hydroxyl shift)  $k \approx 3.3 \times 10^{-5}$ . Many other cases in disparate fields are now turning up which serve to confirm the generality of my view.

The chief lack at present is of crystallographic proof of the presence of 4 coordinated carbon, in any isolated solid, and it is in this direction that some of the current effort in the Cardiff group is going. Among the many available structures of solvated salts of octahedrally complexed N-heterocycles none has yet shown either structural element (A) or (B). We recently checked the most accessible of five polymorphs of  $[\text{Ni}(\text{phen})_3] \text{I}_2 \cdot x\text{H}_2\text{O}$

( $x = 3$ ) and the lower temperature dimorph of  $\text{trans-}[\text{Ir}(\text{py})_4\text{Cl}_2] \text{Cl}6\text{H}_2\text{O}$  (crystallized at  $2^\circ\text{C}$  and isomorphous with a rhodium analogue). The water in both cases was in hydrogen bonded arrays, *not* attached to metal ion or carbon atom.

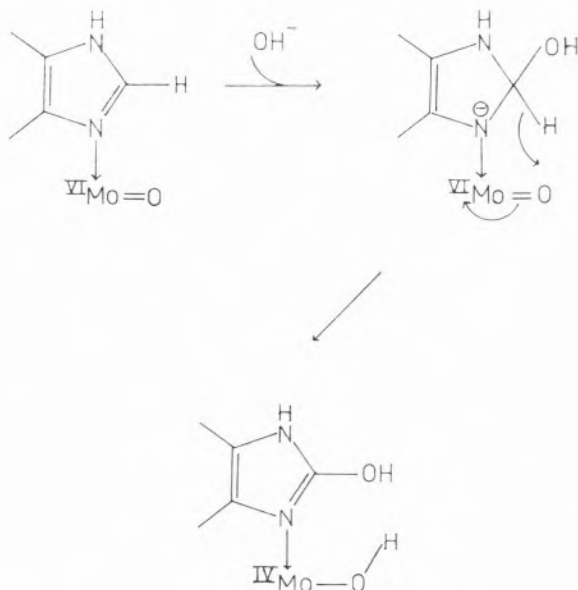
### METALLO-ENZYMIC CENTRES

The imine most often found coordinated to a metal ion at enzyme active sites is imidazole, almost always from the side-chain of an L-histidine residue of the apoprotein. Quaternized imidazoles are highly reactive toward nucleophiles in the now familiar sense, as shown (12  $\rightarrow$  13). This reactivity has been denied<sup>9</sup>, on the authority (sic) of an elementary textbook, but the facts are well known: organic reactivity like 12  $\rightarrow$  13 is established.

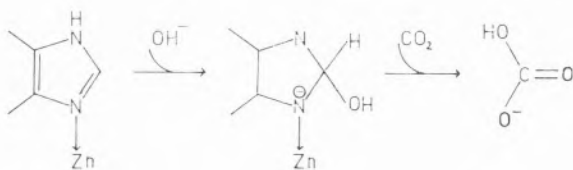


Occasionally, an imidazole is the natural substrate for a metallo-enzyme as in the molybdenum-enzyme xanthine oxidase, where the purine xanthine (a substituted imidazole) binds initially to molybdenum (VI) in the catalytic act. What does this do to the xanthine? From nuclear magnetic resonance work, Sawyer that «the  $\text{MoO}_2^{+2}$  group is nearly as effective as a proton at electron

withdrawing», so it will certainly polarise substrate xanthine, and the Scheme shown is feasible:



The suggestion, *mutatis mutandis*, is parallel to that above for the Cr(VI) oxidation of alcoholate ion by Sarett's reagent. The reducing agent in xanthine oxidase is the incipient hydride ion at the C(8) of the dihydro-imidazole ring of the purine. Any other purine coordinated to an activating metal ion may have nucleophilic addition to C(8), and interpretations of the recent studies of nucleotide and nucleoside binding to the cis-platin moiety may need to be revised in that light.



Finally, the perennial problem of the origin of the anomalous pK<sub>A</sub> (ca 7.0) of carbonic anhydrase has a possible solution which is novel. If one of the three coordinated imidazoles of the L-histidines surrounding the approximately tetrahedral zinc ion were to be attacked by hydroxide ion forming a

pseudo-base, then a bifunctional site for the activation of carbon dioxide would be provided.

## CONCLUSION

The present theory has been accessible for years, but requires certain adjustments in comfortable thinking:

- 1) If in water, a species diagram or property shows an apparent pK<sub>A</sub>, that may arise either from loss of H<sup>+</sup> or gain of OH<sup>-</sup>, but certainly one of the other.
- 2) A positive charge is a positive charge, whether it is the product of an experiment in an organic, inorganic biochemical or enzymology laboratory. Imposition of a positive charge, or reducing the electron density on nitrogen attached to carbon by a double (or aromatic) bond will give similar general effects on reactivity at that carbon.
- 3) The quantity of chemical knowledge is said to double every eight to ten years. We need generalizations which span organic and inorganic systems.

In any system, involving imine groups (whether in heterocyclic rings or not) and -metal ions, the increased likelihood (as in quaternary imines) of nucleophilic attack on some carbon atom of the imine offers opportunity for much new, exciting and useful chemistry.

(Received, 17th June 1985)

## REFERENCES

- [1] (a) R.D. GILLARD. *Coord. Chem Revs.*, **16**, 67, (1975).  
(b) *Idem, ibid*, **50**, 303 (1983).

- [2] D.G. LEE, «The oxidation of Organic Compounds by Permanganate Ion and Hexavalent Chromium» Open Court, LaSalle, Illinois 1980.
- [3] E. PIERS, and P.M. WORSTER, *Canadian J. Chem.*, **55**, 733 (1977).
- [4] F. ORTEGA, E. RODENAS, *Transition Metal Chem.*, **9**, 331 (1984).
- [5] N. SERPONE, G. PONTERINI, M.A. JAMIESON, F. BOLLETTA, M. MAESTRI and Y. TURCI *Coord. Chem. Revs.*, **50**, 209 (1983).
- [6] M. ABU SHARKH, M.Sc. Thesis, Univ. of Wales, 1985.
- [7] P. CARTWRIGHT, E.R.J. SILLANPAA, unpublished research in my laboratory, 1985.
- [8] S.H. MITCHELL, Ph. D. Thesis, Univ. of Wales, 1985.
- [9] D.A. HOUSE, P.R. NORMAN, R.W. Hay, *Inorg. Chim. Acta*, **45**, L117 (1980).

«Mecanismos de Pseudo-base em Química Orgânica, Química de Coordenação e Bioquímica».

Neste artigo apresenta-se, de forma resumida, uma comparação entre o efeito de quaternização (por grupos alquilo e outros) de átomos de azoto em iminas, incluindo N-heterociclos, e o efeito de coordenação a iões metálicos através dos mesmos átomos de azoto. Sugerem-se mecanismos baseados nesta visão dos iões metálicos como agentes de quaternização para sistemas orgânicos, incluindo o reagente de Sarett. Propõe-se, ainda, mecanismos análogos para sistemas enzimáticos, nomeadamente para a imidazola coordenada, quer na oxidase de xantina, quer na anidrase carbónica, onde o  $pK_a$  ( $\approx 7.0$ ) observado poderá ser devido à formação de pseudo-base pelo  $OH^-$  em imidazolas coordenadas a zinco, em vez de se atribuir a ionização de  $H^+$  de um grupo ácido.

DEREK PLETCHER

Department of Chemistry,  
The University,  
Southampton SO9 5NH,  
England



---

## RECENT DEVELOPMENTS IN ORGANIC ELECTROSYNTHESIS \*

*Electrolysis provides a procedure or synthesis both in the laboratory and on an industrial scale; a wide range of reactions have been reported and there have been considerable advances towards practical systems. In addition, electrochemical techniques for the study of synthetic reactions have developed considerably during the past decade and it is now possible to study intermediates with a half life below  $1\mu\text{s}$ . This paper reviews the reasons for organic chemists to take a stronger interest in electrochemistry.*

\* Plenary lecture at the 8th Annual Meeting of the Portuguese Chemical Society, Braga, April 1985.

Attempts to interest organic chemists in the practice of electrode reactions are not new. Indeed, many will be familiar with the contributions of Kolb  [1] in 1849 and Haber [2] in 1898, while industrial processes for the manufacture of organic compounds have probably existed throughout this century. Moreover several exhaustive texts [3-6] have described the extensive studies of organic electrochemistry. Yet electrochemists remain far from satisfied with the impact of their subject on organic synthesis and a theme of this review is the wish to persuade synthetic chemists that electrochemistry has much more to offer.

Following a brief discussion of the concepts which underlie modern organic electrochemistry, I would like to comment on three areas where organic chemistry and electrochemistry overlap. Namely:

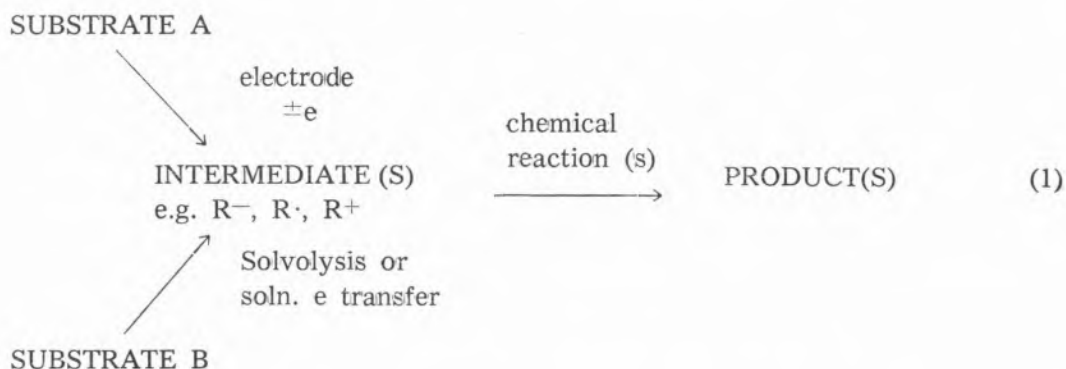
- i organic electrosynthesis in the laboratory,
- ii electrolysis for the manufacture of organic compounds,
- iii electrochemical techniques for the study of synthetic reactions.

Some will think that the distinction between laboratory and commercial scale synthesis is false. Certainly there are many objectives in common, e.g. to develop novel chemistry, to reduce the number of reaction steps, to use cheaper starting materials, to improve selectivity and to avoid hazardous reagents or unpleasant reaction conditions. On the other hand, at least at the present time, there are important differences with regard to the sophistication of the molecules which are investigated and the electrolysis conditions (e.g. solvent, current density) which are considered practicable. In the final section, my aim is to demonstrate that electrochemical techniques are rapidly becoming better matched to the challenges of studying systems of synthetic interest, e.g. with respect to our ability to study short lived intermediates, the

ease of carrying out experiments and the power of the methods to allow clear distinction between similar mechanisms.

## FUNDAMENTAL CONCEPTS OF ORGANIC ELECTROSYNTHESIS

An electrode acts as a source or sink of electrons and by controlling the potential of the electrode (either directly or by controlling



both current density and the concentration of electroactive species), it is possible to control both the thermodynamics and kinetics of electron transfer between the electrode and species in solution. This introduces considerable specificity and selectivity into electrode reactions but this statement should not be taken to mean that electro-syntheses generally give yields approaching 100%. It must be recognised that most electrode reactions take place in at least two steps (i) electron transfer at the electrode surface which converts the electroactive species into a reactive intermediate (ii) decay of the reactive product(s), in the electrolysis medium as the intermediate diffuses away from the surface into the bulk solution. The nature and rate of the reactions (possibly competing reactions leading to different products) of the intermediates will then depend on its chemistry and the selection of the electrolyte medium, not on the electrode potential. In other words the electrode potential will control only the first step in the

overall reaction sequence. Hence we should regard the electrode as generating reactive intermediates and the design of electro-syntheses requires us to control both the generation and reactions of the generation and reactions of the intermediates. Equally, however, the chemistry of the intermediates will depend only slightly on the method by which they are produced and we can therefore predict their behaviour from an understanding of homogeneous chemistry.

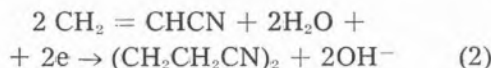
To give a specific example, the oxidation of naphthalene leads initially to its cation radical and the final product depends mainly on which species is the strongest nucleophile in the medium. Thus from electrolysis in acetic acid, methanol and a chloride medium, the major product would be 1-naphthyl acetate, 1-methoxynaphthalene and 1-chloronaphthalene respectively with perhaps side products e.g. oligomers from any cation radical-naphthalene reaction.

While there are many similarities between the behaviour of intermediates produced electrochemically and in homogeneous reactions, it is also necessary to recognise the possibilities for differences. Adsorption of the intermediates on the electrode surface can clearly lead to strong differences in behaviour but its role in electro-synthetic reactions can be over-emphasised; adsorption will be a large influence on some reactions but have little on most systems. More generally differences arise because

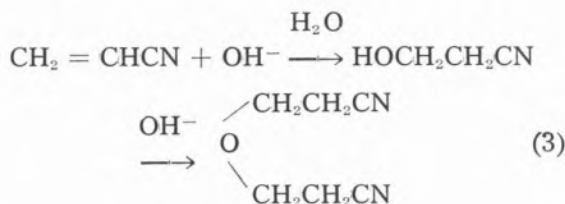


the intermediates are formed on a surface and decay to products completely within a reaction layer very close to the electrode surface (typically this reaction layer has a thickness around 1  $\mu\text{m}$  although this will depend on the kinetics of the chemical reactions). As a result the intermediates react in a region of space where their concentrations are non-uniform, high at the electrode surface and zero outside the reaction layer. Moreover the reaction layer may be atypical of the bulk solution in other ways e.g. pH. This type of difficulty is well illustrated by the Monsanto process [7-9] for the hydrodimerisation of acrylonitrile to adiponitrile.

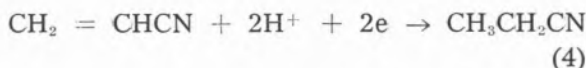
The desired reaction



generates base and if the pH of the reaction layer is not controlled, the side reaction

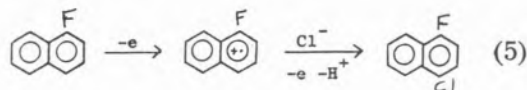


is soon observed. If an acid solution is used, the wrong product predominates



Indeed the only satisfactory way to avoid one of these side reactions is to use a neutral medium but a highly turbulent flow regime so that the  $\text{OH}^-$  is rapidly dispersed into the bulk solution. On the other hand, the fact that the chemical change occurs within a reaction layer can also be turned to advantage. In homogeneous reactions the oxidation (or reduction) of a mixture of two substrates inevitably occurs via oxidation of the most easily oxidised species. This need not be the

case in an electrode processes. For example in  $\text{CH}_2\text{Cl}_2$ ,  $\text{Cl}^-$  oxidises at about +1.2V and 1-fluoronaphthalene at only +1.95V but anodic oxidation of a mixture of the two can occur via the pathway [10]



because of principle of flux balancing [11]. Figure 1 shows the way in which the concentrations of the various species varies with

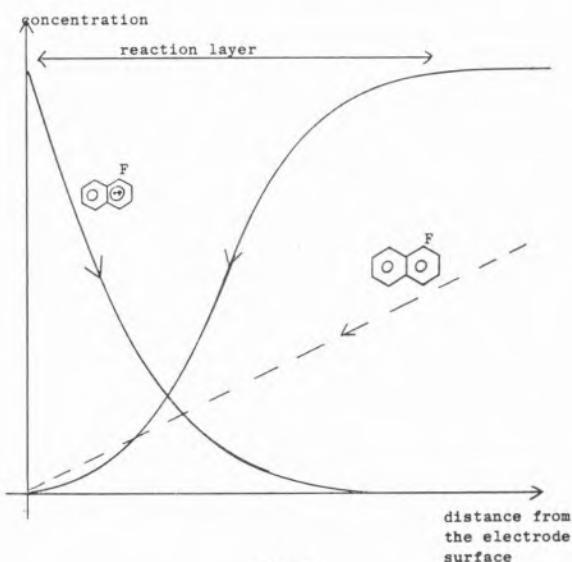


Fig. 1

The principle of flux balancing using the example of the chlorination of fluoronaphthalene. The critical factor is that the cation radical leaving the surface mops up the incoming  $\text{Cl}^-$ , leaving a layer close to the surface where  $C_{\text{Cl}^-} = 0$ .

distance from the electrode surface within the reaction layer. For the electrode reaction to proceed by the pathway indicated by equation (5) the essential feature is that the chloride ion diffusing to the surface reacts with cation radical diffusing in the opposite direction before it can reach the electrode. In fact, the reaction pathway is determined by the relative kinetics of the  $\text{Cl}_2/\text{naphthalene}$  and the  $\text{Cl}^-/\text{cation radical}$  reactions; here the latter is faster by a

factor  $> 10^{10}$  and equation (5) is very much the preferred route. The principle of flux balancing only requires careful selection of

trode potential and without recourse to otherwise forcing conditions. This is illustrated in figure 2 which compares the potential range

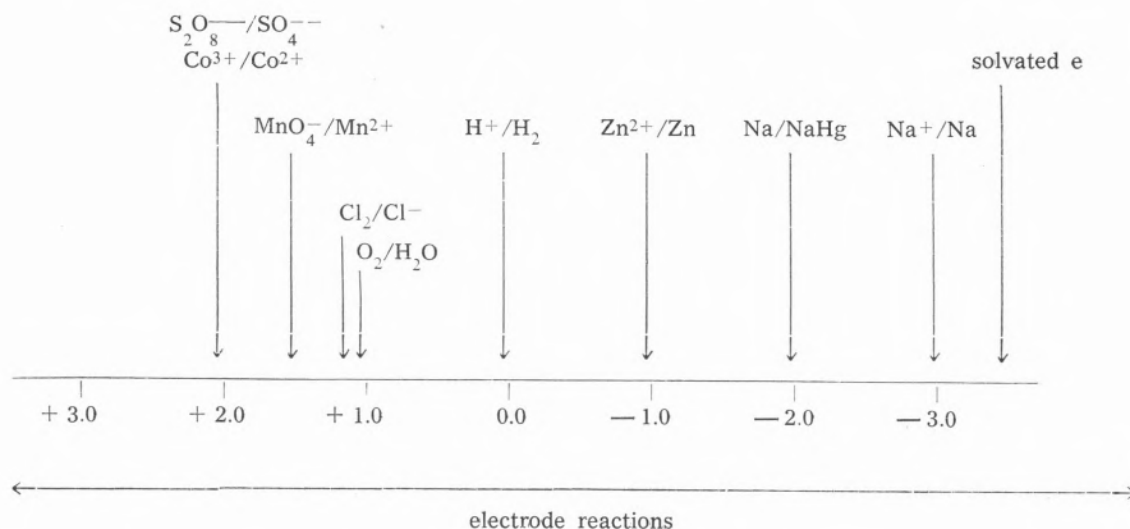
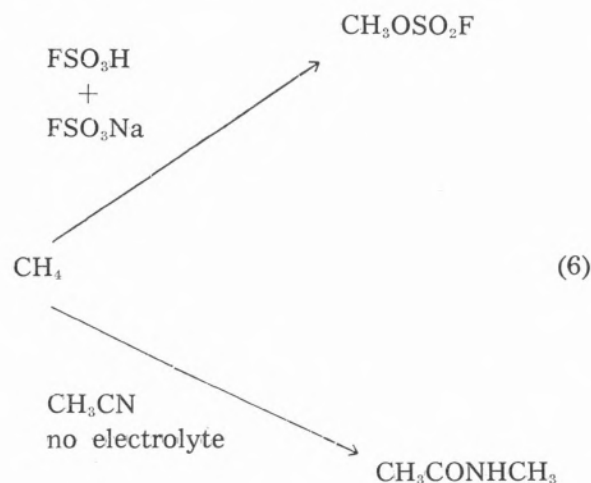


Fig. 2

Comparison of electrode reactions with redox reagents on the basis of the potential or driving force available for oxidation/reduction.

reactant concentrations and extends considerably the range and variety of syntheses which are possible.



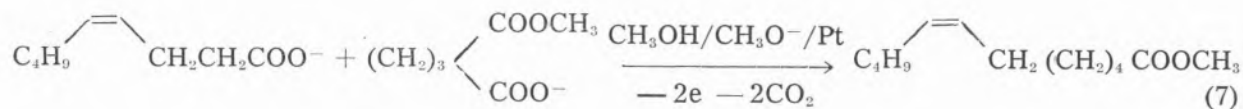
An attractive feature of electrode reactions is that difficult oxidations and reductions are readily carried out by selecting the elec-

trode potential and without recourse to otherwise forcing conditions. This is illustrated in figure 2 which compares the potential range available for electrochemistry with the standard potentials for common redox reagents. As a result the oxidation of methane presents no difficulties provided the electrolysis medium is stable to the conditions, i.e. a very positive potential. The products depend on the solvent [12,13] e.g.

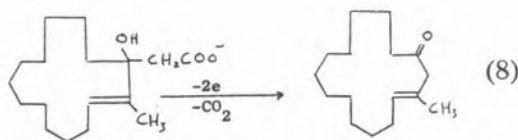
#### SYNTHESIS IN THE LABORATORY

In the organic laboratory, the emphasis is very much on the elegant synthesis of large molecules with selectivity to the desired stereochemistry. Perhaps it is significant that many of the nicest examples are based on an electrode reaction known to all organic chemists, i.e. the Kolbe reaction. This reaction allows large molecules to be synthesised by joining together two dissimilar units, an idea which has been exploited in the

synthesis of the pheromone, looplure [14]. The electrochemical step is



A mixture of the three radical-radical coupling products must be formed but control of the ratio of reactant concentrations can lead to a yield of desired product of 60% (based on the expensive half unit). The oxidation of  $\alpha,\beta$ -dicarboxylic acids is a convenient way of introducing olefinic bonds into large molecules [15,16]. Under modified electrolysis conditions, the oxidation of carboxylic acids occurs by a 2e process to give a carbonium ion. Such reactions provide facile routes to displacing carboxylic acid groups by methoxy or ester groups and rearranged carbon skeletons can result from carbenium ion rearrangements, e.g. [17]



Pattenden has investigated the use of cathodically generated radicals for the synthesis of bicyclic compound following intramolecular reaction. A favoured reaction is the reduction of terminal allenic ketones [18]

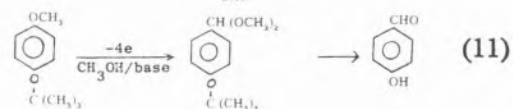
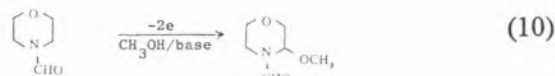


which occurs to give the desired stereochemistry in good yields.

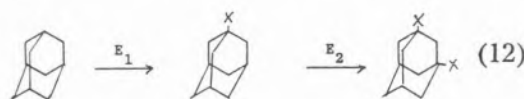
Another modern concept that of the synthon, a key molecule readily synthesised and suitable for a wide range of reactions. Anodic methoxylation is a reaction which can go in very high yields and has been used to pro-

duce such intermediates. To quote two examples, the methoxylation of amides [6,19]

and the production of p-hydroxybenzaldehyde [20]



The ability to control the electrode potential also allows us to control the extent of oxidation. This can be useful, for example, in the anodic substitution of adamantane [21] when it is possible to obtain mono (yield 80%) or disubstitution (yield 55%)



where X = —OH if the electrolysis is carried out in trifluoroacetic acid and X = —NH—COCH<sub>3</sub> if the solvent is acetonitrile.

Another recent trend in the laboratory results from the realisation that electrolyses are possible in a much wider range of media than earlier thought, provided the cell is designed appropriately. One example of an electrolysis in acetonitrile without electrolyte is mentioned above, equation (6). Another example would be the synthesis of lithium alkyl intermediates, a reaction carried out in ether [22].

## INDUSTRIAL SCALE ELECTROSYNTHESIS

A very large number (probably > 10<sup>5</sup>) organic compounds are manufactured each year

(see Aldrich, Kodak, Fluka or Merck catalogues!) but the scale of production will vary between a few kilograms and  $10^7$  tons and the value will likewise vary from a few cents to many dollars per kilogram. Moreover the security of the markets will be totally dissimilar. In such circumstances any generalisations about the economics of processes are difficult. In the case of electroorganic processes, it must also be noted that the electrolysis is only one of several steps between starting material and pure, isolated product.

Even so, it is interesting to consider the factors which influence the success of electrolytic processes. Some of the important factors are shown in table 1. This table has

Table 1

*Factors likely to determine the success of an electrolytic process*

- 
1. Do competing processes present hazards or a pollution problem?
  2. Material yield
  3. Product quality — do any trace impurities cause problems in the use of the product?
  4. Energy consumption — cell voltage  
— current efficiency
  5. Space-time yield — current density  
effective electrode area/unit  
volume cell
  6. Ease of product recovery
  7. Stable electrolysis medium
  8. Cost and lifetime of cell
  9. Patent situation
  10. Market possibilities for the product
  11. Can other compounds be manufactured using the same technology?
- 

many similarities with such a list compiled for any type of technology. Three factors, energy consumption, space time yield and

cell design have features peculiar to electrolytic processes and should therefore perhaps be discussed further.

The energy consumption may be calculated from the equation

$$\text{Energy consumption} = \frac{nFV}{3.6 \times 10^4 \phi M} \text{ (kWh kg}^{-1}\text{)} \quad (13)$$

where  $nF$  is the number of Faradays required to form one mole of product,  $V$  is the cell voltage,  $\phi$  (%) is the current efficiency for product formation and  $M$  the molecular weight of the product (kg). Essentially this equation confirms that we should seek to minimise the cell voltage and maximise the current efficiency. The cell voltage depends on three factors (i) the free energy associated with the overall chemical change in the cell, (ii) the overpotentials  $\eta$ , necessary at the anode and cathode to increase the rate of electron transfer to the required current density and (iii) the energy required to drive the current,  $i$ , through the cell, resistance,  $R$ , i.e.

$$V = -\frac{nF}{\Delta G} - |\eta_A| - |\eta_C| - iR \quad (14)$$

Commonly in organic processes it is the last term which predominates. Hence the desire for a highly conducting medium and to design cells where the interelectrode gap is small.

The space-time yield of the cell depends on the current density and the effective electrode area which can be packed into the cell volume. The former is proportional to the concentration of electro-active species and is also a strong function of the mass transport conditions in the cell. The electrode is only able to have a uniform current density if it is an equipotential surface and this requires that all points on the surface of the electrode are geometrically equivalent with respect to the other electrode. The current density at non-equivalent points on the surface will be lower and may be vanishingly

small, contributing little to the yield of product. An acceptable space-time yield generally requires a current density of at least  $0.1 \text{ A cm}^{-2}$  and hence a concentration of electroactive species of 1 — 10 %, a high solubility. Indeed, much of the literature of organic electrochemistry cannot be considered as synthesis because of the impossibility of reaching such current densities.

Cell design has already been mentioned. It has been noted that the electrodes should be close together and the surfaces should be geometrically equivalent with respect to each other. In addition it is clear that separators should be avoided whenever possible since they will increase cell resistance and it is also helpful to combine other unit operations (e.g. product extraction) into the cell. Clearly cell design is complex but many designs have

been described and may even be available commercially [22,23].

Detailed discussion of cell design is well beyond the scope of this review but I would like to illustrate the advantage to be gained from good engineering — i.e. good cell design and integrating the cell into the total process. The first Monsanto process for the hydrodimerisation of acrylonitrile to adiponitrile was introduced in 1964. Following a decade of R and D, the mark 2 process became available [9,24,25]. The processes are compared in table 2 and the new process may be considered an improvement in terms of energy efficiency, cell costs, simplicity of product extraction and running costs.

Several lists of commercial electroorganic processes have been published [3, 9, 26, 27] and it suffices to comment here that they

Table 2

Comparison of the 1964 and Mark Monsanto Processes for the hydrodimerisation of acrylonitrile to adiponitrile

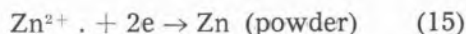
	Early Monsanto Process	Recent Monsanto Process
Cell type	Plate and frame cell with membrane in filter press	Undivided bipolar attack of plates
Cathode	Pb	Cd
Anode	$\text{PbO}_2$ (+ 1 % AgO)	Steel
Separator	Ionics CR 61	None
Electrode gap (mm)	7.1	1.8
Catholyte	$\text{Et}_4 \text{N}^+ \text{EstSO}_4^-$ (40%) $\text{H}_2\text{O}$ (15%) $\text{CH}_2 = \text{CHCN} + (\text{CH}_2\text{CH}_2\text{CN})_2$ (50%)	$\text{EtBu}_2 \text{N}^+(\text{CH}_2)_6 \text{N}^+\text{Bu}_2\text{Et HPO}_4^-$ (0.4 %) $\text{Na}_2\text{HPO}_4$ (10 %) $\text{Na}_2\text{B}_4\text{O}_7$ (2 %) $\text{Na}_4\text{EDTA}$ (0.5 %) Sat. $\text{CH}_2 = \text{CHCN}$ all in $\text{H}_2\text{O}$ / excess $\text{CH}_2 = \text{CHCN}$ as second phase as catholyte
Anolyte	$\text{H}_2\text{SO}_4$ (1M)	
Temperature ( $^\circ\text{C}$ )	50	55
Catholyte velocity ( $\text{m s}^{-1}$ )	2	1 — 1.5
Catholyte resistivity (ohm cm)	38	12
Current density ( $\text{A m}^{-2}$ )	4500	2000
Voltage distribution (V)		
Estimated reversible cell voltage	2.50	2.50
Overpotentials	1.22	0.87
Electrolyte IR	6.24	0.47
Membrane IR	1.69	—
Cell voltage (V)	11.65	3.84
Energy consumption (kWh/lb)	3.0	1.1



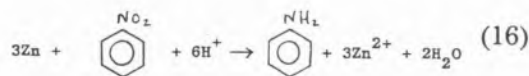
represent a wide range of chemistry (e.g. hydrogenation, epoxidation, substitution, indirect oxidation, functional group oxidation/reduction, hydrodimerisation) and have been successful where the scientist has found it possible to match the chemistry, cell technology and company needs.

Finally, before leaving this section, I would emphasise strongly the need to recognise the technological limitations early in a chemical research programme if the goal is a commercial process. Such thinking has led my group to investigate multiphase electrolysis where the electrolysis medium is an emulsion of an aqueous phase and an immiscible organic solvent. Advantages of such techniques include, (i) they provide a feasible way to apply in industry the many reactions described using aprotic media in the literature, (ii) by continuous extraction of the product into the organic solvent, its isolation can be greatly simplified, (iii) very high current densities can be achieved because it is possible to decouple the link between maximum current density and solubility of the organic compound, (iv) it is possible to design the system so that the working electrode reaction occurs in an organic medium and the counter electrode is simply water electrolysis without recourse to a separator (v) the cell voltage can be greatly reduced by the aqueous phase in most of the inter-electrode gap., (vi) the aqueous solution may be used to buffer the organic medium minimising acid or base catalysed reactions which reduce selectivity in many aprotic electrolyses. To give three illustrations of multiphase electrolysis

- (a) It is possible [28] to reduce nitrobenzene with a current of  $1 \text{ A cm}^{-2}$  by electrolysis an emulsion of nitrobenzene and an aqueous,  $0.4 \text{ M ZnCl}_2 + 1 \text{ M HCl}$ . The cathode reaction is

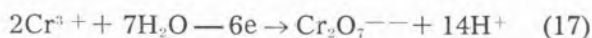


and the high area, oxide free surface, zinc powder then reacts rapidly

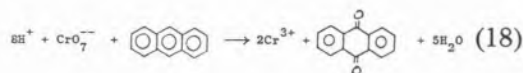


This reaction is quite general for substituted nitrobenzenes and the current density is many orders higher than that achieved in direct reductions.

- (b) The corresponding oxidation reactions employ the anodic generation of an oxidising agent in an aqueous phase. If the oxidising agent is an anion, e.g. hypobromite or dichromate, a possible route to carrying out reactions in the organic medium is to employ phase transfer catalysis. For example [29], the anode reaction in  $\text{H}_2\text{SO}_4/\text{H}_2\text{O}$



can be coupled to the oxidation



in  $\text{C}_2\text{H}_4\text{Cl}_2$  by adding a phase transfer agent e.g.  $\text{Bu}_4\text{N}^+$ .

- (c) The anodic substitution of aromatic hydrocarbons by electrolysis of an emulsion of the substrate in methylene chloride and the nucleophile and a phase transfer catalyst in water. For example, the cyanation [30], chlorination [31] and acyloxylation [32] of naphthalene have all been reported in good yields. The oxidation of the hydrocarbon occurs in a film of  $\text{CH}_2\text{Cl}_2$  on the anode surface while the organic solvent in the emulsion exchanges substrate and product with the film and the aqueous solution acts as a source of nucleophile, to extract proton and as a low resistance path to the cathode.



shows the wide range of half lives which it is now possible to study. Of course, most interest centres on the short-lived intermediates since these are the ones most commonly of interest in synthesis.

(Received, 4th June 1985)

## REFERENCES

- [1] H. KOLBE, *Ann. Chem.*, **69**, 257 (1849).
- [2] F. HABER, *Z. Electrochem.*, **4**, 506, (1898).
- [3] «Organic Electrochemistry», Eds M.M. Baizer and H. Lund, Marcel Dekker, 1983.
- [4] «Techniques of Electroorganic Synthesis» Ed. N.L. Weinberg, Wiley Interscience, 1974.
- [5] F. BECK, «Elektroorganische Chemie», Verlag Chemie, Weinheim, 1974.
- [6] T. SHONO, «Electroorganic Chemistry as a New Tool in Organic Synthesis», Springer Verlag, Berlin, 1984.
- [7] M.M. BAIZER, *J. Electrochem. Soc.*, **111**, 215 (1965).
- [8] Chapters by M.M. Baizer and D.E. Danley in ref. 3.
- [9] D. PLETCHER, «Industrial Electrochemistry», Chapman and Hall Ltd., 1982.
- [10] S.S. FORSYTH, D. PLETCHER, unpublished work.
- [11] G. FAITA, M. FLEISCHMANN, D. PLETCHER, *J. Electroanal. Chem.*, **25**, 455 (1970).
- [12] D. PLETCHER, C.Z. SMITH, *Chem. Ind.*, 371 (1976).
- [13] S.B. PONS, unpublished work.
- [14] W. SEIDEL, J. KNOLLE, H.J. SCHAFER, *Chem. Ber.*, **110**, 3544 (1977).
- [15] M.H. WESTBERG, H. DAUBEN, *Tet. Letters*, 5123 (1968).
- [16] K.R. KOPECKY, M-P LAU, *J. Org. Chem.*, **43**, 525 (1978).
- [17] T. SHONO, J. HAYASHI, H. OMOTO, Y. MATSUMURA, *J. Org. Chem.*, **44**, 2303 (1979).
- [18] G. PATTENDEN and G.M. ROBERTSON, *Tet. Letters*, 4617 (1983).
- [19] K. NYBERG, R. SERVIN, *Acta Chem. Scand.* B**33**, 640 (1979).
- [20] D. Degner, RSC Meeting «Electroorganic Synthesis», Wrexham, 1982.
- [21] A. BEWICK, G.J. EDWARDS, J.M. MELLOR, S.R. JONES, *Tet. Letters*, 631 (1976).
- [22] F.C. WALCH, R.J. MARSHALL, *Surface Technol.*, **24**, 45 (1985).
- [23] R.E.W. JANSSON, *Phil. Trans. R. Soc. London*, A**302**, 285 (1981).
- [24] D.E. DANLY, *Hydrocarbon Processing*, 161 (1981).
- [25] D.E. DANLY, *J. Electrochem. Soc.*, **131**, 435C (1984).
- [26] R.E.W. JANSSON, *C and E News* Nov. 43 (1984).
- [27] M.M. BAIZER, *J. Applied Electrochem.*, **10**, 285 (1980).
- [28] N.E. GUNAWARDENA, D. PLETCHER, *Acta Chem. Scand.*, B**37**, 549 (1983).
- [29] L-C JIANG, D. PLETCHER, *J. Electroanal. Chem.*, **152**, 157 (1983).
- [30] L. EBERSON, B. HELGEE, *Chem. Scripta*, **5**, 47 (1974).
- [31] S.R. ELLIS, D. PLETCHER, W.N. BROOKS, K.P. HEALY, *J. Applied Electrochem.*, **13**, 735 (1983).
- [32] S.R. ELLIS, D. PLETCHER, P.H. GAMLEN, K.P. HEALY, *J. Applied Electrochem.*, **12**, 693 (1982).
- [33] A.J. BARD, L.R. FAULKNER, «Electrochemical «Methods» John Wiley and Sons, 1980.
- [34] «Laboratory Techniques in Electroanalytical Chemistry», Eds. P.T. Kissinger and W.R. Heineman, Marcel Dekker, 1984.
- [35] R. GREEF, R. PEAT, L.M. PETER, D. PLETCHER, J. ROBINSON, «Instrumental Methods in Electrochemistry», Ellis Horwood Ltd., 1985.
- [36] J. ROBINSON in «Specialist Periodical Reports in Electrochemistry» Royal Society of Chemistry, **9**, 101 (1984).
- [37] A. BEWICK, J.M. MELLOR, B.S. PONS, *Electrochim. Acta*, **25**, 931 (1980).
- [38] R.M. WIGHTMAN, *Anal. Chem.*, **53**, 1125A (1981).
- [39] M.I. MONTENEGRO, *Port. Electrochim. Acta*, in press.
- [40] J.O. HOWELL, R.M. WIGHTMAN, *Anal. Chem.*, **56**, 524 (1984).

### Progressos em electrossíntese.

A electrólise pode constituir um processo de síntese quer à escala laboratorial quer à escala industrial. Existem publicados grande número de reacções usadas em electrossíntese e tem sido feitos progressos significativos em sistemas de utilidade prática. Simultaneamente as técnicas electroquímicas usadas no estudo de reacções de síntese desenvolveram-se bastante durante a última década o que tornou possível o estudo de intermediários com tempo de vida inferior a  $\mu$ s. Este artigo revê as razões para que um químico orgânico se interesse mais profundamente pela Electroquímica.

NOSRAT M. ABED  
 NADIA S. IBRAHIM  
 SUZAN I. AZIZ

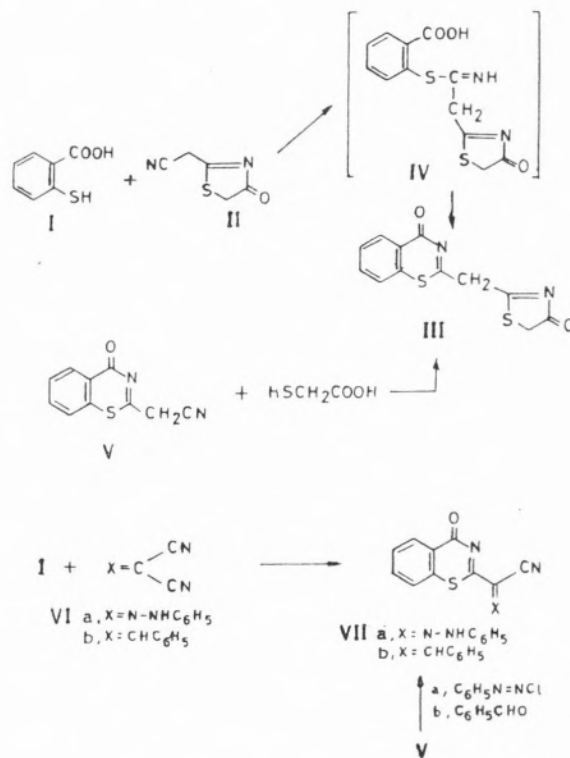
Chemistry Department,  
 Faculty of Science,  
 Cairo University,  
 Giza, A. R. Egypt.



## NITRILES IN HETEROCYCLIC SYNTHESIS: A ROUTE FOR SYNTHESIS OF FUNCTIONALLY SUBSTITUTED THIAZINONES

The reaction of thiosalicylic acid with a variety of activated nitriles is described. Several new benzo [e]-1,3-thiazinones are reported.

As a part of our program aiming to develop new procedures for synthesis of azoles and azines utilising simple inexpensive starting materials, we have recently reported a novel synthesis of 2-thiazin-4-ones via reaction of thiosalicylic acid [1] with malononitrile and with ethylcyanoacetate [1]. Now, in order to define the scope and limitation of this approach for thiazin-4-one synthesis, the behaviour of a variety of activated nitriles toward I was investigated.



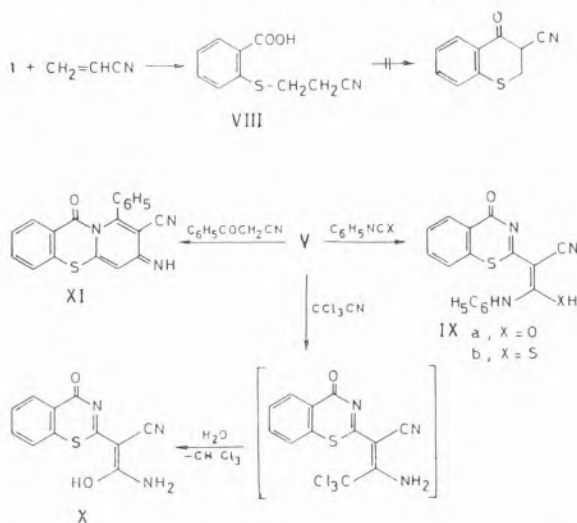
Thus, it has been found that I reacts with 2-cyanomethyl-2-thiazolin-4-one (II) recently prepared by Elnagdi et al. [2] to yield a product of molecular formula C<sub>12</sub>H<sub>8</sub>N<sub>2</sub>O<sub>2</sub>S<sub>2</sub>. The IR spectrum of the product revealed the absence of CN absorption. The thiazine structure III was established for the reaction product by its synthesis via the reaction of 2-cyanomethylbenzo[e]-1,3-thiazine-4-one (V) with thioglycolic acid. Compound III was assumed to be formed through the intermediate IV. Similar to the behaviour of I with II, the malononitrile derivatives VIa,b reacted with I to yield the thiazinones VII,a,b. The struc-



ture of which was established also via synthesis of the reaction products from the reaction of V with benzene diazonium chloride and with benzaldehyde respectively.

The reaction of I with acrylonitrile under our experimental conditions was also investigated. Similar to previous literature [3], the reaction afforded the cyanoethylated product VIII. Attempted cyclization of VIII under a variety of conditions failed to afford the desired product.

The thiazinone derivatives IXa,b, and X were prepared via reaction of V with phenylisocyanate, phenylisothiocyanate, and with trichloroacetonitrile as trials of direct synthesis of these derivatives from the reaction of I with the appropriate activated nitrile failed to afford the desired products.



Fusion on V with benzoylacetonitrile at 160°C for 1 h. yielded 2-cyano-3-imino-1-phenylpyrido [2,1-b] benzthiazin-10-one XI.

#### Experimental Section:

All melting points are uncorrected. IR spectra were recorded on a Beckman spectrophotometer, <sup>1</sup>H NMR on Varian EM-390—90 MHz spectrometer. The microanalyses were performed by the microanalytical unit at Cairo University. Reaction of active nitriles with thiosalicylic acid (General procedure):

Thiosalicylic acid (0.01 mol) was refluxed with 0.01 mol of the appropriate nitrile (II; VIa,b; and acrylonitrile) in 20 cm<sup>3</sup> of pyridine for 2 h. The reaction mixture was triturated with ice-cold water and the solid product, so formed, was collected by filtration and crystallized from the proper solvent. (cf. table 1).

Reactions of 2-cyanomethylbenzo [e] 1,3-thiazin-4-one (V) with:

#### a) Thioglycollic acid :

Equimolecular amounts of compound V (0.01 mol) and thioglycollic acid (0.01 mol) were refluxed in 20 cm<sup>3</sup> pyridine for 2 h. The reaction mixture was poured on ice-cold water and the resulting solid product (2 g, 72 %) was identified as compound III (m.p. and mixed m.p. 252°C).

#### b) Benzenediazonium chloride :

An ice-cold solution of diazotized aniline (0.01 mol) was added to an ethanolic solution of V (0.01 mol) in the presence of sodium acetate (0.01 mol). The solid product so formed was collected by filtration, washed with water and crystallized from the proper solvent as compound VIIa (m.p. and mixed m.p.) 222°C, yield 72 %.

#### c) Benzaldehyde :

Benzaldehyde (0.01 mol) was heated with V at 160°C (bath T) for 1 h. the product, so formed, was collected and crystallized from the proper solvent as compound VIIb (m.p. and mixed m.p.) 245°C; yield 62 %.

#### d) Phenylisocyanate and phenyl isothiocyanate :

Compound V (0.01 mol) was heated with either phenylisocyanate (0.01 mol) or pheny-



Table 1

Compound	Solvent	M.P./°C	Yield (%)	Mol. Formula (mol. wt.)	Analysis Formed/(Calcd.)		
					% C	% H	% N
III	Acetic acid	252	65	C <sub>12</sub> H <sub>8</sub> N <sub>2</sub> O <sub>2</sub> S <sub>2</sub> 276	52.5 (52.17)	2.60 (2.89)	10.50 (10.14)
VII a	Ethanol	222	70	C <sub>16</sub> H <sub>10</sub> N <sub>4</sub> OS 306	62.56 (62.74)	3.00 (3.26)	18.50 (18.30)
VII b	Acetic acid	245	60	C <sub>17</sub> H <sub>10</sub> N <sub>2</sub> OS 290	70.60 (70.34)	3.10 (3.44)	9.90 (9.65)
VIII	Ethanol	180	80	C <sub>10</sub> H <sub>9</sub> NO <sub>2</sub> S 207	58.30 (57.97)	4.20 (4.34)	6.80 (6.76)
IX a	Acetic acid	250	70	C <sub>17</sub> H <sub>11</sub> N <sub>3</sub> O <sub>2</sub> S 321	63.80 (63.55)	3.20 (3.42)	13.30 (13.08)
IX b	Ethanol	260	75	C <sub>17</sub> H <sub>11</sub> N <sub>3</sub> OS <sub>2</sub> 337	60.10 (60.53)	3.00 (3.26)	12.50 (12.46)
X	Ethanol	230	60	C <sub>11</sub> H <sub>7</sub> N <sub>3</sub> O <sub>2</sub> S 245	53.80 (53.87)	2.40 (2.85)	17.00 (17.14)
XI	Acetic acid	225	70	C <sub>19</sub> H <sub>11</sub> N <sub>3</sub> OS 329	69.00 (69.30)	3.50 (3.34)	12.80 (12.76)

Table 2

Compound	IR/cm <sup>-1</sup>	<sup>1</sup> H NMR/ppm.
III	1730 1690 (two ring C=O); 1640, 1630 (two C=N).	3.25 (q, 2H, CH <sub>2</sub> ); 4.15 (q, 2H, CH <sub>2</sub> ); 7.3-7.8 (m, 4H, aromatic protons).
VII a	3200 (NH); 2200 (CN); 1680 (ring C=O); 1640 (C=N).	7.2 -8O (m, 9H, aromatic protons); 8.25 (d, 1H, NH).
VII b	2190 (CN); 1700 (ring C=O) 1660 (C=N).	
VIII	2220 (CN); 1700 (acid C=O).	2.9 (t, 2H, CH <sub>2</sub> ); 3.25 (t, 2H, CH <sub>2</sub> ); 4.8 (s, br, 1H, CO <sub>2</sub> H); 7.16 — 7.9 (m, 4H, aromatic protons).
IX a	3360 (NH); 2210 (CN); 1720 (exocyclic C=O); 1690 (ring C=O); 1640 (C=N)	3.45 (s, 1H, CH); 7.5-7.8 (m, 9H, aromatic protons); 8.45 (s, br, 1H, NH).
IX b	3330 (NH); 2200 (CN); 1690 (ring C=O); 1650 (C=N); 1550 (C=S).	
X	3600 (OH); 3320 (NH <sub>2</sub> ); 2200 (CN); 1690 (ring C=O); 1640 (C=N).	
XI	3350 (br. NH); 2200 (CN) and 1690 (CO).	7.9 (m, 9, phenyl protons + methine proton + 3 of phenylene proton); 8.5 (m, 2, NH + the phenylene proton near the carbonyl group).

isothiocyanate (0.01 mol) at 160°C (bath T) for 1 h. The solid product, so formed, was crystallized from the proper solvent (cf. Table 1).

e) *Trichloroacetonitrile* :

Compound V (0.01 mol) was refluxed with trichloro-acetonitrile (0.01 mol) in toluene (30 cm<sup>3</sup>) in the presence of 0.1 cm<sup>3</sup> of triethylamine for 3 h. The reaction mixture was poured on ice-cold water. The solid product was collected by filtration and crystallized from the proper solvent (cf. Table 1).

f) *Benzoylacetonitrile* :

Compound V (0.01 mol) was heated with benzoylacetonitrile (0.01 mol) at 160°C (bath T) for 1 h. The solid product, so for-

med, was crystallized from the proper solvent (cf. Table 1).

(Received, 5th February 1985)

#### REFERENCES

- [1] N.S. IBRAHIM; N.M., ABED, Z.E. KANDEEL *Heterocycles*, **22**, 1677 (1984).
- [2] M.H. ELNAGDI, M.R.H. ELMOGHAYAR A.E.G., HAMMAM and S.A. KHALLAF *J. Heterocycl. Chem.*, **16**, 1541 (1979).
- [3] H.A. BRUSON, «Cyanoethylation In Organic Reactions», Ed. by Adams, R. Academic Press, New York 1952, V, 79.

#### RESUMO

«Nitrilos em síntese heterocíclica: uma via para a síntese de tiazinonas funcionalmente substituídas.»

*Descrevem-se as reações do ácido tiosalicílico com uma série de nitrilos activados. Descrevem-se pela primeira vez várias benzo[e]-1,3-tiazinonas.*



## NÚMEROS DE TRANSFERÊNCIA DO SULFATO DE ZINCO EM ÁGUA A 25° C

*Foram feitas determinações dos números de transferência catiónicos e aniónicos do sulfato de zinco em água a 25°C às concentrações 0,01 0,025 e 0,069 M pelo método directo da fronteira móvel. Os valores limites dos números de transferência catiónicos,  $T_+$ , foram calculados usando as várias equações de Fuoss-Onsager e Pitts e comparados com os obtidos a partir dos resultados de transferência de Dye e colaboradores e com dados de condutância da literatura. Um teste destas equações teóricas estendido a soluções aquosas de sulfato de cobre, usando números de transferência colhidos na literatura, mostra que tal como sucede com o sulfato de magnésio previamente estudado, também para aqueles dois electrólitos, as teorias de Fuoss-Onsager fornecem um melhor ajuste dos dados experimentais que a teoria de Pitts.*

## 1 — INTRODUÇÃO

Numerosas determinações de números de transferência têm sido efectuadas para electrólitos 1:1, tendo os resultados obtidos sido recentemente utilizados para comparar as diversas teorias interiónicas [1].

O ajuste dos resultados experimentais aqueles modelos teóricos apresenta-se mais crítico para o caso dos electrólitos 2:2, embora para estes a informação experimental seja muito escassa.

Soluções aquosas de sulfato de cobre foram investigadas por Fritz e Fuget [2] com determinações dos números de transferências aniónicos pelo método da fronteira móvel. Contudo, além da ausência de valores para os números de transferência catiónicos, a precisão das determinações aniónicas é estimada pelos autores em apenas  $\pm 0,001$ .

Um estudo bastante rigoroso foi o efectuado recentemente em soluções aquosas de sulfato de magnésio por Lima et al [3] com determinações dos números de transferência aniónicos e catiónicos pelo método da fronteira móvel.

Um estudo prévio dos números de transferência catiónicos do sulfato de zinco em água foi realizado por Dye e colaboradores [4]. Embora as determinações tenham sido efectuadas pelo método da fronteira móvel, os autores apenas estudaram fronteiras catiónicas, ignorando assim uma regra fundamental para trabalho de precisão. Não deveria ter havido qualquer dificuldade em encontrar um anião indicador conveniente como iodato ou benzenossulfonato (ambos usados no presente trabalho) ou mesmo oxalato para seguir a fronteira aniónica. A independência dos números de transferência com a concentração da solução indicadora e com a corrente eléctrica também não foi devidamente verificada para todas as concentrações estudadas. Aparentemente Dye e colaboradores variaram a corrente em apenas 10-20 %, o que poderia ter concluído uma pequena variação com a corrente produzida por efeito de Joule.

Decidimos por isso efectuar um estado mais preciso do sulfato de zinco com determinações aniónicas e catiónicas de modo a dispormos de dados de números de transferência que nos permitissem testar adequadamente as várias teorias inter-iónicas para electrólitos 2:2.

## 2 — EXPERIMENTAL

### 2.1 — EQUIPAMENTO

As células de fronteira móvel usadas no presente trabalho são do tipo ascendente e descendente, feitas de vidro Pyrex com tor-

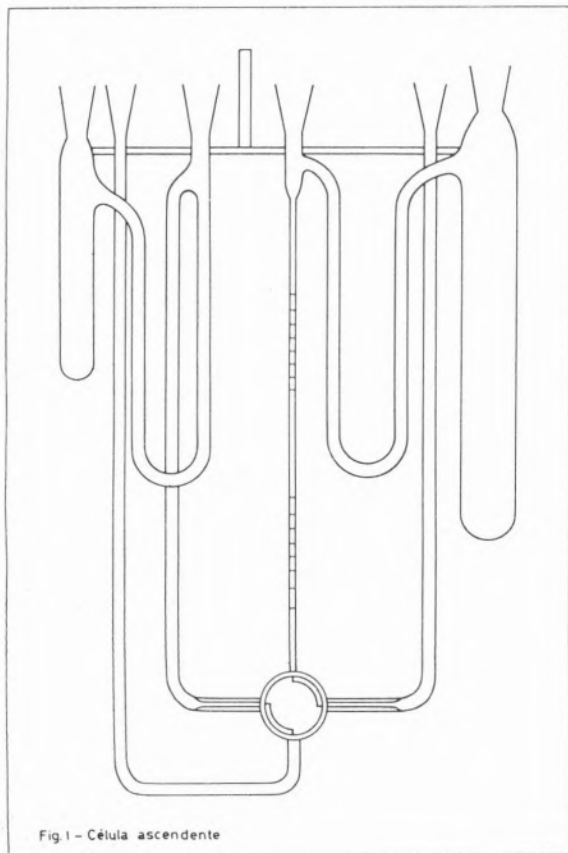


Fig. 1 - Célula ascendente

neiras de quatro vias em teflon. As figuras 1 e 2 ilustram ambos os tipos de células. As torneiras têm duas ranhuras cavadas na parte exterior do teflon de modo a permitir que as soluções fiquem em contacto directo

com o encaixe de vidro, onde são arrefecidas por um banho termostático. A vantagem das torneiras de teflon é a de dispensarem o uso de qualquer lubrificante, embora o arre-

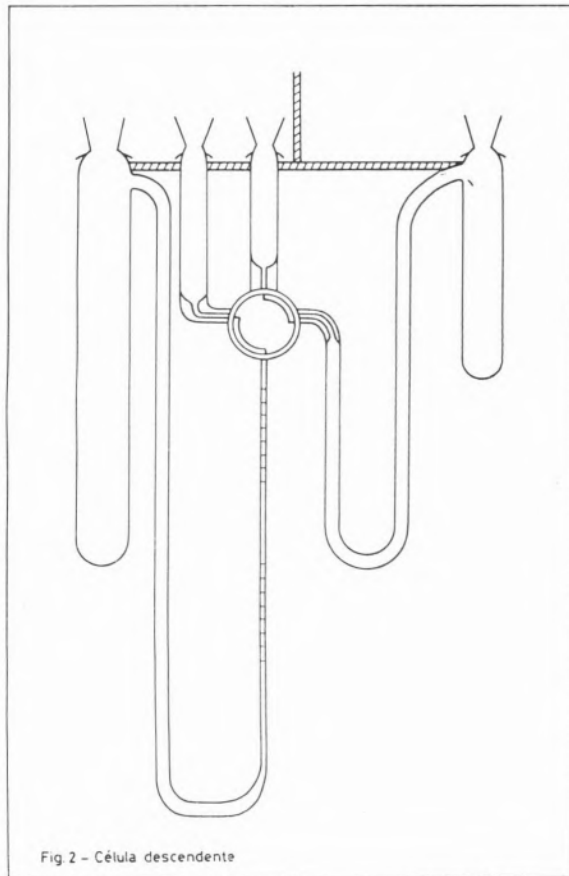


Fig. 2 - Célula descendente

fecimento da solução dentro das torneiras não seja tão eficiente como no caso destas serem de vidro oco. Como as figuras ilustram, as células possuem dois compartimentos destinados à colocação dos eletrodos. Os tubos da fronteira móvel com 2 mm de diâmetro interno têm sobre eles gravados dois grupos de marcas como se mostra nas figuras. A calibração das células ascendente e descendente foi efectuada usando os sistemas  $KCl \leftarrow KIO_3$  e  $KCl \leftarrow LiCl$  respectivamente, para os quais os números de transferência são conhecidos. Em ambos os casos o cátodo era um fio em espiral de platina colocado em compartimento aberto da célula e o ânodo era um eletrodo de prata (prata

electrodepositada sobre um fio em espiral de platina) colocado em compartimento fechado.

Quer na calibração quer nas determinações experimentais dos números de transferência do sulfato de zinco, após cheias com as respectivas soluções inicialmente separadas pelas torneiras de teflon, as células são imersas num banho de óleo termostático à temperatura de  $25.00^{\circ}\text{C} \pm 0,005$ . Após atingido o equilíbrio térmico, as soluções são postas em contacto por rotação de  $90^{\circ}$  das torneiras e imediatamente aplicada uma diferença de potencial entre os eléctrodos.

O controlo da temperatura é efectuado por meio dum termorregulador de mercúrio e tolueno em espiral usado em conjunção com uma resistência de aquecimento de nitrógeno colocada no interior daquela espiral para se obter maior sensibilidade. A observação da fronteira é feita usando o método de detecção óptica descrito por Spiro [5] baseado na diferença de índices de refração das soluções «chefe» e indicadora. Os tempos de percurso da fronteira entre as marcas gravadas nos tubos das células são medidos com um cronómetro digital de quartzo de precisão 1/100 s.

Para as medições da intensidade de corrente, as células são colocadas em série com uma resistência padrão de  $1000 \Omega$ , nos terminais da qual é medida a diferença de potencial com um voltímetro digital de precisão.

A alimentação do circuito das células é feita com uma fonte de corrente constante de alta tensão [6]. A regulação electrónica da corrente é essencial dado que a resistência das soluções no interior das células varia acentuadamente no decorrer das experiências.

## 2.2 — MATERIAIS

$\text{ZnSO}_4 \cdot 7\text{H}_2\text{O}$  Analar obtido comercialmente da Merck foi recristalizado duas vezes a partir de água tridestilada. Após secagem inicial à temperatura de  $150^{\circ}\text{C}$  como heptahidrato, foi convertido em sal anidro até peso cons-

tante numa mufla a  $400^{\circ}\text{C}$ . Aquecimento a  $300^{\circ}\text{C}$  produziu resultados semelhantes. As soluções foram preparadas por pesagem.

KCl Analar obtido comercialmente da BDH foi recristalizado duas vezes a partir de água tridestilada e seco a  $100^{\circ}\text{C}$ .

$\text{KIO}_3$  Analar obtido comercialmente da Merck foi recristalizado duas vezes a partir de água tridestilada e seco a  $110^{\circ}\text{C}$ .

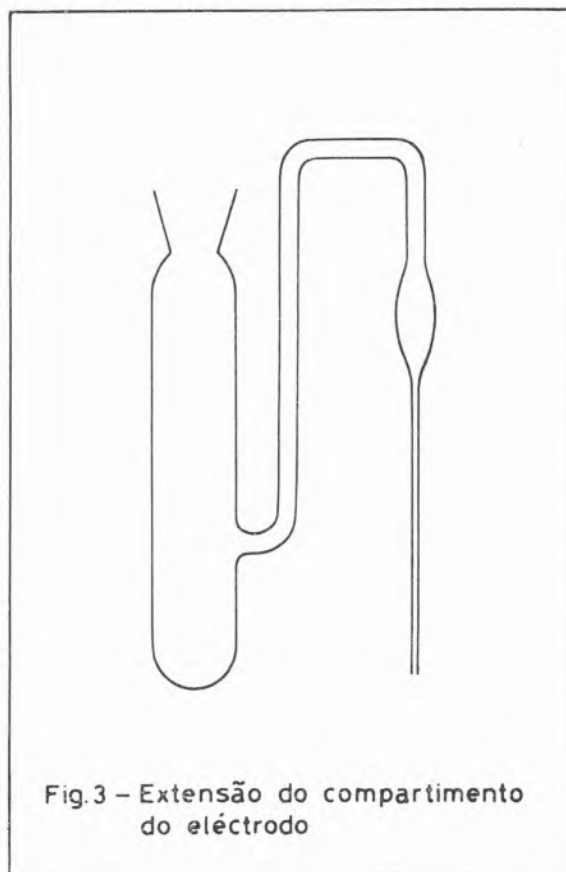


Fig.3 - Extensão do compartimento do electrodo

$\text{LiCl}$  foi obtido da BDH e purificado especialmente para trabalhos de absorção atómica.  $\text{NaPhSO}_3$  obtido comercialmente da BDH foi recristalizado a partir de água tridestilada e seco a  $65^{\circ}\text{C}$  sob pressão reduzida.

Dada a dificuldade de obtenção de cristais de  $(n\text{-Bu}_4\text{N})_2\text{SO}_4$ , foi preparada uma solução de  $(n\text{-Bu}_4\text{N})_2\text{SO}_4$  por neutralização duma solução de  $n\text{-Bu}_4\text{NOH}$  a 40% (BDH) com ácido



sulfúrico Analar (BDH) em atmosfera de azoto.

Todas as soluções foram preparadas com água tridestilada de condutância específica  $0,95 \times 10^{-6} \Omega^{-1} \text{cm}^{-1}$ .

Eléctrodos de cádmio foram preparados por electrodeposição sobre um fio em espiral de platina de uma solução [7] contendo 12,5 g de CdO e 45 g de NaCN Analar em 500 cm<sup>3</sup>, usando uma vareta de cádmio como ânodo e correntes entre 1-3mA.

Eléctrodos de prata foram também preparados electroliticamente a partir de uma solução de KAg(CN)<sub>2</sub> 1% (p/V) usando uma corrente de 1 mA.

Eléctrodos de prata/cloreto de prata foram obtidos anodisando parte da prata em cloreto de prata por electrólise de uma solução de KCl 0,05 M, usando uma corrente de 1 mA. Nas experiências realizadas com NaPhSO<sub>3</sub> como indicador, usou-se uma extensão do compartimento catódico cujo esquema se mostra na fig. 3. Esta extensão tinha o fim de evitar que produtos resultantes da reacção de eléctrodo atingissem a fronteira, alterando assim a sua velocidade.

## SISTEMAS ESTUDADOS

Várias tentativas foram feitas no sentido de encontrar electrólitos indicadores convenientes, com ZnSO<sub>4</sub> como solução «chefe». Não apareceram fronteiras catiónicas visíveis com KCl e ZnCl<sub>2</sub>, mas foi observada uma fronteira descendente bastante definida quando (Bu<sub>4</sub>N)<sub>2</sub>SO<sub>4</sub> foi usado como electrólito indicador. Foram também observadas fronteiras aniónicas com NaPhSO<sub>3</sub> (descendente) e KIO<sub>3</sub> (ascendente) como indicadores.

Nos sistemas  $\oplus \text{ZnSO}_4 \leftarrow \text{NaPhSO}_3 \ominus$  e  $\oplus \text{ZnSO}_4 \leftarrow \text{KIO}_3 \ominus$ , os solutos Zn(PhSO<sub>3</sub>)<sub>2</sub> e Zn(IO<sub>3</sub>)<sub>2</sub> na solução de Kohlrausch foram produzidos por acção da corrente eléctrica. Estimativas das concentrações iniciais dos electrólitos indicadores foram feitas a partir dos valores limites de condutâncias colhidos na literatura [8].

## RESULTADOS E DISCUSSÃO

Os números de transferência foram obtidos a partir da equação  $cVF/it$  em que  $c$  é a concentração molar da solução de sulfato de zinco,  $V$  é o volume em centímetros cúbicos varrido pela fronteira em  $t$  segundos pela intensidade de corrente de  $i$  mA e  $F$  é a constante de Faraday (96487C).

A tabela 1 sumariza as condições experimentais e os valores médios dos números de transferência catiónicos ( $T_+$ ) e aniónicos ( $T_-$ ) obtidos para o sulfato de zinco às três concentrações estudadas.

Para comparação, incluem-se na tabela os valores dos números de transferência catiónicos ( $T_+^*$ ) calculados às mesmas concentrações, usando uma equação indicada por Dye e colaboradores [4], à qual os referidos autores ajustaram os valores experimentais dos números de transferências catiónicos como uma função da concentração de sulfato de zinco.

Nas condições experimentais indicadas não se observou variação dos números de transferência com a corrente eléctrica, excepto nas experiências catiónicas onde se verificou uma diminuição significativa dos números de transferência para correntes acima de 2 mA. A concentração inicial do electrólito indicador não teve qualquer efeito sobre os números de transferência.

Como se ilustra no tabela 1, os valores obtidos para  $T_-$  quando o KIO<sub>3</sub> é usado como indicador são acentuadamente mais baixos que os obtidos com NaPhSO<sub>3</sub>. Isto poderá ser possivelmente atribuído ao facto de o KIO<sub>3</sub> não ser um electrólito conveniente em virtude de a solução de Zn(IO<sub>3</sub>)<sub>2</sub> ser mais densa que a de KIO<sub>3</sub>, produzindo-se assim instabilidade gravitacional.

A natureza do eléctrodo no compartimento fechado não teve qualquer influência sobre os valores de  $T_+$ . Assim, o uso de um ânodo de cádmio ou o de um cátodo de prata/cloreto de prata no compartimento fechado conduziu aos mesmos resultados.

A tabela 2 mostra os valores das correcções efectuadas para o solvente e para o volume

Tabela 1

Condições experimentais na determinação dos números de transferência do ZnSO<sub>4</sub>

C/mol dm <sup>3</sup>	Indicador	Corrente/ma	T <sub>+</sub>	T <sub>-</sub>	T <sub>+</sub> <sup>*</sup>
0,0100	(Bu <sub>4</sub> N) <sub>2</sub> SO <sub>4</sub> NaPhSO <sub>3</sub>	0,50 — 2,00 0,80 — 2,00	0,3822	0,6170	0,3802(4)
0,0250	(Bu <sub>4</sub> N) <sub>2</sub> SO <sub>4</sub> NaPhSO <sub>3</sub> KIO <sub>3</sub>	0,50 — 2,00 0,80 — 2,00 2,00	0,3750	0,6250 (0,6190 †)	0,3750(4)
0,0690	(Bu <sub>4</sub> N) <sub>2</sub> SO <sub>4</sub> NaPhSO <sub>3</sub>	0,50 — 2,00 0,80 — 2,00	0,3583	0,6410	0,3657(4)

† Valor médio obtido com KIO<sub>3</sub> como electrólito indicador nas experiências aniónicas.

Tabela 2

Números de transferência corrigidos do ZnSO<sub>4</sub> a 25°C

C/mol dm <sup>3</sup>	2CΔV (corr. volume)	1 + k <sub>H<sub>2</sub>O</sub> /k <sub>sol</sub> (corr. solvente)	T <sub>+</sub> (corr) média	T <sub>-</sub> (corr) média	T <sub>+</sub> (corr) + T <sub>-</sub> (corr)
0,0100	0,2540	1,0004	0,3821	0,6175	0,9996
0,0250	0,3590	1,0002	0,3747	0,6255	1,0002
0,0690	0,5710	1,0000	0,3577	0,6416	0,9993

bem como os valores dos números de transferência obtidos após efectuadas estas correcções. Nas experiências aniónicas e nas experiências catiónicas em que se usou um ânodo de cádmio no compartimento fechado a variação de volume (ΔV) foi calculada através da equação

$$\Delta V = -1/2 V(\text{Cd}) + 1/2 \phi(\text{CdSO}_4) - 1/2 T(\text{ZnSO}_4) \times \phi(\text{ZnSO}_4) \quad (\text{eq. 1})$$

em que V é o volume molar do cádmio sólido e φ o volume molar aparente do electrólito indicado.

Os valores de φ(ZnSO<sub>4</sub>) às respectivas concentrações bem como os de φ(CdSO<sub>4</sub>) às con-

centrações de Kohlrausch correspondentes foram calculados a partir de dados de densidade [9].

A correcção para o solvente foi calculada a partir de medidas de condutividade (K) do solvente e da solução de ZnSO<sub>4</sub> às várias concentrações estudadas.

Assim a equação final dos números de transferência contendo ambas as correcções é dada por:

$$T(\text{corr.}) = (T \pm 2\Delta V/1000) \times (1 + K_{\text{H}_2\text{O}}/K_{\text{sol.}}) \quad (\text{eq. 2})$$

usando-se o sinal + ou - consoante a fronteira se move em direcção ao eléctrodo

colocado no compartimento fechado ou na direcção oposta à deste, respectivamente. As somas dos números de transferência catiónicos e aniónicos medidos independentemente são próximas da unidade às três concentrações de  $ZnSO_4$ : 0,9996 e 0,9993 às concentrações mais baixa e mais alta respectivamente e 1,0002 à concentração intermédia. Dividindo os números de transferência  $T_+$  (corr.) e  $(T_-)$  (corr.) pela respectiva soma obtemos os «melhores» números de transferência  $T_+$  (m) e  $T_-$  (m), cujos valores se mostram na tabela 3.

Tabela 3

Os «Melhores» números de transferência do  $ZnSO_4$  a  $25^\circ C$

C/mol dm <sup>-3</sup>	$T_+$ /m	$T_-$ /m
0,0100	0,3823	0,6177
0,0250	0,3746	0,6254
0,0690	0,3580	0,6420

Os valores de  $T_+$  (m) assim obtidos foram usados para investigar até que ponto a variação dos números de transferência com a concentração poderá ser explicada pelas várias teorias interiónicas.

Como foi referido anteriormente, este teste efectuado também sobre os números de transferência catiónicos de  $ZnSO_4$  obtidos por Dye e colaboradores [4], foi estendido às soluções de  $CuSO_4$  para as quais se conhecem os números de transferência aniónicos [2].

Os valores de  $T_+$  ( $ZnSO_4$ ) obtidos por Dye et al. [4] foram modificados pelos presentes autores de modo a permitir a introdução das correcções para o volume e solvente, considerando que aqueles investigadores usaram o ânodo de cádmio colocado no compartimento fechado. Os números de transferência assim obtidos, são mais concordantes com a equação dos mínimos quadrados dada por Dy et al [4] do que os calculados tomando

o cátodo de prata/cloreto de prata como eléctrodo fechado.

A variação de volume foi obtida a partir da equação [1] e a correcção para o solvente foi calculada usando valores de condutividade derivados de dados de condutância obtidos por Dye et al [4].

A tabela 4 sumariza os valores dos números de transferência catiónicos assim corrigidos para o  $ZnSO_4$  às várias concentrações estudadas por estes autores [4] assim como os valores de  $T_+$  obtidos para  $CuSO_4$  por Fritz e Fuget [2].

Tabela 4

Números de transferência catiónicos do  $ZnSO_4$  e  $CuSO_4$  a  $25^\circ C$

C/mol dm <sup>-3</sup>	$T_+$ ( $ZnSO_4$ ) †
0,004846	0,3832
0,01135	0,3802
0,017745	0,3780
0,025475	0,3752
0,03755	0,3727
0,045135	0,3705

C/mol dm <sup>-3</sup>	$T_+$ ( $CuSO_4$ ) Δ
0,1249	0,3548
0,1557	0,3472
0,2801	0,3237
0,4230	0,3055
0,5131	0,3040

† Dye et al (4) após correcção efectuada pelos presentes autores.

Δ Fritz e Fuget.

Aparentemente, estes últimos autores aplicaram uma correcção para o volume mas não há menção no seu trabalho da aplicação de uma correcção para o solvente. Embora normalmente a concentrações elevadas esta última correcção seja praticamente desprezável no caso das soluções de  $CuSO_4$  ela é importante. Efectivamente, este

sal hidroliza-se dando origem a soluções ácidas, sendo por isso parte da corrente transportada por H<sup>+</sup>. Aliás, Fritz e Fuget estudaram o efeito do pH sobre T<sub>+</sub>, verificando que uma extrapolação para pH=7 reduzia o seu valor em cerca de 0,001.

Por uma questão de generalidade, as várias equações interiónicas serão escritas para um electrólito z : z.

De acordo com a teoria de Fuoss-Onsager [10].

$$T_+^o = T_+ - (T_+ - 1/2) \Delta\Lambda^e / \Lambda^o \quad (\text{eq. 3})$$

em que T<sub>+</sub><sup>o</sup> e Λ<sup>o</sup> são respectivamente os valores limites do número de transferência e condutância e ΔΛ<sup>e</sup> é o termo electroforético. A forma primitiva de ΔΛ<sup>e</sup> é dada pela equação, à qual designaremos aqui por (F—O)<sub>1</sub>

$$\Delta\Lambda^e = B_2 \sqrt{\alpha c} / (1 + y) \quad (\text{eq. 4})$$

em que

$$B_2 \sqrt{\alpha c} = ze^2 kN / 3\pi\eta = 82,48z^2 \sqrt{\alpha c} / \eta (DT)^{1/2}$$

$$y = kd = d (8\pi Nz^2 e^2 \alpha c / 1000 DKT)^{1/2} = 50,29 dz (\alpha c / DT)^{1/2}$$

sendo α o grau de dissociação do electrólito à concentração c, e a carga do protão, N o número de Avogadro, K a constante de Boltzmann, T a temperatura absoluta, D a constante dieléctrica do solvente e η a sua viscosidade, e d a distância de máxima aproximação do catião e anião.

Uma forma mais exacta do efeito electroforético desenvolvida por Fuoss e Onsager [11] deu origem à equação (F—O)<sub>2</sub>

$$\Delta\Lambda^e = B_2 \sqrt{\alpha c} - B_3 \quad (\text{eq. 5})$$

em que

$$B_3 = [2 Z^5 e^6 N^2 \alpha c / 3000 \eta (DKT)^2] F(b) \\ b = Z^2 e^2 / dDKT$$

e F(b) é uma função complexa de b. Independentemente, Pitts [12] desenvolveu a seguinte equação para os números de transferência

$$T_+^o = T_+ - (T_+ - 1/2) Y_3 / (\Lambda' + Y_3) \quad (\text{eq. 6})$$

em que

$$\Lambda' = \Lambda^o - \Lambda^o Y_1 + Y_2 - Y_3$$

e

$$Y_1 = \frac{Z^2 e^2 k}{3DKT (1 + \sqrt{2}) (1 + y) (\sqrt{2} + y)} + \frac{Z^4 e^4 k^2 S_1}{3 (DKT)^{1/2}}$$

$$Y_2 = \frac{\sqrt{2} - 1}{(\sqrt{2} + y) (1 + y)^2} \left( \frac{N}{3\pi\eta} \right) \left( \frac{Z^4 e^4 k^2}{3DKT} \right)$$

$$Y_3 = \frac{z^2 e^2 k}{(1 + y)} \left( \frac{N}{3\pi\eta} \right) \left( 1 - \frac{z^2 e^2 k T_1}{3DKT} \right)$$

onde S<sub>1</sub> e T<sub>1</sub> são funções de y.

O ajuste destas diferentes equações teóricas aos resultados dos números de transferência para os dois electrólitos foi efectuado por cálculo, tendo sido elaborado um programa de computador para a resolução do problema.

O método usado no teste efectuado consiste em verificar que sendo a equação teórica válida para um dado valor de d, então o valor limite do número de transferência, T<sup>o</sup>, calculado, deve ser independente da concentração. Assim, os números de transferência obtidos experimentalmente para o ZnSO<sub>4</sub> bem como os valores colhidos da literatura para este electrólito (corrigidos pelos presentes autores) e para o CuSO<sub>4</sub> foram do mesmo modo que as correspondentes concentrações iónicas substituídos nas respectivas equações para uma sequência de valores de d. O valor de d seleccionado foi o correspondente ao desvio padrão mínimo, σ, dos valores de T<sub>+</sub><sup>o</sup> calculados. Dado que as teorias são mais falíveis para forças iónicas elevadas, no caso dos valores dos números de transferência colhidos na literatura, em



que as determinações foram efectuadas a mais que três concentrações, os cálculos foram repetidos sucessivamente, excluindo sempre a concentração mais elevada até que se atingissem as três concentrações mais baixas. Dado que se trata de electrólitos parcialmente dissociados, estes cálculos requerem um conhecimento dos graus de dissociação  $\alpha$ . Estes foram calculados através da equação

$$\alpha = 1 - c \gamma_{\pm}^2 K_A$$

em que os coeficientes de actividade estequiométricos médios  $\gamma_{\pm}$  às concentrações  $C$  a 25°C foram colhidos da literatura [13]. Um problema que se pôs foi o do cálculo da constante de associação,  $K_A$ . Da literatura foi colhido um largo espectro de constantes de associação para os dois electrólitos. As tabelas 5 e 6 sumarizam estes valores para o  $ZnSO_4$  e  $CuSO_4$  respectivamente.

Da sua observação, verifica-se que a concordância entre eles é claramente pobre. Efectivamente, a comparação directa entre os valores de  $K_A$  não é possível dado que os cálculos estão baseados em diferentes valores das distâncias de máxima aproximação,  $d$ , entre os iões livres. Assim, quanto maior for o valor de  $d$ , maior deverá ser a correspondente constante de associação. Os dados das tabelas foram por isso recalculados de modo a poderem ser referidos à mesma distância. Escolheu-se o valor de 14,3 Å que é a distância de Bjerrum para um electrólito 2:2 em água a 25°C. As tabelas 5 e 6 mostram os valores de  $K'_A$  obtidos deste modo através da equação de Bjerrum

$$K'_A = K_A + \frac{4\pi N}{1000} \left( \frac{z^2 e^2}{DKT} \right) Q \quad (b)$$

$$b = z^2 e^2 / DKTd$$

Os valores de  $K'_A$  são ainda demasiado diferentes para os dois electrólitos. Tomámos como ponto de referência a 14,3 Å, os valores médios de 228 e 296  $dm^3 mol^{-1}$  para o  $ZnSO_4$  e  $CuSO_4$  respectivamente.

Através de cálculos preliminares efectuados com o computador em que se usaram diferentes valores de  $K_A$  verificou-se que os valores de  $d$  correspondentes a um melhor ajuste decresciam com o aumento de  $K_A$ , contrariamente ao que prevê o modelo de Bjerrum. Assim, foi possível para cada teoria, F-O<sub>1</sub>, F-O<sub>2</sub> e Pitts encontrar um único valor de  $K_A$ , ao qual o valor de  $d$  correspondente ao melhor ajuste fosse o mesmo do valor de Bjerrum consistente com este valor de  $K_A$ .

A tabela 7 sumariza os resultados de ajuste obtidos através do computador para os dois electrólitos.

Da observação desta tabela poderemos concluir que para o  $ZnSO_4$ , as teorias de Fuoss-Onsager se ajustam melhor aos resultados experimentais que a teoria de Pitts, usando três parâmetros como critério: desvio padrão,  $\sigma$ , distância de máxima aproximação entre os iões,  $d$  e valor limite do número de transferência catiónico,  $T_+^0$ .

Relativamente aos valores de  $\sigma$ , verifica-se que não há apreciável diferença entre os resultados obtidos quando se usam os valores dos números de transferência de Dye et al ou os determinados pelos presentes autores.

No primeiro caso, a média  $T_+^0$  (0,3940) é cerca de 0,004 mais baixa que o valor 0,3975 obtido a partir dos valores limites de condutâncias iónicas<sup>(8)</sup> e no segundo caso a média  $T_+^0$  (0,4002) é 0,003 mais elevada que aquele valor. Também se verifica que no primeiro caso, a média  $T_+^0$  decresce continuamente e o melhor valor obtido para  $d$  aumenta à medida que as concentrações mais altas são excluídas. No presente trabalho os cálculos foram efectuados na gama de concentrações estudadas sem exclusão da concentração mais elevada.

Os valores de  $d$  produzidos pela equação F-O<sub>1</sub> são mais razoáveis que os produzidos pela equação F-O<sub>2</sub> quando comparados com a distância cristalográfica metal-enxofre (3,46 Å<sup>0</sup>)



Tabela 5

Constantes de Associação para  $ZnSO_4$  a 25°C

Ref.	Método	$K_A/dm^3 mol^{-1}$	d/A°	$K'_A/dm^3 mol^{-1}$
8	Recálculo dos dados da ref. (1)	227	14,3	227
13	Coefs. osmóticos	200	14,3	200
14	Condutimétrico	204	3,64	540
15	f. e. m.	240	4,3	452
16	Condutimétrico	215	10,7	258
17	Condutimétrico	185	—	—
18	Condutimétrico	189	—	—

Tabela 6

Constantes de Associação para  $CuSO_4$  a 25°C

Ref.	Método	$K_A/dm^3 mol^{-1}$	d/A°	$K'_A/dm^3 mol^{-1}$
13	Coef. osmóticos	250	14,3	250
14	Condutimétrico	233	3,64	567
15	Condutimétrico	250	10,7	293
17	Espectrofotométrico	250	10	302
17	Espectrofotométrico	286	14	289
17	Espectrofotométrico	125	4,3	350
17	Condutimétrico	204	4,3	429
17	Condutimétrico	250	10	302
17	Condutimétrico	256	14	256
18	Condutimétrico	218	—	—
19	Espectrofotométrico	125	—	—
20	Espectrofotométrico	213	—	—

Tabela 7

Resultados computacionais dos números de transferência do  $ZnSO_4$  e  $CuSO_4$ 

Teoria	$10^3 C/mol\ dm^3$	Melhor $d/A^\circ$	$K_A\ dm^3\ mol^{-1}$	$10^4\sigma$	Média $T_+^\circ$
F-O <sub>1</sub>	10 — 69	3,6	5	5,37	4,4002
F-O <sub>2</sub>	10 — 69	6,1	100	5,99	0,4005
Pitts	10 — 69	10,9	180	10,22	0,4104
$ZnSO_4$ (Dye et al)					
F-O <sub>1</sub>	4,8 — 45,1	6,6		4,29	0,3943
	4,8 — 37,5	7,2	140	3,26	0,3940
	4,8 — 25,5	7,7		3,23	0,3937
	4,8 — 17,7	9,3		0,99	0,3930
F-O <sub>2</sub>	4,8 — 45,1	7,3		6,77	0,3957
	4,8 — 37,5	7,5	145	5,43	0,3953
	4,8 — 25,5	7,8		4,69	0,3948
	4,8 — 17,7	8,4		1,97	0,3940
Pitts	4,8 — 45,1	16,4		7,09	0,4014
	4,8 — 37,5	17,5	228	5,43	0,4006
	4,8 — 25,5	18,9		4,52	0,3997
	4,8 — 17,7	21,0		1,72	0,3986
$CuSO_4$					
F-O <sub>1</sub>	125 — 513	2,9		14,5	0,4091
	125 — 423	2,7	10	4,37	0,4112
	125 — 280	2,6		1,62	0,4122
F-O <sub>2</sub>	125 — 513	5,7		15,7	0,4118
	125 — 423	5,7	150	13,1	0,4123
	125 — 280	5,7		0,71	0,4131
Pitts	125 — 513	6,7		7,89	0,4534
	125 — 423	6,7	180	8,07	0,4535
	125 — 280	6,9		2,57	0,4499

para o sal anidro. Este valor está em perfeita concordância com o produzido pela equação F-O<sub>1</sub>, quando se usam os resultados de transferência obtidos pelos presentes autores.

Relativamente ao ajuste dos dados experimentais à teoria de Pitts, embora este seja razoável em termos dos valores obtidos para  $\sigma$ , os valores de  $d$  produzidos são anormalmente elevados.

A teoria F-O<sub>1</sub>, é por isso, a que melhor se ajusta.

Quanto ao CuSO<sub>4</sub>, as teorias ajustam-se mal, embora os valores de  $d$  produzidos pelas teorias F-O<sub>2</sub> e Pitts sejam fisicamente razoáveis. Os valores das médias  $T_{+}^{\circ}$  são extremamente elevados para todas as teorias quando comparados com o valor da literatura, 0.4011 [8]. De facto, a gama de concentrações estudada para o CuSO<sub>4</sub> fica bastante acima dos limites superiores de validade das teorias.

Se tivermos em consideração os resultados obtidos para o MgSO<sub>4</sub> [3], poderemos concluir que para os três electrólitos 2:2 as teorias de Fuoss-Onsager, fornecem um melhor ajuste dos dados experimentais que a teoria de Pitts. Os parâmetros  $d$  e  $T_{+}^{\circ}$  obtidos a partir da teoria de Pitts são mais elevados que os derivados das teorias de Fuoss-Onsager contrariamente ao que acontece para electrólitos 1:1 [1], para os quais a teoria de Pitts fornece valores praticamente concordes.

(Recebido em 18 de Julho de 1894)

## AGRADECIMENTO

Os autores manifestam o seu reconhecimento ao Instituto Nacional de Investigação Científica pelo apoio financeiro concedido para a realização deste trabalho.

## BIBLIOGRAFIA

- [1] D.P. SIDEBOTTOM, M. SPIRO, *J.C.S. Faraday I*, **69**, 1287 (1973).
- [2] J.J. FRITZ, C.R. FUGET, *J. Phys Chem.*, **62**, 303 (1958).
- [3] M.C.P. LIMA, S. KUMARASINGHE, M. SPIRO, *J.C.S. Faraday Trans. I*, **74**, 1036 (1978).
- [4] J.L. DYE, M.P. FABER, D.J. KARL, *J. Am. Chem. Soc.*, **82**, 314 (1960). **83**, 5047 (1961).
- [5] M. SPIRO, *Transference Numbers*, Chapter IV in *Physical Methods of Chemistry*, Vol. 1, Part II A. A. Weissberger and B.W. Rossiter, eds (Wiley, New York, 1971), p. 205.

- [6] A. TRAÇA, M.C.P. LIMA, *J. Physics E Sci. Instrum.*, **13**, 387 (1980).
- [7] Kirk-Othmer Encyclopedia of Chemical Technology (Wiley-Interscience, New York, 2nd edn, 1965), vol. 8, p. 55.
- [8] R.A. ROBINSON, R.H. STOKES, *Electrolyte Solutions* (Butterworths, London, 2nd edn, 1959).
- [9] *International Critical Tables* (Mc Graw-Hill, New York, 1928), Vol. III, p. 66.
- [10] R. FERNANDEZ-PRINI, in *Physical Chemistry of Organic Solvent Systems*, ed. A.K. Covington and T. Dickinson (Plenum Press, London, 1973), p. 530.
- [11] R.M. FUOSS, L. ONSAGER, *J. Phys. Chem.*, **67**, 628 (1963).
- [12] E. PITTS, B.E. TABOR, J. DALY, *Trans. Faraday Society*, **65**, 849 (1969).
- [13] K.S. PITZER, B.E. TABOR, J. DALY, *Trans. Faraday Society*, **65**, 849 (1969).
- [14] B.B. OWEN R.W. GURRY, *J. Am. Chem. Soc.*, **60**, 3074 (1938).
- [15] V.S.K. NAIR, G.H. NANCOLLAS, *J. Chem. Soc.* 3706 (1958).
- [16] E.M. HANNA, A.D. PETHYBIRDGE, S.E. PRUE, *Electrochim. Acta*, **16**, 677 (1971).
- [17] C.W. DAVIES, *J. Chem. Soc.* 2093 (1938).
- [18] P.A.H. WYATT, *Trans. Faraday Society*, **47**, 656 (1951).
- [19] R. NASANEM, *Acta Chem. Scand.* **3**, 179 (1949).
- [20] E.W. BALE, C.B. MONK, *Trans. Faraday Society*, **52**, 816 (1956).

## ABSTRACT

**Transference Numbers of zinc sulphat in Water at 25°C.**

The cation- and anion—constituent transference numbers of zinc sulphate in water at the concentrations 0.01, 0.025 and 0.069 mol dm<sup>-3</sup> have been measured by the direct moving boundary at 25°C. The limiting values of the cation transference numbers,  $T_{+}^{\circ}$ , have been calculated using the various equations of Fuoss-Onsager and Pitts and compared with those obtained from the transference work of Dye et al and with literature conductance data. A test of these theoretical equations has been extended to aqueous solutions of copper sulphate, using literature transference numbers and shows that as for magnesium sulphate, previously studied, also for those two electrolytes, the Fuoss-Onsager theories provide a better fit to the experimental data than Pitts theory.

HIGUINALDO J. CHAVES DAS NEVES

Faculdade de Ciências e Tecnologia da  
Universidade Nova de Lisboa  
Quinta da Torre  
2825 Monte da Caparica

HARTMUT FRANK

Institut fuer Toxikologie  
Universidade de Tuebingen  
7400 Tuebingen, R. F. A.



## ANÁLISE DE MONOSSACARIDOS POR CROMATOGRÁFIA GÁS-LÍQUIDO: CGL E CGL/EM DE N,O- -TRIMETILSILIL AMINODEOXIALDITÓIS

*Apresenta-se um processo de derivatização para a produção de derivados voláteis de monossacaridos, apropriados para a sua análise por cromatografia gás-líquido e, eventualmente por cromatografia gás-líquido associada à espectrometria de massa (CGL/EM). O método envolve a preparação de metóximas e a sua ulterior redução pelo borano-tetra-hidrofurano aos correspondentes aminodeoxialditóis. Estes são tornados voláteis por trimetilsililação, segundo um processo que introduz reprodutivelmente dois grupos TMS no átomo de azoto. Obtêm-se, assim, cromatogramas simplificados, uma vez que o processo conduz a um único derivado por cada aldose. A estrutura dos derivados foi estabelecida por CGL/EM. Embora o processo de derivatização possa ser conduzido na presença de cetoses, estas originam dois picos cromatográficos correspondentes aos dois diastêromeros esperados. A aplicação do processo a misturas contendo dissacaridos é discutida.*

## 1 — INTRODUÇÃO

A inequívoca identificação de monossacaridos é um objectivo de importância muitas vezes fundamental, quer em química de produtos naturais quer em bioquímica. A semelhança estrutural entre os membros deste importante grupo de compostos, exige métodos analíticos de elevada resolução. Dada a sua elevada sensibilidade, poder de separação e rapidez de análise, a cromatografia gás-líquido em colunas tubulares abertas (capilares) é o método de eleição para a análise de misturas complexas. Porém, no caso dos açúcares, surgem complicações adicionais.

A elevada polaridade dos açúcares torna-os inadequados à análise em fase de vapor. Para tal, torna-se necessária a preparação de derivados voláteis. A partir dos trabalhos iniciais de Bayer [1] e Sweeley [2] sobre as propriedades cromatográficas de ésteres trimetilsilílicos de monossacaridos, dissacaridos e poliálcoois, desenvolveu-se um intenso trabalho de investigação que tem encontrado expressão nas propostas de numerosos derivados voláteis para a análise por CGL de hidratos de carbono. Com maior ou menor sucesso, derivados como os acetatos [3] e trifluoroacetatos [4] de alditóis n-butilboronatos [5], aldonitrilos [6], trifluoroacetatos de O-metil-glicosidos [8], ésteres e éteres trimetilsilílicos de óximas e metóximas [9, 10], ditioacetais de anidro-hexoses [11], têm sido propostos e utilizados na análise cromatográfica em fase gasosa de hidratos de carbono.

A maior dificuldade encontrada na generalidade dos processos de derivatização, consiste na formação de isómeros que conduzem, com frequência, ao aparecimento de picos múltiplos para um único composto, produzindo-se cromatogramas complicados que tornam difícil ou mesmo impossível, a análise de misturas complexas. Picos correspondentes a um mesmo açúcar podem eluir

conjuntamente, interferindo na análise qualitativa e quantitativa dos componentes da mistura. Dada a simplicidade de alguns dos métodos de derivatização a utilização de colunas tubulares abertas (capilares) tem sido tentada, aproveitando-se o seu alto poder de resolução para uma separação completa de todos os picos múltiplos correspondentes a cada um dos monossacaridos de uma mistura [13-15].

A formação de picos múltiplos tem origem no equilíbrio que se estabelece entre as formas carbonílicas, furanósicas e piranósicas. Este equilíbrio pode ser eliminado por recurso à destruição do grupo carbonilo. A análise de monossacaridos sob a forma de ésteres de alditóis veio, por esta razão, a ocupar uma posição destacada, tornando-se um método clássico na análise de monossacaridos por cromatografia gás-líquido. Contudo, em muitos casos, não é fácil conseguir uma separação completa, para além do facto que cetoses e aldoses produzem poliálcoois idênticos. O recurso a éteres trimetilsilílicos de N-etoxycarbonil aminodeoxialditóis permite a resolução de todas estas dificuldades [16]. O processo é, porém, trabalhoso e uma simplificação do mesmo princípio torna-se importante quando se pretende aplicá-lo a análises de rotina.

## 2 — PARTE EXPERIMENTAL

### MATERIAIS

Trimetilcloro-silano (TMCS), trimetilsilimidazol (TMSI) e cloridrato de metoxilamónio (Pierce Chemical Co), solução 1 molar de borano em tetra-hidrofurano (Ega Chemie) e piridina seca, (Pierce Chemical Co.), foram utilizados sem tratamento prévio. As soluções padrão foram preparadas a partir de substâncias puras especialmente preparadas para ensaios cromatográficos, da marca Alltech Associates.

### INSTRUMENTOS

As análises cromatográficas foram executadas num cromatógrafo gás-líquido, adaptado a cromatografia em colunas tubulares abertas da marca Pye Unicam, modelo PU 4500, equipado com repartidor de fluxo e detector de ionização de chama (DIC). Utilizou-se uma coluna de vidro de paredes revestidas de 25 m × 0,25 mm d.i. Fase líquida: OV-101; temperatura do injetor e detector, 300°C. As análises foram efectuadas com programação de temperatura: temp. inicial 160°C durante 10 min., seguindo-se incremento linear de temperatura a 2 ou 4°/min., até 220°C. Ensaios de CGL/EM foram levados a efeito num instrumento Finningan modelo 4021, equipado com uma base de dados INCOS. Os espectros de massa de impacto electrónico (IE) foram obtidos sob as condições seguintes: energia de ionização 70 eV; temperatura da fonte iónica 270°C; temperatura da interface 340°C. Multiplicador 2500 V. Nos ensaios de CGL/EM utilizou-se uma frequência de varrimento de 50-700 U.M.M./2 s. As determinações quantitativas, curvas de calibração e cálculo de factores de resposta foram efectuados num integrador — computador SP 4100.

### PREPARAÇÃO DOS DERIVADOS

Preparam-se soluções aquosas padrão contendo 1-2 mg/cm<sup>3</sup> de cada monossacarido e 2 mg/cm<sup>3</sup> de D(—)-Manitol como padrão interno. Um volume de 200 µl de cada solução foi transferido para um frasco de derivatização de 1 cm<sup>3</sup>, de paredes espessas e tapado com septo de borracha revestido com PTFE apertado com tampa de rosca (Reacti-Vial, Pierce). O solvente foi evaporado sob uma ligeira corrente de azoto e o resíduo seco em vácuo, sob pentóxido de fósforo. Ao resíduo seco, foram adicionados 200 µl de uma solução de 25 mg/cm<sup>3</sup> de cloridrato de



metoxilamônio em piridina. O frasco foi fechado e o conjunto aquecido a 80°C durante 1 hora. Ao fim deste tempo após, arrefecimento à temperatura ambiente, o solvente foi evaporado sob, corrente de azoto. Ao resíduo seco, adicionaram-se 200  $\mu$ l de uma solução 1 molar de borano em tetra-hidrofurano, a mistura foi agitada vigorosamente e aquecida no frasco fechado, a 80°C durante 2 horas. O conteúdo foi arrefecido em banho de gelo e o excesso de borano destruído pela adição cuidadosa de metanol. Após ter cessado a libertação de gás, o solvente foi evaporado sob corrente de azoto e o resíduo tratado por três vezes com 100  $\mu$ l de metanol a 80°C por 30 min.

Após destruição dos complexos de borano, o metanol foi evaporado sob corrente de azoto e o resíduo tratado com uma mistura de piridina: TMCS:TMSI (4:1:1). Após agitação vigorosa a mistura foi aquecida a 50°C durante trinta minutos, arrefecida e centrifugada. O sobrenadante foi directamente usado para CGL.

### 3 — RESULTADOS E DISCUSSÃO

A análise de açúcares redutores por cromatografia gás-líquido pode ser muito simplificada pela utilização de derivados voláteis acíclicos. Se bem que os ésteres trimetilsilílicos das metóximas possam ser directamente utilizados em CGL, tais derivados dão frequentemente origem a dois picos correspondentes às formas *sin* e *anti*. A redução das metóximas pelo borano-tetrahidrofurano permite obter os correspondentes aminodeoxialditóis com rendimento elevado [16]. As condições de reacção conduzem a um mínimo de produtos secundários e o excesso de reagente é facilmente eliminado por tratamento com metanol e evaporação sob corrente de azoto.

Para que os aminodeoxialditóis sejam utilizáveis em cromatografia gás-líquido é neces-

sário torná-los voláteis. A trimetilsilação oferece as vantagens da simplicidade e rapidez. Os produtos secundários são voláteis e não interferem com a análise. Porém, para que a sililação possa ser utilizada com sucesso, é condição indispensável que ela se produza de modo reprodutível e seja com-

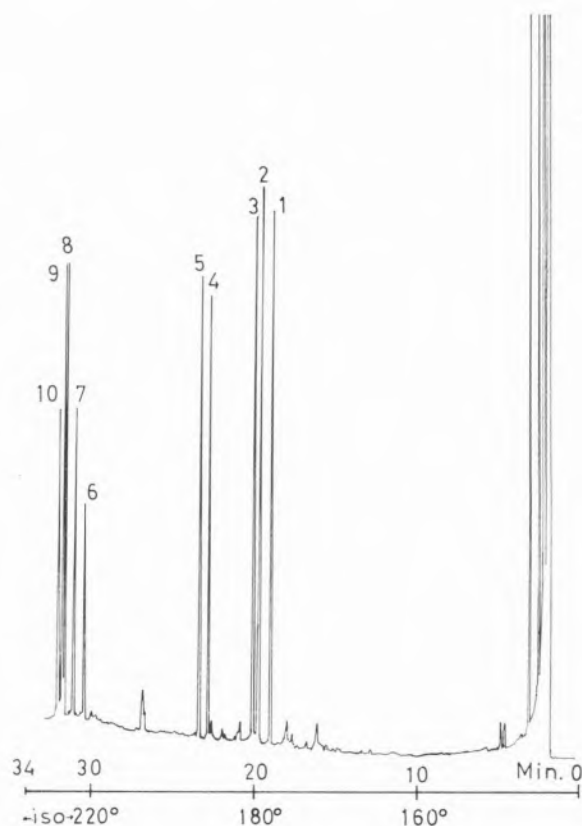


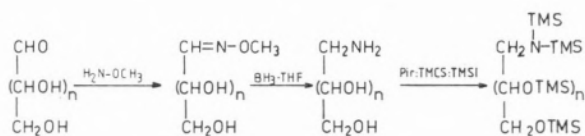
Fig. 1

Cromatograma de éteres trimetilsilílicos de N-di(trimetilsilil) aminodeoxialditóis. Condições na parte experimental. 1 — Xilose; 2 — Ribose; 3 — Arabinose; 4 — Rammose; 5 — Fucose 1; 6 — Frutose 1; 7 — Frutose 2; 8 — Glucose; 9 — Manose; 10 — Galactose.

pleta. O átomo de azoto pode tomar um ou dois grupos TMS. Reagentes sililantes fortes como a bis-(trimetilsilil)trifluoroacetamida (BSTFA) são capazes de introduzir dois grupos TMS no átomo de azoto mas, esta dupla sililação não é completa. Juntamente com os produtos N-dissililados, aparecem sem-

pre quantidades significativas de produtos N-monossililados. Uma dupla sililação completa é conseguida apenas em condições violentas (150°C, 2 horas) que reconhecidamente afectam a integridade dos açúcares. O estudo das condições de sililação revelou que, pela utilização de uma mistura de piridina: TMCS:TMSI (4:1:1), é possível obter em condições suaves uma trime-tilsilação completa dos aminodeoxialditóis, incluindo dupla sililação do átomo de azoto. Nestas condições, o método de derivatização conduz a um único pico por cada aldose (Esquema 1). Xilose, ribose, arabinose, ramnose, fucose, glucose, manose galactose puderam assim ser separados, identificados

e quantificados num único ensaio (Fig. 1). Como cetose que é, a frutose origina dois picos. Estes são, porém, bem separados, per-



Esquema 1

mitindo a sua identificação e quantificação. Os factores de resposta relativos foram calculados em relação ao TMS-D (—)-manitol (Fig. 3).

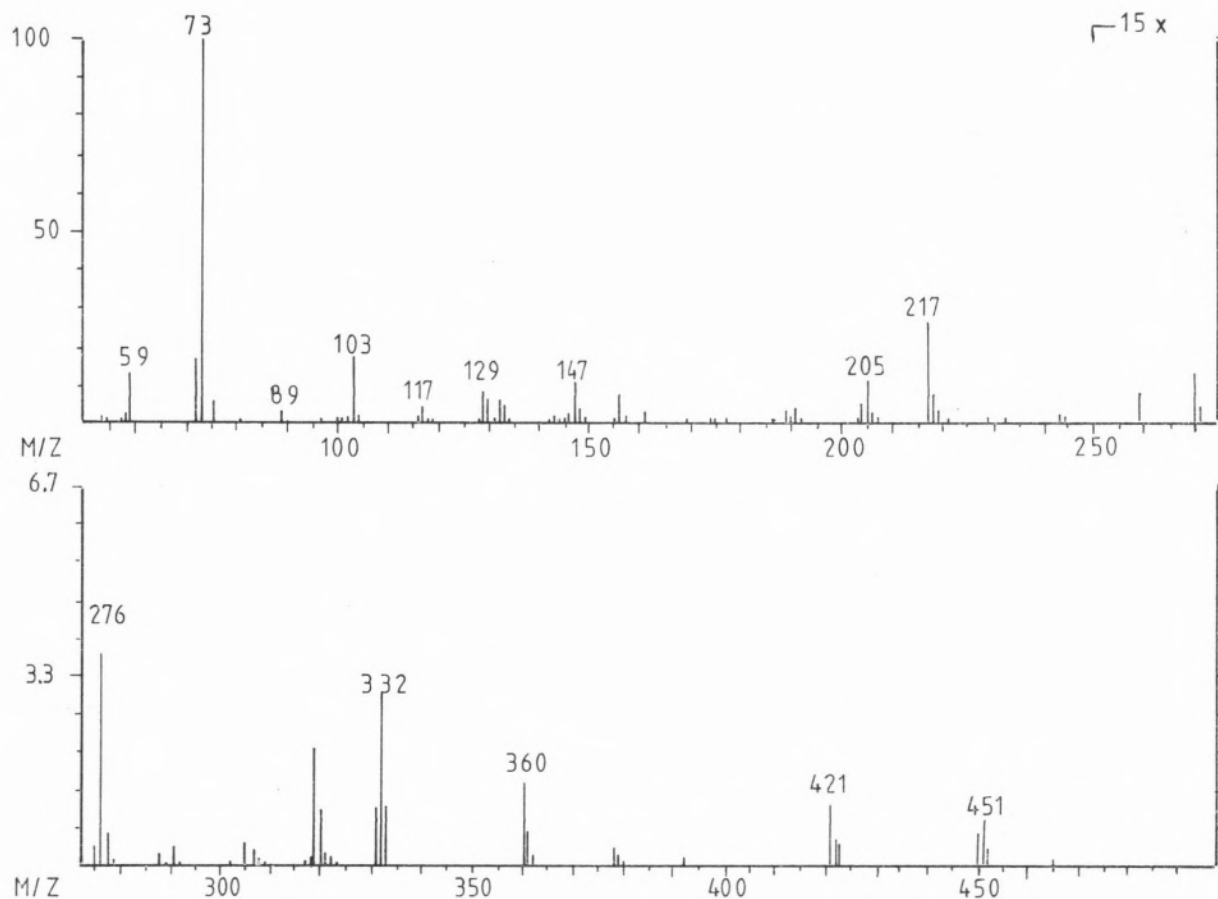


Fig. 2

Spectro de Massa de Impacto Electrónico (EM-IE) de N,N-di(trimethylsilyl)-pentakis-2,3,4,5,6-O-(trimethylsilyl)-amino-deoxyglucitol. Condições na parte experimental.

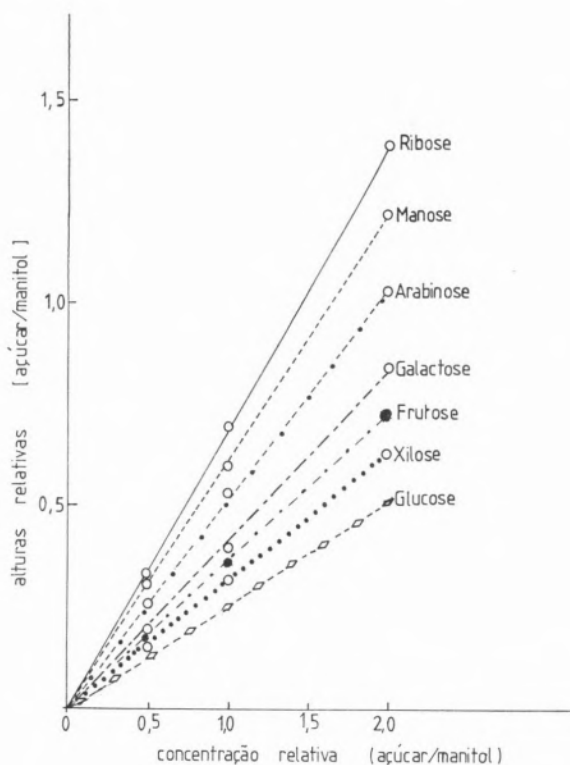


Fig. 3

Resposta Relativa (DIC) dos éteres trimetilsilílicos dos N,N-di-(trimetilsilil)aminodeoxialditóis, relativas ao TMS-D(—)-manitol como padrão interno. No caso da frutose, o cálculo teve em conta a soma dos dois picos.

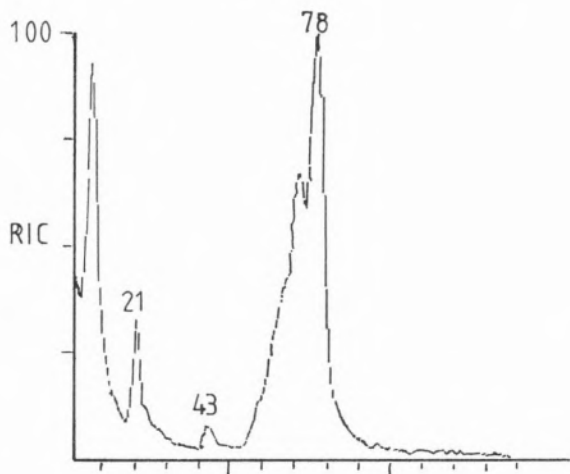
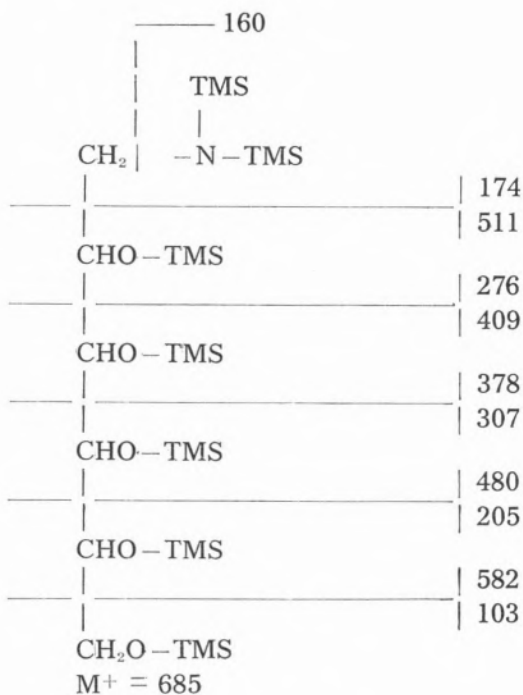


Fig. 4

Registo de Corrente Iónica Total obtido a partir de uma amostra de monossacaridos, derivatizados como descrito, quatro dias após a derivatização. Os varrimentos de 50 a 100 correspondem ao conjunto glucose, manose e galactose.

A identidade dos derivados foi estabelecida por CGL/EM. O aspecto de impacto electrónico do N,N-di-(trimetilsilil)-pentakis-2, 3, 4, 5, 6-O-(trimetilsilil)-aminodeoxiglucitol (Fig. 2), mostra um ião a m/z 276 correspondente ao fragmento (TMS)<sub>2</sub>-N-CH<sub>2</sub>-CH<sub>2</sub>-OTMS. Juntamente com os iões a m/z 161 e m/z 368, a presença de dois grupos TMS no átomo de azoto fica demonstrada (esquema 2). Outro ião de valor diagnóstico



Esquema 2

e m/z 421, resultante da eliminação de NH-(TMS)<sub>2</sub> a partir de m/z 582, ou por perda de 90 U.M.M. a partir de M<sup>+</sup> - 174. Como é característico dos poliálcoois pertrimetilsililados, m/z 421 perde novamente 90 U.M.M. para originar m/z 331. Os iões m/z 73, 103, 117, 129, 147, 205, e 319 são característicos dos éteres trimetilsilílicos dos poliálcoois [17]. O ião de massa mais elevada m/z 451 corresponde à perda de um grupo TMS a partir de M<sup>+</sup> - 161.

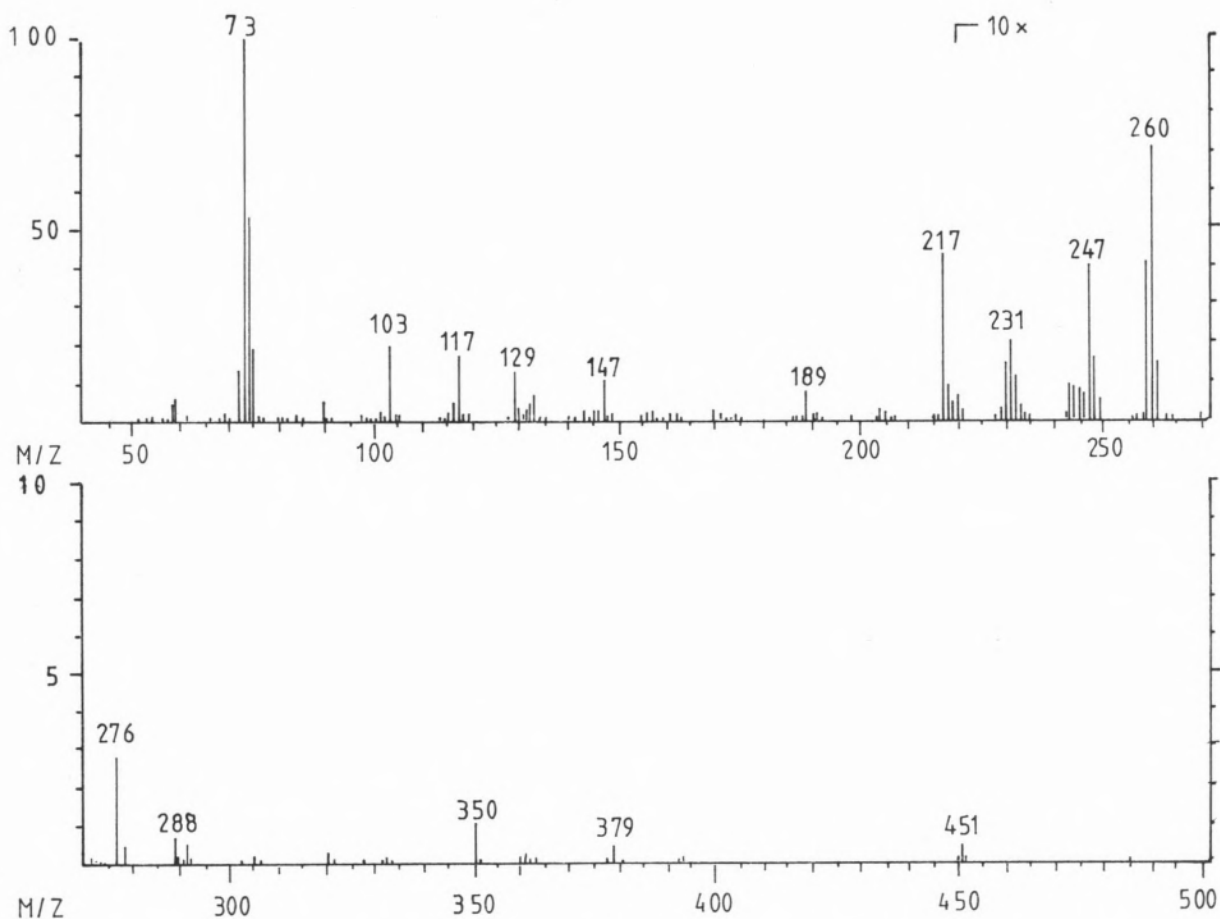


Fig. 5

Espectro de Massa de Impacto Electrónico obtido por CGL/EM, correspondente ao varrimento n.º 78 do RCI da Fig. 4.

A linearidade da resposta do DIC foi determinada para cada açúcar a partir de misturas contendo quantidades crescentes de monossacarido para uma quantidade fixa de D (-)-manitol e as relações das áreas comparadas com as relações das concentrações (Fig. 3). Dentro dos limites estudados observa-se resposta linear do DIC.

### 3.1 — ESTABILIDADE DOS DERIVADOS

Os compostos N-trimetilsililados apresentam, de um modo geral, uma resistência diminuída ao armazenamento. No caso particular dos

presentes derivados, amostras armazenadas em frigorífico apresentam ao fim de 72 horas evidentes sinais de alteração que se manifesta por deformação acentuada dos picos cromatográficos. A Fig. 4 mostra o registo da corrente iónica total, obtido com uma amostra em tais condições. A análise por CGL/EM do pico correspondente ao derivado da glucose (Fig. 5) mostra ausência do ião  $m/z$  421. Os iões  $m/z$  305, 319 e 332 existentes no EM-IE de amostras frescas aparecem agora deslocados de 72 U.M.M. Na amostra armazenada um novo ião  $m/z$  203 é mais intenso que o ião  $m/z$  205. Igualmente ausentes estão  $m/z$  89 e  $m/z$  306.

### 3.2 — AMOSTRAS CONTENDO DISSACARIDOS

Em princípio, o método de derivatização descrito é igualmente aplicável a amostras contendo dissacaridos redutores. No entanto, ao

comportamento da sacarose nas condições de reação. Misturas contendo apenas dissacaridos foram tratadas com borano-tetra-hidrofurano nas condições descritas e trimetilsililadas segundo o método original de Sweeley [2]. O cromatograma respectivo,

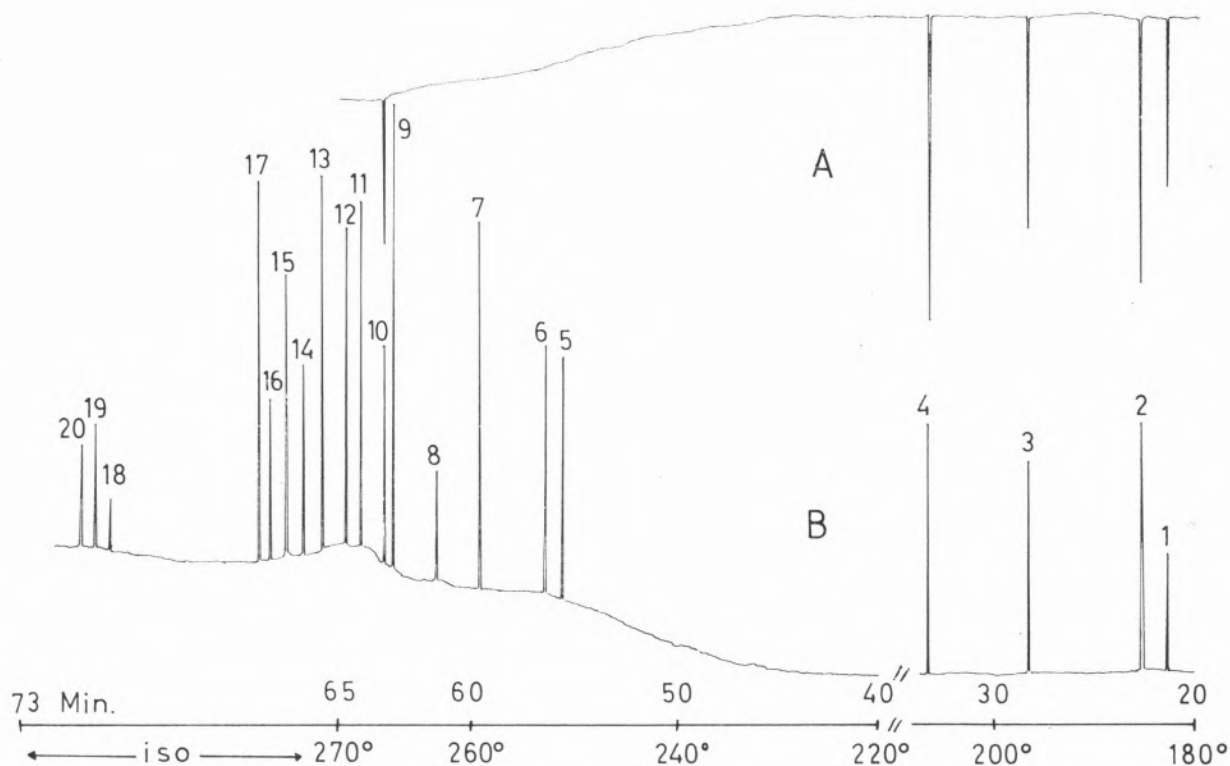


Fig. 6

Cromatograma de uma mistura de Dissacaridos após tratamento como borano-tetra-hidrofurano (V. Texto).  
 B — Mistura de Dissacaridos analisados sob a forma de TMS-éteres: 1 —  $\alpha$ -O-Metilfrutósido; 2 —  $\beta$ O-Metilfrutósido; 3 —  $\alpha$ -Glucose; 4 —  $\beta$ -Glucose; 5, 6, 7 — Galacto-arabinose; 8 — Lactulose; 9, 15 — Lactose; 10 — Sacarose; 11,13 — Maltose; 12, 17 — Celobiose; 14 — Turanose; 16 — Trealose; 18, 20 — Melibiose; 19 — Gentiobiose;  
 B — Cromatograma de sacarose após tratamento com borano-tetra-hidrofurano.

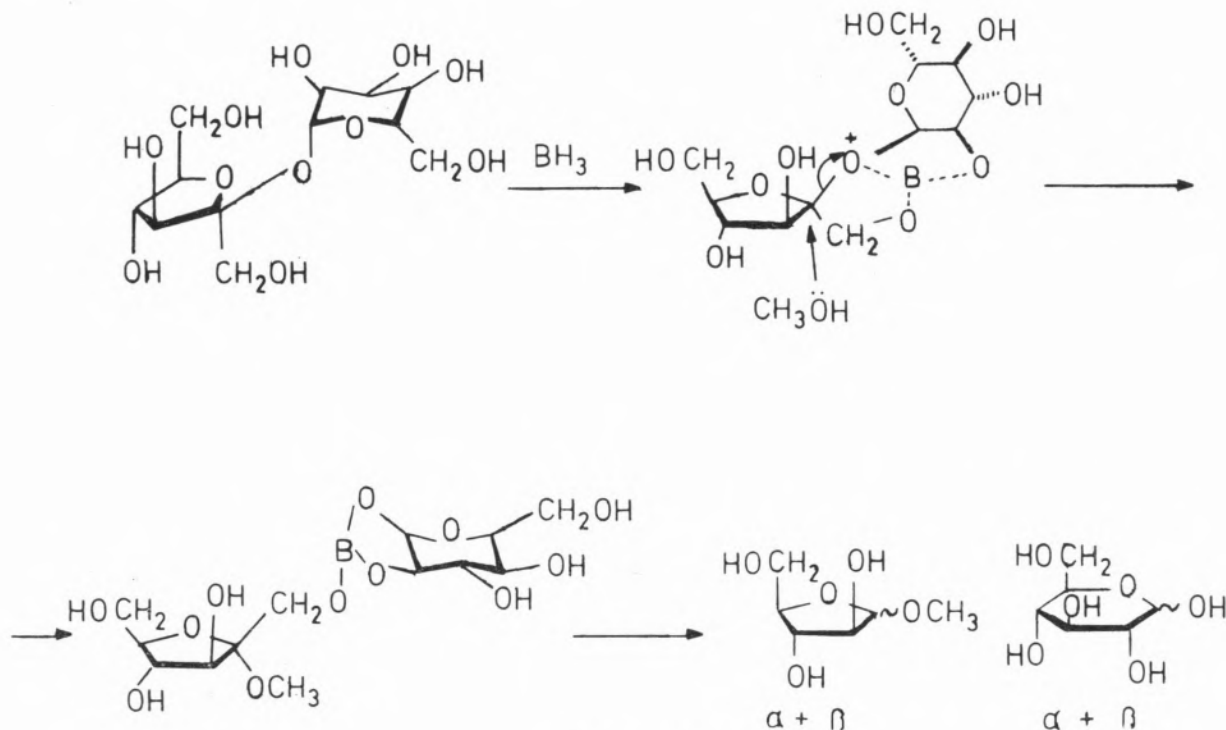
aplicar o processo a amostras contendo dissacaridos redutores e sacarose, tal como se encontram em numerosos secretados vegetais, verificou-se um comportamento anômalo da sacarose, caracterizado por fatores de recuperação muito baixos ou mesmo o seu desaparecimento. Este surpreendente comportamento anômalo levou a estudar o

mostrou o aparecimento de quatro picos adicionais (Fig. 6). Ensaio individuais revelaram ser a sacarose a origem dos picos adicionais. Estes picos foram identificados por CGL/EM como sendo os éteres trimetilsilílicos de  $\alpha$  e  $\beta$ -glucose e  $\alpha$  e  $\beta$ -O-metilfrutósido. Estes resultados mostram que o tratamento com borano-tetra-hidrofurano e subsequente



metanólise dos complexos açúcar-borano, conduz à rotura da ligação glicosídica da sacarose em que o metanol ataca preferencialmente a metade frutofuranósica (Esquema 3).

ria à análise é baixa. A derivatização foi efectuada sobre quantidades de cerca de 1  $\mu\text{mol}$  e a análise conseguida com quantidades da ordem dos 0,1-1 nmol.



Esquema 3

#### 4 — CONCLUSÕES

A análise de misturas de monossacaridos por cromatografia gás-líquido é significativamente simplificada por uma derivatização que conduza a um único pico por cada açúcar. A grande parte dos processos correntes de derivatização originam mais do que um pico cromatográfico por cada monossacarido. Os derivados trimetilsililados dos aminodeoxialditóis foram preparados segundo um processo que conduz reprodutivelmente a uma dupla sililação completa do átomo de azoto, originando assim um único pico cromatográfico por cada aldose. A identificação dos derivados foi levada a efeito por CGL/EM. A quantidade de amostra necessá-

A estabilidade dos derivados ao armazenamento recomenda que as análises sejam efectuadas de fresco.

(Recebido, 30 de Novembro de 1984)

#### AGRADECIMENTOS

Os autores agradecem à Fundação Volkswagen Werk o generoso apoio financeiro e à Lic.<sup>a</sup> Maria Manuela Araújo Mantas o apoio técnico prestado.

#### REFERÊNCIAS

- [1] E. BAYER, *Gaschromatographie*, Berlin, 2.<sup>a</sup> Ed., 1962, p. 143.
- [2] C.C. SWEELLEY, R. BENTLEY, M. MAKITA, W.W. WELLS, *J. Amer. Chem. Soc.*, **85**, 2497 (1963).
- [3] J.S. SAWARDEKER, J.H. SLONEKER, A. JEANES *Anal. Chem.*, **37**, 1602 (1965).

- [4] W.A. KOENIG, H. BAUER, W. VOELTER, E. BAYER, *Chem. Ber.*, **106**, 1905 (1973).
- [5] F. EISENBERG, JR., *Carbohydr. Res.*, **19**, 135 (1971).
- [6] P.J. WOOD, I.R. SIDDIQUI, *Carbohydr. Res.*, **19**, 283 (1971)
- [7] D.C. DEJONGH, S. HANESSIAN, *J. Amer. Chem. Soc.* **87**, 3744 (1965).
- [8] P. ZANETTA, W.C. BRECKENRIDGE, G. VINCENDON, *J. Chromatogr.*, **69**, 291 (1972).
- [9] R.A. LAINE, C.C. SWEELEY, *Carbohydr. Res.*, **27**, 199 (1974).
- [10] G. PETERSSON, *Carbohydr. Res.*, **33**, 47 (1974).
- [11] S. HONDA, K. KAKEHI, K. OKADA, *J. Chromatogr.*, **176**, 367 (1979).
- [12] P.E. REID, B. DONALDSON, D.W. SECRET, B. BRADFORD, *J. Chromatogr.*, **47**, 199 (1970).
- [13] G. EKLUND, B. JOSEFSSON, C. ROOS, *J. Chromatogr.*, **142**, 575 (1977).
- [14] G. GERWIG, J.P. CAMERLING, J.F.G. VLIAGENTHART, *Carbohydr. Res.*, **62**, 349 (1978).
- [15] H. ZEGOTA, *J. Chromatogr.*, **192**, 446 (1980).
- [16] H. FRANK, H.J. CHAVES DAS NEVES, E. BAYER, *J. Chromatogr.* **207**, 213 (1981).
- [17] G. PETERSSON, *Tetrahedron*, **25**, 4437 (1969).

**Gas chromatography of monosaccharides: GLC and GCMS of N,O-trimethylsilyl aminodeoxyalditols.**

A new derivatization method for the production of volatile derivatives of monosaccharides is presented, which affords only one chromatographic peak for each aldose. The method involves the preparation of supar methoximes and their reduction with borane-tetrahydrofurane to the corresponding aminopoliols. Trimethylsilylation with a mixture of Pyridine:TMCS: TMSI (4:1:1) affords the corresponding TMS derivatives with two TMS groups on the nitrogen atom. Thus, simplified chromatograms are obtained with mixtures, since only one peak is formed for each aldose. The structure of the derivatives was established by GCMS. Although the same process is applicable to cetoses, it affords the two expected diastereomers. Some disaccharides are partially cleaved under the reaction conditions. This is the case of Saccharose were extra peaks corresponding to the TMS ethers of the glucose and fructose moities are formed



# STUDIES ON THE OXIDATION REACTIONS OF THE DINITROGEN COMPLEX *trans*- -[ReCl(N<sub>2</sub>)(Ph<sub>2</sub>PCH<sub>2</sub>CH<sub>2</sub>PPh<sub>2</sub>)<sub>2</sub>]

Complex *trans*-[ReCl(N<sub>2</sub>)(dppe)<sub>2</sub>] (A, dppe = Ph<sub>2</sub>PCH<sub>2</sub>CH<sub>2</sub>PPh<sub>2</sub>) undergoes oxidation by AgBF<sub>4</sub> to give the derived analogous cationic species with a labile N<sub>2</sub> ligand which undergoes ready replacement by CNMe to afford *trans*-[ReCl(CNMe)(dppe)<sub>2</sub>][BF<sub>4</sub>]; alternatively, a rearrangement of the unsaturated [ReCl(dppe)<sub>2</sub>][BF<sub>4</sub>] complex appears to afford an ortho-metalated species. Photochemical chlorination of A by CH<sub>2</sub>Cl<sub>2</sub> gives [Re<sub>2</sub>Cl<sub>3</sub>(dppe)<sub>4</sub>], whereas the oxo compound [ReOCl(dppe)<sub>2</sub>] is formed in the presence of dioxygen; photolysis of a solution of A in the absence of any substrate affords the possible dimeric ortho-metalated complex [Re<sub>2</sub>Cl<sub>2</sub>(dppe)<sub>3</sub>].

## 1 — INTRODUCTION

Electron-rich dinitrogen complexes are easily oxidizable species and their oxidations generally result in dinitrogen evolution [1] in agreement [2] with expectations based upon some simplified  $\pi$ -MO schemes. However, in some cases where the metal-dinitrogen bond is strong enough, e.g., in *trans*-[ReCl(N<sub>2</sub>)(dppe)<sub>2</sub>], A, a stable mono-oxidized species with bonded N<sub>2</sub> may be formed upon oxidation of the parent complex [3]; nevertheless, a weakening of the N-N<sub>2</sub> bond is expected [2] to result from the metal oxidation, and this behaviour was tested in the present work by studying the reaction of *trans*-[ReCl(N<sub>2</sub>)(dppe)<sub>2</sub>]<sup>+</sup> with isocyanide.

The evolution of the dinitrogen ligand may also result from photochemical excitation and the unsaturated complex [ReCl(dppe)<sub>2</sub>], with a trigonal bipyramidal structure, was isolated from a toluene solution of complex A, under tungsten filament light [4]. In the present work we looked for other products of this reaction, also in the absence of any substrate but under stronger irradiation conditions; moreover, the behaviour of the unsaturated centre, generated *in situ*, in the presence of an oxidizing agent (dichloromethane or dioxygen) was also the object of this study.

## 2 — RESULTS AND DISCUSSION

### 2.1 — Oxidation of *trans*-[ReCl(N<sub>2</sub>)(dppe)<sub>2</sub>], A, by Ag<sup>+</sup> followed by reaction with CNMe or by rearrangement of the metal centre

Complex A undergoes oxidation by AgBF<sub>4</sub> in thf to afford the cationic species *trans*-[ReCl(N<sub>2</sub>)(dppe)<sub>2</sub>][BF<sub>4</sub>], B, as very dark green or purple platelets, with i. r.  $\nu$ (N<sub>2</sub>) at 2030 cm<sup>-1</sup>, in agreement with studies quoted by other authors [3]; the observed differen-

ces in colour may correspond to different dppe distortional isomers since differences in their infrared spectra were detected in the 600-800  $\text{cm}^{-1}$  phenyl region.

The higher i.r.  $\nu(\text{N}_2)$  value ( $2030 \text{ cm}^{-1}$ ) observed for complex B, compared to the value ( $1960 \text{ cm}^{-1}$ ) shown by compound A, suggests a weaker Re-N<sub>2</sub> bond for the former. Since

Table 1

Physical data for complexes  $\text{trans-[ReCl(N}_2\text{)(dppe)}_2\text{][BF}_4\text{]}$  (B),  $\text{trans-[ReCl(CNMe)(dppe)}_2\text{][BF}_4\text{]}$  (C),  $[\text{ReCl(dppe)}_2\text{][BF}_4\text{]}$  (D, *ortho-metallated*),  $[\text{ReCl(dppe)}_2]_2(\mu\text{-Cl})$  (E),  $[\text{ReOCl(dppe)}_2]$  (F) and  $[\text{ReCl}_2(\text{dppe})_3]$  (G, *ortho-metallated*)

Complex	Colour	Elemental microanalysis <i>a</i>			Relevant i.r. data <i>b</i>	$\Delta_M^c$	$\mu_{\text{eff}}$ B.M.	Molecular weight <i>a,d</i>
		% C	% H	% N				
B	Very dark red/green	55.3(55.1)	4.6(4.3)	2.9(2.5)	2030m[ $\nu(\text{N}_2)$ ] 1050vs( $\text{BF}_4^-$ )	80	1.9	—
C	Red	56.9(56.6)	5.0(4.5)	1.0(1.2)	2070s[ $\nu(\text{CN})$ ] 1050vs( $\text{BF}_4^-$ )	80	1.8	—
D	Yellow	56.1(56.5)	4.5(4.4)	—	1585sh, 1570m 1555m, 1525sh } <i>e</i> 1050vs( $\text{BF}_4^-$ ) 340ms[ $\nu(\text{ReCl})$ ]	70	3.95	$1.0 \times 10^3(1105.3)$
E	Yellow	60.2(60.3)	4.9(4.7)	—	280wm[ $\nu(\text{ReCl})$ ]	<i>f</i>	1.8	$1.94 \times 10^3(2072.4)$
F	Rose	49.4(49.1)	4.0(3.8)	—	903s[ $\nu(\text{Re} = \text{O})$ ]	<i>g</i>	<i>h</i>	$1.03 \times 10^3(1034.5)$
G	Pink	57.6(57.3)	4.6(4.4)	—	785m <i>e</i>	<i>g</i>	<i>h</i>	$1.59 \times 10^3(1638.5)$

*a* Required values in parentheses. *b* In Nujol null. *c* In  $\Omega^{-1} \text{ cm}^2 \text{ mol}^{-1}$ , measured in nitromethane, unless stated otherwise. *d* Measured in 1,2-dichloroethane. *e* Associated to *ortho*-metallated phosphine. *f* Non-electrolyte in nitromethane solution. *g* Non-electrolyte in 1,2-dichloroethane solution. *h* Diamagnetic.

complex B (Table 1) is paramagnetic ( $\mu_{\text{eff}} = 1.9 \text{ B. M.}$  in accordance with the presence of one unpaired electron), 1:1 electrolyte in nitromethane ( $\Delta_M = 80 \Omega^{-1} \text{ cm}^2 \text{ mol}^{-1}$ ) and a singlet due to the  $\text{BF}_4^-$  anion is observed in the  $^{19}\text{F}$  n.m.r. spectrum. No  $^{31}\text{P}$  n.m.r. was observed, possibly due to the paramagnetism, and the  $^1\text{H}$  n.m.r. spectrum displays very unusual sharp multiplet patterns along a wide range (Table 2) due to paramagnetic contact shifts.

the Re-N<sub>2</sub> bond in complex A presents a remarkable strength and, e.g., the replacement of dinitrogen by CNMe in a considerable extension requires a long refluxing time (above one week with partial decomposition) in thf, under argon, it would be advantageous to find a way to accelerate the loss of N<sub>2</sub> from the rhenium centre in order that the dinitrogen complex could be applied as a much more convenient starting material for the preparation of other

Table 2

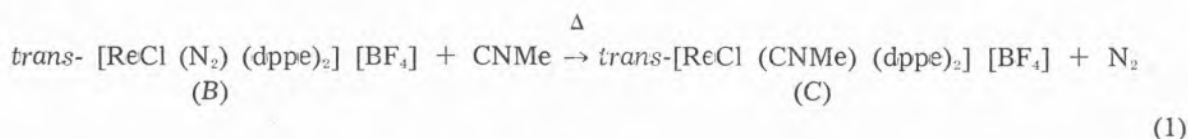
$^1\text{H}$  and  $^{31}\text{P}$  n.m.r. data <sup>a</sup> for complexes  $\text{trans-}[\text{ReCl}(\text{N}_2)(\text{dppe})_2][\text{BF}_4]$  (B),  $\text{trans-}[\text{ReCl}(\text{CNMe})(\text{dppe})_2][\text{BF}_4]$  (C),  $[\text{ReCl}(\text{dppe})_2][\text{BF}_4]$  (D, ortho-metalated),  $[\{\text{ReCl}(\text{dppe})_2\}(\mu\text{-Cl})]$  (E),  $[\text{ReOCl}(\text{dppe})_2]$  (F) and  $[\text{Re}_2\text{Cl}_2(\text{dppe})_3]$  (G, ortho-metalated).

Complex	$\delta$ ( $^1\text{H}$ ) ppm	Integration	Assignment	
B	9.56 s,br	2	$\text{C}_6\text{H}_5$ (dppe)	
	9.11 t b	2		
	8.05 t b	4		
	7.34 s	3		
	ca. 7.34-5.9 m,br c	29		
	2.11 s	2		8.5 (8)
	1.25 s	4		
	-4.55 d b	2.5		
	16.28 d d	3		
	16.15 d d	3		
C	10.16 br	1.5	$\text{C}_6\text{H}_5$ (dppe)	
	9.57 s	2		
	9.42 d b	2		
	9.13 t b	2		
	8.47 t b	3		
	8.08 t b	3		
	7.82 d b	1		
	7.34-7.08 m	19.5		
	5.6 m,br	3		11
	2.85 s	2		
	2.42 t d	3		
	1.60 s e	3		
	16.33 d f	2		
16.19 d f	5			
ca. 10.2 m,br	3			
9.59 d g	2			
9.44 d h	4			
9.15 t b	2			
8.50 t b	6			
8.10 t b	3			
7.97 s	1			
7.84 d h	3			
7.33 s,br	8			
5.6 d,br h	6	8		
ca. 3.2-2.3 m,br	1			
1.57 s	1			
E	ca. 13.5-6.0 m,br	80	$\text{C}_5\text{H}_5$ (dppe)	
	ca. 4.5-1.0 m,br	16	$\text{CH}_2$ (dppe)	
F i	8.4-6.6 m	40	$\text{C}_6\text{H}_5$ (dppe)	
	3.4-1.2 m,br	8	$\text{CH}_2$ (dppe)	
G j	8.3-7.9 m	8	$o\text{-C}_6\text{H}_4$ (dppe)	
	7.8-6.9 m	50	$\text{C}_6\text{H}_5$ (dppe)	
	3.0-1.9 m,br	12	$\text{CH}_2$ (dppe)	
	-2.2 br	ca. 2	Hydrides	

<sup>a</sup> In  $\text{CD}_2\text{Cl}_2$  solution.  $\delta$  ( $^1\text{H}$ ) relative to internal TMS.  $\delta$  ( $^{31}\text{P}$ ) relative to external TMP. <sup>b</sup>  $J = 7.3\text{Hz}$ . <sup>c</sup> Four broad resonances centered at  $\delta$  ca. 7.3, 6.9, 6.45 and 6.15 ppm. <sup>d</sup>  $J = 8.2\text{Hz}$ . <sup>e</sup> No further resonances were observed up to  $\delta = -15.7\text{ppm}$ . <sup>f</sup>  $J = 8.0\text{Hz}$ . <sup>g</sup>  $J = 4.6\text{Hz}$ . <sup>h</sup>  $J = 6.8\text{Hz}$ . <sup>i</sup>  $\delta$  ( $^{31}\text{P}$ ) =  $-130\text{s (ppm)}$ . <sup>j</sup>  $\delta$  ( $^{31}\text{P}$ ) =  $-106.9\text{d (43.2Hz)}$ ,  $-125.6\text{s}$ ,  $-129.6\text{s}$ ,  $-137.3\text{s}$ ,  $-147.6\text{d (43.2Hz)}$ ,  $-159.4\text{d (43.2Hz) (ppm)}$ .



complexes with related ligands (such as, isocyanides, carbonyl, nitriles, acetylenes, etc). Hence, the reaction of complex *B* with CNMe (ca. 3 molar excess) was studied in thf and, upon only 3h reflux under  $N_2$ , a red compound, *C*, could be isolated which, on the basis of microanalytical, i.r., magnetic, molar conductivity and  $^1H$  n.m.r. data (Tables 1 and 2), is formulated as the expected isocyanide complex *trans*-[ReCl(CNMe)(dppe) $_2$ ][BF $_4$ ], obtained through replacement of  $N_2$  by CNMe (equation 1).



Complex *C* exhibits, in the i.r. spectrum, a strong band at 2070  $cm^{-1}$  assigned to  $\nu(CN)$  (much higher than that observed in the neutral *trans*-[ReCl(CNMe)(dppe) $_2$ ] at ca. 1800-1830  $cm^{-1}$ ) and a very strong one at ca. 1050  $cm^{-1}$  associated to the BF $_4^-$  counterion; the i.r. data agree with those observed for another sample of complex *C* which was prepared independently by oxidation of the parent neutral isocyanide compound [5]. Compound *C* is paramagnetic ( $\mu_{eff} = 1.8$  B.M. in agreement with a  $d^5$  Re $^{II}$  octahedral centre) and a 1:1 electrolyte in nitromethane ( $\Lambda_M = 85 \Omega^{-1} cm^2 mol^{-1}$ ); its  $^1H$  n.m.r. spectrum exhibits unusual complex sets of sharp multiplets spread over a wide range (Table 2) and no resonance was found in the  $^{31}P$  n.m.r. spectrum, as it was observed in the related paramagnetic complex *B*.

The reaction of the oxidized dinitrogen complex *B* with CNMe in refluxing thf was described above.

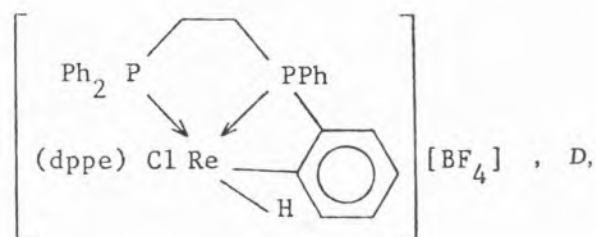
However, another, species, *D*, yellow in colour is also isolated from the reaction mixture as well as from a simple refluxing thf solution of complex *B*, in the absence of isocyanide.

No bands assignable to  $\nu(NN)$  or  $\nu(CN)$  are observed in the i.r. spectrum of *D* which only exhibits, as main bands and apart from those

due to dppe, a very strong one at 1050  $cm^{-1}$  (BF $_4^-$ ) and a medium/strong band at 340  $cm^{-1}$  which may conceivably be assigned to  $\nu(Re-Cl)$ . Microanalytical, molar conductivity ( $\Lambda_M = 70 \Omega^{-1} cm^2 mol^{-1}$  in nitromethane) and molecular weight ( $1.0 \times 10^3$  compared to the expected value, 1105.3) data (Table 1) agree with the formulation [ReCl(dppe) $_2$ ][BF $_4$ ] for species *D*. However, such a formulation would correspond to a 15-electron complex and it would be unacceptable particularly in the strong isocyanide ligand.

Complex *D*, however, presents a high paramagnetism ( $\mu_{eff} = 3.95$  B.M. which correspond to three unpaired electrons), its  $^1H$  n.m.r. spectrum consists of a series of sharp multiplets spread over a wide range (Table 2) and its i.r. spectrum exhibits, in the region just below 1600  $cm^{-1}$ , a complex pattern which may be diagnostic [6] of an *ortho*-metalated phosphine ligand: 1585 sh, 1570 m, 1555 m and 1525 sh, whereas, in the absence of *ortho*-metalation, only two bands would be expected, as it is usually observed in other dppe complexes.

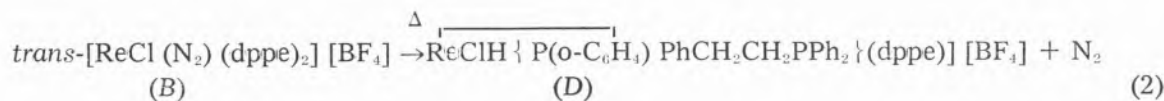
Hence, species *D* is tentatively formulated as an *ortho*-metalated compound of the type



with Re(IV),  $d^3$ , in agreement with the paramagnetic properties; it is a 17-electron complex which is coordinatively saturated (the coordination number is seven) which accounts

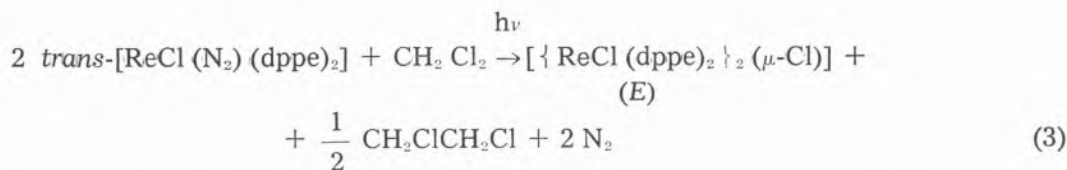
for its stability towards the addition of an isocyanide ligand

Complex *E* appears to be formed according to overall reaction (3) where the dichlorome-



Hence, one may possibly conclude that the dinitrogen ligand in the oxidized *trans*-[ReCl(N<sub>2</sub>)dppe]<sub>2</sub><sup>+</sup> complex presents a considerable lability and, upon heating, it is evolved to generate an unsaturated 15-elec-

thane, under irradiation, behaves as a chlorinating agent (giving possibly 1,2-dichloroethane) of the {ReCl(dppe)<sub>2</sub>} centre to afford a mixed valence Re(I)/Re(II) dimeric species. Hence, dichloromethane is able to oxi-



tron centre which may bind another substrate (such as an isocyanide, reaction 1) or, alternatively may rearrange through an *ortho*-metalation (undergoing a phenyl C-H bond oxidative addition, reaction 2) to afford a different saturated complex.

dize that electron-rich centre, although presenting, as expected, a milder oxidizing power than chlorine since the dichloro complex of Re(III), [ReCl<sub>2</sub>(dppe)<sub>2</sub>]Cl, is the product [3] of the reaction of the dinitrogen complex *A* with an excess of chlorine in chloroform.

## 2.2 — Reaction of *trans*-[ReCl(N<sub>2</sub>)(dppe)<sub>2</sub>], *A*, with dichloromethane

If a benzene solution of complex *A* with dichloromethane is irradiated with tungsten-filament light for ca. 2 days, a yellow species, *E*, may be isolated; it is formulated as the dimeric compound (possibly with a bridging chloro ligand) [<sub>2</sub>ReCl(dppe)<sub>2</sub>]<sub>2</sub>(μ-Cl), on the basis of microanalytical, molecular weight (1.94 × 10<sup>3</sup> in 1,2-dichloroethane, compared to the expected value of 2072.4), magnetic susceptibility (μ<sub>eff</sub> ≈ 1.8BM, which corresponds to one unpaired electron per two metal atoms), molar conductivity (non-electrolyte in nitromethane) and infrared data [a weak/medium band at 280 cm<sup>-1</sup> is assigned to ν(ReCl)] (Table 1). On account of the paramagnetism, the <sup>1</sup>H n.m.r. spectrum of *E* exhibits very broad resonances for the phenyl and the methylene protons (Table 2).

## 2.3 — Reaction of *trans*-[ReCl(N<sub>2</sub>)(dppe)<sub>2</sub>], *A*, with dioxygen and photolysis in the absence of any substrate.

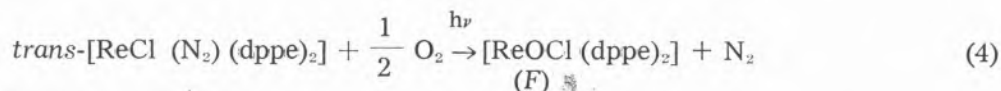
In the previous section the photochemical reaction of complex *A* with CH<sub>2</sub>Cl<sub>2</sub> in benzene (toluene) was mentioned. However, in the absence of CH<sub>2</sub>Cl<sub>2</sub> but in the presence of traces of air, a different oxidized species, *F*, is isolated, being formulated as the oxo complex [ReOCl(dppe)<sub>2</sub>], possibly formed according to equation (4).

It is rose in colour, a strong i.r. band observed at 903 cm<sup>-1</sup> is assigned to ν(Re=O), its molecular weight in 1,2-dichloroethane (1.03 × 10<sup>3</sup>) agrees with the expected value (1034.5) and it is a non-electrolyte in this solvent.

Complex *F* is diamagnetic and its <sup>1</sup>H and <sup>31</sup>P n.m.r. spectra (Table 2) agree with the

proposed formulation. It is also a product of the deoxygenation reaction of carbon dioxide

In the  $^1\text{H}$  n.m.r. spectrum (Table 2), a broad resonance (which integrates for  $2\text{H}^+$ ) is



by complex A, which will be described separately.

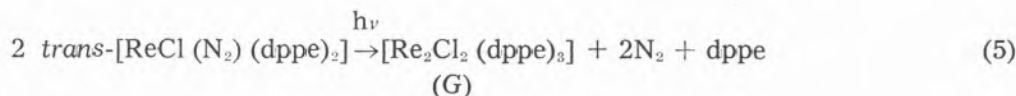
If the photolysis of a toluene solution of complex A (under one 100 Watt tungsten filament bulb) is carried out in the absence of any substrate, the unsaturated complex  $[\text{ReCl}(\text{dppe})_2]$ , whose structure was authenticated by X-rays, was isolated [4].

However, under stronger irradiation conditions [e.g., by using four 100 Watt tungsten filament bulbs at a short distance from the toluene reaction solution or by irradiating a thf solution of complex A with two 150 watt tungsten filament bulbs for an extended period of 5 days] the reaction appears to proceed with liberation of phosphine to afford a pink species formulated as  $[\text{Re}_2\text{Cl}_2(\text{dppe})_3]$ , G, (reaction 5) mainly on account of microanalytical data, molecular weight measurements ( $1.59 \times 10^3$  in 1,2-dichloroethane, compared to the expected value of 1638.5) and conductivity data (it is a non-electrolyte in this

observed at high field ( $\delta = -2.2$  ppm) whereas a complex multiplet (which integrates for  $8\text{H}^+$ ) occurs at low field ( $\delta = 8.3 - 7.9$  ppm), below the usual phenyl proton range; these resonances may be assigned [7] to the hydride ligands and to the aromatic  $o\text{-C}_6\text{H}_4$  groups involved in the *ortho*-metalation. Moreover, although the i.r. region just below  $1600\text{ cm}^{-1}$  is not clear enough, extra bands with a high intensity are observed at  $785\text{ cm}^{-1}$  (sharp),  $1095\text{ cm}^{-1}$  (broad) and  $1190\text{ cm}^{-1}$  and, at least the first two of them, have been assigned [7,8] to a phenyl group involved in *ortho*-metalation.

The  $^{31}\text{P}$  n.m.r. spectrum of compound G is a complex multiplet (Table 2) which spans over a wide range, as expected in view of the presence of different types of phosphorus nuclei involved in chelate rings of distinct sizes.

The lowest field  $^{31}\text{P}$  resonance occurs at a chemical shift [ $\delta = -106.9$  ppm relative to



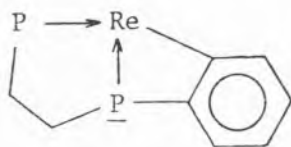
solvent) (Table 1). The dimeric structure would result from chloro or/and dppe bridges between the two metal centres.

However, this simple formulation of species G would correspond to a highly unsaturated metal site unless, as it was suggested for complex D, an *ortho*-metalation is postulated to occur. Moreover, this proposal is substantiated by some n.m.r. and i.r. data as follows.

$\text{P}(\text{OMe})_3$ ] which is similar to those observed for chelating dppe ligands in related complexes [e.g.  $-108.6$  and  $-109.8$  ppm for *trans*- $[\text{ReCl}(\text{CNMe})(\text{dppe})_2]$  [9] and *trans*- $[\text{ReCl}(\text{C}=\text{CHPh})(\text{dppe})_2]$ , [10], respectively]; hence, it is associated to a phosphorus nucleus in a 5-membered ring of a chelating dppe ligand.

The chemical shift of the highest field  $^{31}\text{P}$  resonance ( $\delta = -159.4$  ppm) occurs  $52.5$  ppm

upfield from the abovementioned resonance, and this shift is identical to that expected (ca. 52 ppm) [11] for the contribution of a 4-membered ring which, in complex G, conceivably results from an *ortho*-metalation. Hence, the resonance at  $\delta = -159.4$  ppm is tentatively assigned to a phosphorus atom of a chelating dppe ligand which is also involved in an *ortho*-metalation, *i.e.*,



The  $^{31}P$  n.m.r. spectrum also exhibits resonances which are intermediate between the abovementioned limits and, possibly, they may be associated, in part, to a non-chelating (bridging) dppe ligand whose phosphorus resonance would be expected [11] to occur at ca. 33 ppm upfield from that ( $\delta = -106.9$  ppm) of the P atom in the chelating ligand.

### 3 — FINAL COMENTS

Chemical oxidation or photochemical excitation promotes the lability of  $N_2$  at the  $trans-[ReCl(N_2)(dppe)_2]$  complex which can then undergo a ready replacement of the  $N_2$  ligand by a non-oxidizing substrate (such as isocyanide) or which, upon  $N_2$  loss, may be further oxidized by an oxidizing agent (*e.g.*, being chlorinated by dichloromethane or oxygenated by dioxygen). In the absence of any substrate, dinitrogen evolution is followed by an internal oxidative-addition reaction (*ortho*-metalation) to afford coordinatively saturated oxidized species.

The easy oxidation of the electron-rich centre  $\{ReCl(dppe)_2\}$  and the ability of this unsaturated site to bind various substrates are well patent in the reactions described in this study.

### 4 — EXPERIMENTAL

All the reactions (unless otherwise stated) were carried out in the absence of air using standard inert gas flow and vacuum techniques. Solvents were purified by standard techniques and  $trans-[ReCl(N_2)(dppe)_2]$ , A, was prepared by a published method [3]. Infrared measurements were carried out on a Perkin-Elmer 683 spectrometer  $^1H$  and  $^{31}P$  n.m.r. spectra were recorded on a Jeol JNM-PS-100, a Bruker CXP 300 or a Jeol PFT 100 Fourier-transform spectrometer. Molecular weights and magnetic susceptibilities were determined using a Perkin-Elmer osmometer and a Faraday balance, respectively. Conductivities were measured using a Portland Electronics P 310 conductivity bridge.

#### — Preparation of $trans-[ReCl(N_2)(dppe)_2][BF_4]$ , B

$AgBF_4$  (0.282 g) was added to a stirred solution of  $trans-[ReCl(N_2)(dppe)_2]$  (0.329 g) in thf (140 cm<sup>3</sup>). An immediate formation of a fine black precipitate of metal silver occurred, whereas the solution became very dark. After ca. 1h, the solution was filtered, concentrated under vacuum and a very dark purple (violet) solid precipitated out upon addition of pentane. This solid was filtered-off, washed with a mixture of thf/pentane and dried under vacuum; it was then recrystallised from  $CH_2Cl_2/Et_2O$  to afford complex B as very dark/violet platelets (ca. 0.3 g) which were filtered-off, washed with a mixture of  $CH_2Cl_2/Et_2O$  and dried under vacuum (very dark green was the final colour of the dried product).

#### — Preparation of $trans-[ReCl(CNMe)(dppe)_2][BF_4]$ , C, and $[ReCl(dppe)_2][BF_4]$ , D.

A solution of  $trans-[ReCl(N_2)(dppe)_2][BF_4]$ , B (0.309 g), with CNMe (0.15 ml, *i.e.*, in a



3.2 molar excess) in thf (60 cm<sup>3</sup>) was refluxed under N<sub>2</sub> for ca. 3h; during this period the solution colour changed from dark violet to red. It was then concentrated under vacuum, with heating, until complex *D* precipitated as a yellow solid (ca. 0.090 g) which was filtered-off, washed with a mixture of thf/pentane dried under vacuum (the same compound may be prepared, in a better yield, by carrying out the reaction in the absence of CNMe and under identical experimental conditions).

The mother liquor solution (red in colour) separated from *D* by filtration was concentrated and complex *C* precipitated out (ca. 0.20 g) as a red solid upon addition of pentane; it was filtered-off, washed with a mixture of thf/pentane and dried under vacuum.

— Preparation of  $[\mu\text{-ReCl}(\text{dppe})_2]_2$ , *E*

A benzene (250 cm<sup>3</sup>) solution of *trans*-[ReCl(N<sub>2</sub>)(dppe)<sub>2</sub>], *A* (0.40 g), with CH<sub>2</sub>Cl<sub>2</sub> (ca. 0.1 ml) was prepared under argon (this addition of CH<sub>2</sub>Cl<sub>2</sub> may not be required provided that complex *A* was previously recrystallized from CH<sub>2</sub>Cl<sub>2</sub>: the solvent of crystallization is enough for the reaction to occur). The stirred solution was then irradiated, under reduced pressure, by two 100 Watt tungsten-filament bulbs for ca. 2 days. The reaction solution was then heated to dryness, under vacuum, and the resulting solid was washed with hot benzene. The yellow residue of complex *E* (ca. 0.15 g) was then dried under vacuum.

— Preparation of [ReOCl(dppe)<sub>2</sub>], *F*

To a solution of complex *trans*-[ReCl(N<sub>2</sub>)(dppe)<sub>2</sub>] (0.35 g) in toluene (250 cm<sup>3</sup>), which was prepared under argon, a portion of air was admitted. The solution was then irradiated by four 100 Watt tungsten filament bulbs for about 2 days, concentrated, with heating, under vacuum, until complex *F* precipitated as a rose solid which was filtered-off,

washed with toluene and dried under vacuum. A further crop of species *F* could be obtained upon concentration of the mother liquor and addition of petroleum ether 40-60; the precipitate was washed with toluene and the residue (species *F*) was dried under vacuum (the total amount of *F* was ca. 0.10 g).

— Preparation of [Re<sub>2</sub>Cl<sub>2</sub>(dppe)<sub>3</sub>], *G*

A stirred solution of *trans*-[ReCl(N<sub>2</sub>)(dppe)<sub>2</sub>], *A* (0.30 g), in toluene (200 cm<sup>3</sup>), which was prepared under argon, was irradiated by four 100 Watt tungsten filament bulbs for about 2 days. It was then concentrated under vacuum and pentane was added until a brownish solid precipitated out. The solution was filtered and a brownish pink solid was obtained upon addition of petroleum ether 40-60; this solid was filtered-off and recrystallized from hot toluene to afford complex *G* as a brownish pink solid which was filtered-off, washed with a mixture of toluene/petroleum ether and dried under vacuum (ca. 0.070 g).

Complex *G* may also be prepared by irradiating a thf solution (250 cm<sup>3</sup>) of compound *A* (0.20 g) with two 150 Watt tungsten filament bulbs for 5 days. The solution was then concentrated under vacuum and pentane was added until appearance of a yellowish solid which was filtered-off. The resulting solution was again concentrated and complex *G* precipitated as a pink solid upon addition of pentane; it was filtered-off, washed with a mixture of thf/pentane and dried under vacuum (ca. 0.060 g).

Received, 13th May, 1985

## REFERENCES

- [1] A.J.L. POMBEIRO, «Preparation, Structure, Bonding and Reactivity of Dinitrogen Complexes», Ch. 6, in «New Trends in the Chemistry of Nitrogen Fixation», J. Chatt, L.M.C. Pina, R.L. Richards, eds., Academic Press, 1980; Academy of Sciences of Lisbon, 1982; MIR Editions, 1983 (Russian Translation).



- [2] A.J.L. POMBEIRO, *Rev. Port. Quím.*, **21**, 90 (1979).
- [3] J. CHATT, J.R. DILWORTH, G.J. LEIGH, *J.C.S. Dalton*, **1973**, 612; J. Chatt, J.R. Dilworth, H.P. Gunz, G.P. Leigh, J.R. Sanders, *Chem. Comm.*, **1970**, 90
- [4] D.L. HUGHES, A.J.L. POMBEIRO, C.J. PICKETT, R.L. RICHARDS, *J. Organometal. Chem.*, **248**, C26 (1983).
- [5] M.F.N.N. CARVALHO, A.J.L. POMBEIRO, unpublished work.
- [6] D.P. ARNOLD, M.A. BENNETT, *X Intern. Conf. Organometal. Chem.*, Toronto, Canada, 1981, 2E86; M.A. Bennett, D.L. Milner, *J. Am. Chem. Soc.*, **91**, 6983 (1969).
- [7] E.W. AINSCOUGH, S.D. ROBINSON, *J. Chem. Soc. (A)* **1971**, 3413.
- [8] J.J. LEVISON, S.D. ROBINSON, *J. Chem. Soc. (A)*, **1970**, 639.
- [9] A.J.L. POMBEIRO, M.F.N.N. CARVAHO, P.B. HITCHCOCK, R.L. RICHARDS, *J.C.S. Dalton*, **1981**, 1629.

[10] A.J.L. POMBEIRO, unpublished work.

[11] P.E. GARROU, *Chem. Rev.*, **81**, 229 (1981).

## RESUMO

Estudo de reacções de oxidação do complexo *trans*-[ReCl(N<sub>2</sub>)(Ph<sub>2</sub>PCH<sub>2</sub>CH<sub>2</sub>PPh<sub>2</sub>)<sub>2</sub>]

A oxidação do complexo *trans*-[ReCl(N<sub>2</sub>)(dppe)<sub>2</sub>] (A, dppe = Ph<sub>2</sub>PCH<sub>2</sub>CH<sub>2</sub>PPh<sub>2</sub>) por AgBF<sub>4</sub> conduz à formação de uma espécie catiónica em que o ligando N<sub>2</sub> apresenta acentuada labilidade sendo facilmente substituído por CNMe formando *trans*-[ReCl(CNMe)(dppe)<sub>2</sub>][BF<sub>4</sub>]; em alternativa, pode ocorrer um rearranjo do complexo insaturado [ReCl(dppe)<sub>2</sub>][BF<sub>4</sub>] com formação de uma espécie orto-metalada. Por cloração fotoquímica de A por CH<sub>2</sub>Cl<sub>2</sub> forma-se [Re<sub>2</sub>Cl<sub>3</sub>(dppe)<sub>4</sub>], enquanto que o composto oxo [ReOCl(dppe)<sub>2</sub>] é gerado na presença de dioxigénio; fotólise de uma solução de A na ausência de qualquer substrato conduz à formação de uma espécie, [Re<sub>2</sub>Cl<sub>2</sub>(dppe)<sub>3</sub>], possivelmente dimérica e orto-metalada.

ANA M. LOBO  
SUNDARESAN PRABHAKAR  
M. AMÉLIA SANTOS

Centro de Química Estrutural,  
Complexo I,  
Av. Rovisco Pais,  
1096 Lisboa Codex  
and Secção de Química Orgânica Aplicada, FCT,  
New University of Lisbon,  
Quinta da Torre,  
2825 Monte da Caparica, Portugal

HENRY S. RZEPA

Department of Chemistry,  
Imperial College of Science and Technology,  
London SW7 2AY, UK.



# MAGNETIC NON-EQUIVALENCE IN THE LOW-TEMPERATURE NUCLEAR MAGNETIC RESONANCE SPECTRA OF *N*-BENZYL- *N*-METHYLHYDROXYL- AMINE AND ITS ANION— COMPARISON WITH SCF —MO CALCULATIONS

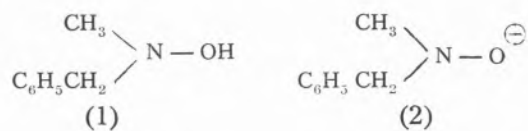
From the  $^1\text{H}$  n.m.r. analysis of *N*-benzyl-*N*-methylhydroxylamine and its anion the observed magnetic non-equivalence of the benzylic protons is rationalised in terms of slow nitrogen inversion being the rate determining step in the dynamic process. Molecular orbital calculations (MNDO and *ab initio*) carried out on the model *N,N*-dimethylhydroxylamine and the corresponding anion lend further support to this hypothesis.

## INTRODUCTION

The conformational analysis of compounds containing single bonds between atoms bearing pairs of nonbonding electrons have attracted considerable attention, [1] including hydroxylamine and its derivatives.

Since the observation of magnetic non-equivalence in the low-temperature  $^1\text{H}$  n.m.r. spectra of some hydroxylamines derivatives, there has been controversy concerning the nature of the measured rate process. Whereas in the case of cyclic hydroxylamines there seems to exist general agreement as to the origin of the observed magnetic non-equivalence, which is attributed to pyramidal inversion at *N*, [2-4] the opposite holds for acyclic hydroxylamines. In the latter case a competitive intramolecular conformational process leading to a substantial barrier to rotation about the *N*-O bond cannot be dismissed *a priori*.

Previous work [5] had shown that *N*-benzyl-*N*-methylhydroxylamine does exhibit magnetic non-equivalence of the benzylic hydrogens at low temperature.



It is the aim of our work to contribute to the clarification of the factors involved in the observed magnetic non-equivalence of the methylene group in the low temperature  $^1\text{H}$  n.m.r. spectra of *N*-benzyl-*N*-methylhydroxylamine 1 and its anionic derivative 2.

## RESULTS AND DISCUSSION

$^1\text{H}$ . n.m.r. analysis. — At room temperature (probe temperature at  $300 \pm 3$  K) and in  $\text{CD}_3\text{OD}$ , the  $^1\text{H}$  n.m.r. spectra of 1 (see Table 1) showed, for the two benzylic protons, a sharp singlet at  $\delta$  3.85, while its corresponding anion showed for the same methylene group a broad absorption at ca.

$\delta$  3.73 (see Table 1). The upfield shift can be accounted for by the shielding effect of the adjacent negative oxygen.

On lowering the temperature, the signals due to the methylene protons of (1) and (2) broadened, and finally became AB quartets (see Table 2), the temperature of coalescence being approximately 266 and 289 K

observed in the anion is noteworthy. For this kind of compound this can only be rationalised by the larger anisochrony resulting from a different orientation of the benzylic protons and the lone pair in the nitrogen atom of 2, relative to 1. We also note that the broadening as a function of temperature was fully reversible, indicating that broadening

Table 1

<sup>1</sup>H N.M.R. data at 300 ± 3 K

Compound	Solvent	$\delta$ * (number of protons, multiplicity **)		
		CH <sub>3</sub>	CH <sub>2</sub>	Ar-H
PhCH <sub>2</sub> NMeOH	CD <sub>3</sub> OD	2.61 (3, s)	3.85 (2, s)	7.30-7.32 (5, m)
PhCH <sub>2</sub> NMeO <sup>⊖</sup> Na <sup>⊕</sup>	CD <sub>3</sub> OD	2.47 (3, s)	3.73 (2, b)	7.20-7.34 (5, m)

\* p.p.m. from T.M.S.

\*\* s = singlet, b = broad singlet, m = multiplet.

for the neutral and charged species respectively.

The limit of exchange broadening was approximately 220 K for 1, while for the corresponding anion no significant changes were observed below 238 K. The much larger difference between the chemical shifts of the diastereoisotopic protons (anisochrony)

due to the presence of paramagnetic impurities from oxidation of the hydroxylamine can be discounted.

The rate constants of chemical exchange at different temperatures were determined by lineshape analysis of the AB quartets. These were obtained by visual comparison between the experimental spectrum and the com-

Table 2

Low temperature <sup>1</sup>H n.m.r. data for the methylene protons

Compound *	$\Delta\nu_{AB}$ /Hz	$J_{AE}$ /Hz	$T_C$ /K
PhCH <sub>2</sub> NMeOH (219.8 K)	31.29	— 12.67	265.8
PhCH <sub>2</sub> NMeO <sup>⊖</sup> Na <sup>⊕</sup> (238.2 K)	137.82	— 11.65	287.9

\* In brackets the temperature below which no further changes in lineshape could be observed.

puted line shape for the hydroxylamine and its anion (see Fig. 1 and Fig. 2).

Kinetic data with the corresponding Eyring parameters can be found in Table 3 and 4,

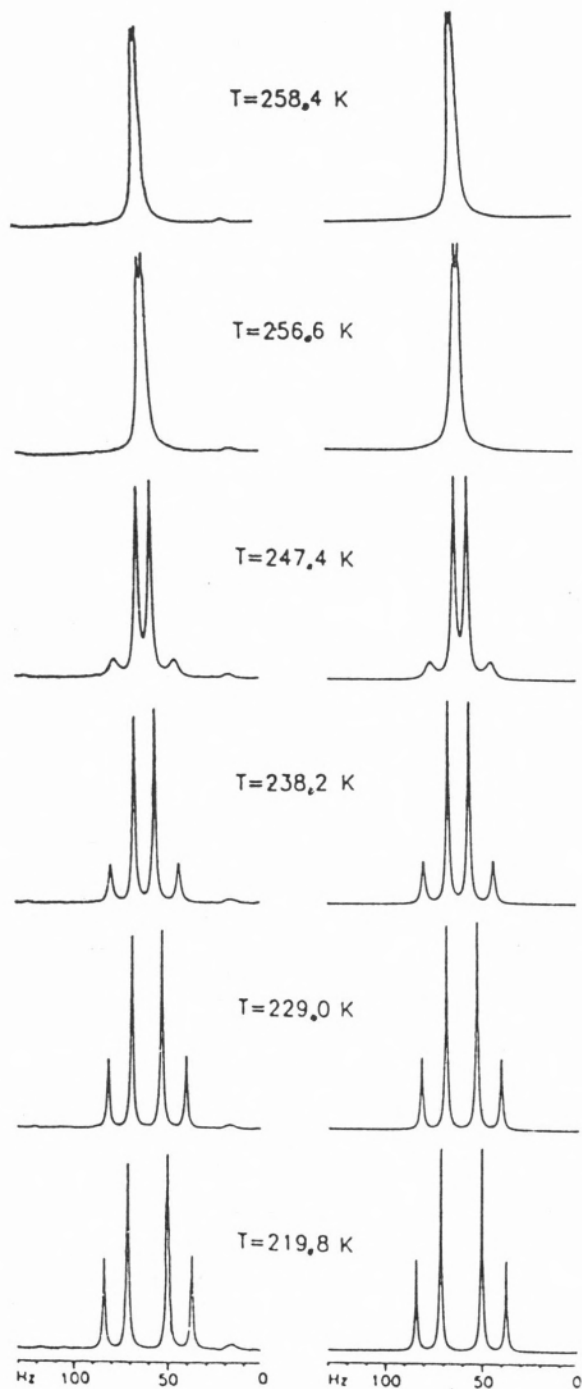


Fig. 1

Experimental (left) and computed (right) d.n.m.r. spectra of  $\text{PhCH}_2\text{NMeOH}$ .

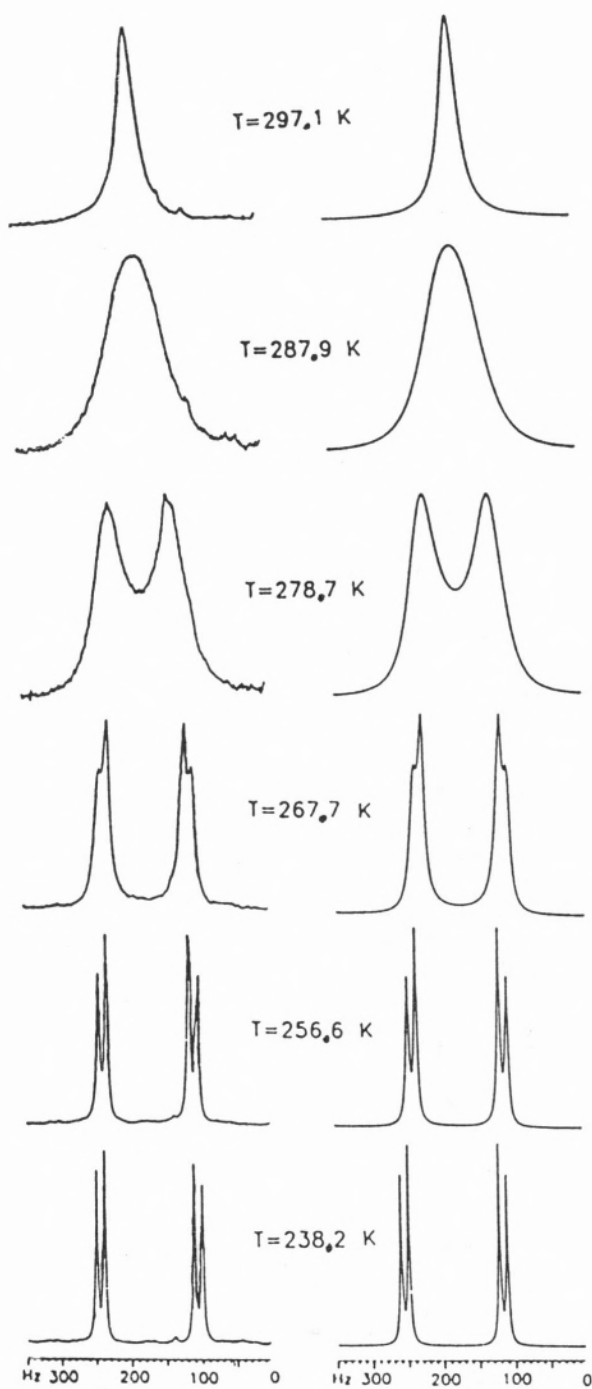


Fig. 2

Experimental (left) and computed (right) d.n.m.r. spectra of  $\text{PhCH}_2\text{NMeO}^- \text{Na}^+$ .

Table 3

Kinetic data for  $\text{PhCH}_2\text{NCH}_3\text{OH}$   
 ( $\sim 0.02 \text{ M}$  in  $\text{CD}_3\text{OD}$ ;  $T_2 = 0.25 \text{ s}$ )

Temperature K	$k/\text{s}^{-1}$	$\Delta\nu/\text{Hz}$	$10^3 (1/T)/\text{K}^{-1}$	$\ln(k/T)$
229.0	0.5	25.5	4.367	-6.126
238.2	2.0	19.9	4.198	-4.780
247.4	8.0	15.3	4.042	-3.432
256.6	26.6	12.0	3.897	-2.267
258.4	32.0	10.0	3.870	-2.089

Table 4

Kinetic data for  $\text{PhCH}_2\text{NCH}_2\text{O}^-\text{Na}^+$   
 ( $\sim 0.02 \text{ M}$  in  $\text{CD}_3\text{OD}/\text{CD}_3\text{O}^-\text{Na}^+$ ;  $T_2 = 0.15 \text{ s}$ )

Temperature K	$k/\text{s}^{-1}$	$\Delta\nu/\text{Hz}$	$10^3 (1/T)/\text{K}^{-1}$	$\ln(k/T)$
256.6	9.5	128.0	3.897	-3.244
267.7	29.5	120.2	3.736	-2.009
278.7	136.0	114.1	3.588	-0.881
287.9	296.0	108.7	3.473	-0.004
297.1	660.0	103.2	3.365	0.818

while the Eyring plots are shown in Fig. 3 and 4 respectively.

The activation parameters displayed in Table 5 indicate:

1 — A good agreement between the value of  $\Delta G^\ddagger$  ( $53.6 \text{ kJ mol}^{-1}$ ) for **1** in deuterated methanol and the reported [5] value ( $51.9 \text{ kJ mol}^{-1}$ ) in deuterated acetone.

2 — The free energy of activation for the anion **2**, relative to **1** is only marginally higher, ( $2.9 \text{ kJ mol}^{-1}$ ), lending support to the importance of electronic differences. In **2**, there are three lone pairs on the oxygen, resulting in greater repulsion with the nitrogen lone pair in the transition state. Furthermore in **2**, magnetic nonequivalence must arise as the result of slow nitrogen inversion, because the angle of rotation about the N-O bond remains undefined.



As pointed out earlier, [5] the steric acceleration found for *N*-benzyl-*N*,*O*-dimethylhydroxylamine ( $\Delta G_c^\ddagger$  41.4 kJ mol<sup>-1</sup> in ace-

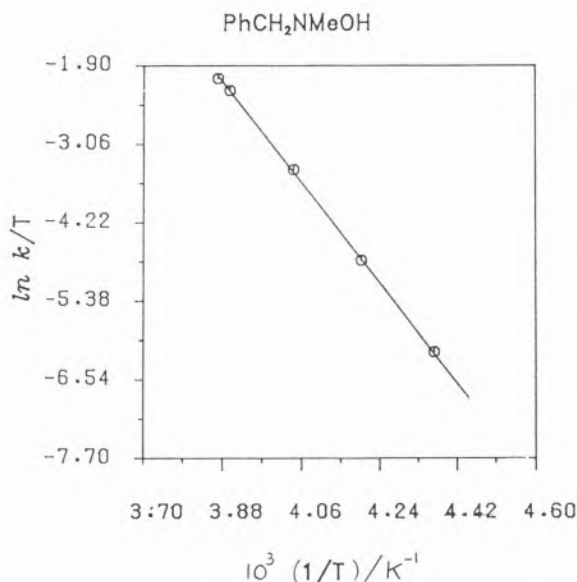


Fig. 3

Eyring plot for PhCH<sub>2</sub>NMeOH.

tone-d<sub>6</sub>) relative to *N*-benzyl-*N*-methylhydroxylamine ( $\Delta G_c^\ddagger$  51.9 kJ mol<sup>-1</sup> in the same

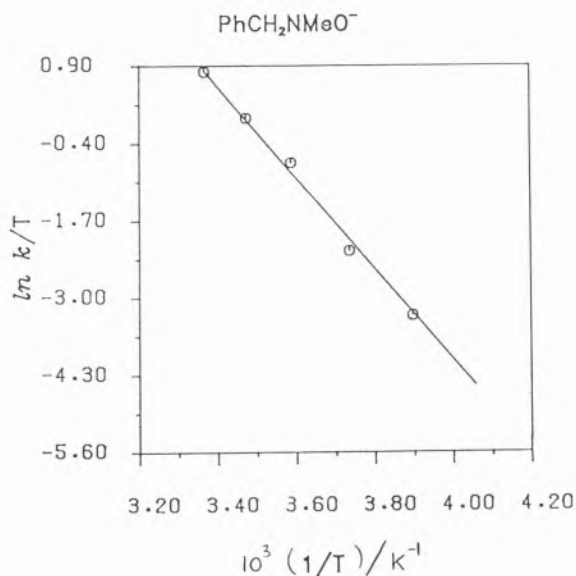
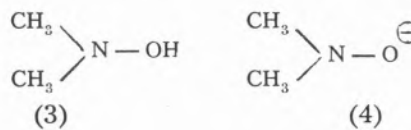


Fig. 4

Eyring plot for PhCH<sub>2</sub>NMeO<sup>-</sup>Na<sup>+</sup>

solvent) has been taken to confirm likewise that nitrogen inversion is the rate determining step of the dynamic process associated with the diastereotopicity of the methylene protons. A similar conclusion was reached by Hall [7] and his group, studying various *N*-arylethyl-*N*,*O*-dimethylhydroxylamines, but increase in the bulkiness of the groups attached to *N* and *O* can dramatically change this situation as found more recently by Iwamura [8] and coworkers. The Japanese chemists, who assigned the slow step to restricted rotation around one of the skeletal C-N-O-C bonds, based their conclusion on the fact that practically no change in the energetic barriers were found when a benzyl group attached to nitrogen was replaced by a phenyl in a similar hydroxylamine derivative. In our hands however, *N*-benzyl-*N*-phenylhydroxylamine failed to show any magnetic non-equivalence of the methylene protons when the temperature was as low as 190 K.

*SCF - MO Calculations*—The results of molecular orbital calculations, by the MNDO [14] and *ab initio* [15] methods using a STO-3G basis set, carried out on the models *N*, *N*-dimethylhydroxylamine 3 and the corresponding anion 4 are summarised in Table 6.



A generally greater value of  $\Delta G_c^\ddagger$  was found for the anionic derivative 4 than for the neutral molecule 3, the differences being however bigger in the theoretical calculations, ( $\Delta\Delta G_c^\ddagger$  37.7 kJ mol<sup>-1</sup>—MNDO; 13.6 kJ mol<sup>-1</sup>—STO-3G // MNDO) than in the actual result ( $\Delta\Delta G_c^\ddagger$  2.9 kJ mol<sup>-1</sup>). A better agreement with experimental values is thus found when using the STO-3G // MNDO method.

A smaller theoretical value for the activation entropy is found for the anion relative

Table 5

Coalescence temperature and activation parameters for *N*-benzyl-*N*-methylhydroxylamine and its anion

Compound	Solvent	$T_c/K$	$\Delta H^\ddagger/kJ\ mol^{-1}$	$\Delta S^\ddagger/JK^{-1}\ mol^{-1}$	$\Delta G_{298}^\ddagger/kJ\ mol^{-1}$
PhCH <sub>2</sub> NMeOH	CD <sub>3</sub> OD	265.8	68.2 ± 2.9	49.0 ± 0.8	53.6 ± 2.9
PhCH <sub>2</sub> NMeO <sup>⊖</sup> Na <sup>⊕</sup>	CD <sub>3</sub> OD	287.9	65.7 ± 10.0	36.5 ± 2.9	56.5 ± 10.0

Table 6

Molecular orbital calculations for the nitrogen inversion of *N,N*-dimethylhydroxylamine and its anion

	$\Delta H^\ddagger$ (method) KJ mol <sup>-1</sup>	$\Delta S^\ddagger$ (method) JK <sup>-1</sup> ml <sup>-1</sup>	$\Delta G_{298}^\ddagger$ (method) KJ mol <sup>-1</sup>
Me <sub>2</sub> NHOH	31.1 (a) (MNDO) 60.3 (b) (STO-3G // MNDO)	12.3 (MNDO) —	27.4 (MNDO) 58.8 (c) (STO-3G // MNDO)
Me <sub>2</sub> NHO <sup>⊖</sup> Na <sup>⊕</sup>	65.6 (a) (MNDO) 72.9 (b) (STO-3G // MNDO)	1.8 (MNDO) —	65.1 (MNDO) 72.4 (c) (STO-3G // MNDO)

(a) Difference between the transition and ground state heat of formation.

(b) Difference between the transition and ground state absolute energy.

(c) MNDO values were used to calculate  $\Delta G^\ddagger$ :

to the neutral hydroxylamine ( $\Delta\Delta S^\ddagger$  10.5 Jk<sup>-1</sup> mol<sup>-1</sup>), which is nevertheless less than the experimental difference ( $\Delta\Delta S^\ddagger$  18.4 Jk<sup>-1</sup> mol<sup>-1</sup>). However the fact that  $\Delta S^\ddagger$  is the parameter most dependent on errors in the lineshape analysis would limit the weight of any theoretical interpretation advanced.

## CONCLUSIONS

Given the good theoretical concordance found with the experimental results obtained, and the similarity of the values of the free energy of activation for the dynamic processes occurring with 3 and 4, the best rationale for the origin of the rate-limiting process governing the non-equivalence of the

an aqueous solution of *N*-methylhydroxylamine group in both 1 and 2 is slow-nitrogen inversion. This process is in any case the only conceivable explanation for the behaviour presented by 2.

The slightly greater value for the free energy of activation observed for the anion can be explained in terms of an increase in instability experienced by its nitrogen planar transition state, due to a greater repulsive effect between the electronic nitrogen lone pair and the negative charge in the oxygen atom.

## EXPERIMENTAL

### *N*-Methylbenzaloxime

To a suspension of benzaldehyde (2.6 g) in 2 N sodium hydroxide (70 cm<sup>3</sup>) was added

an aqueous solution of *N*-methylhydroxylamine (2.2 g in 5 cm<sup>3</sup>). T.l.c. control showed that, after 1 hour of stirring at room temperature, all the aldehyde had disappeared, and the *N*-methylbenzaloxime, remaining in solution, was extracted several times with dichloromethane (3 × 10 cm<sup>3</sup>). The organic phase was dried with magnesium sulfate, the solvent was evaporated under reduced pressure, giving rise to a solid residue. On crystallisation from benzene-*n*-hexane white crystals (3.13 g, 94 %) of *N*-methylbenzaloxime were obtained with m.p. 83-84° (lit. [9] 84°).

#### *N*-Methyl-*N*-benzylhydroxylamine

A solution of *N*-methylbenzaloxime (3.04 g) in a mixture of benzene (10 cm<sup>3</sup>) and ether (30 cm<sup>3</sup>) was added to a suspension of lithium hydride (0.45 g) in ether (10 cm<sup>3</sup>) and the mixture refluxed for 4 hours.

The reaction mixture was treated with a small amount of water (ca. 2 cm<sup>3</sup>), the white inorganic precipitate filtered off and extracted with diethyl ether (3 × 10 cm<sup>3</sup>).

The combined extracts were dried with anhydrous sodium sulfate, the organic solution was concentrated under reduced pressure and the residue recrystallised from *n*-hexane to give *N*-methyl-*N*-benzylhydroxylamine (2.83 g, 98 %), m.p. 40-41° lit. [10] 40-41°.

#### *N*-Methyl-*N*-benzylhydroxylamine anion

To solution of *N*-methyl-*N*-benzylhydroxylamine in CD<sub>3</sub>OD was added carefully with stirring an excess of sodium metal.

#### <sup>1</sup>H N.M.R. Spectroscopy

Spectra were recorded on a Brüker WM 250 spectrometer and the sample temperature calibrated using a standard methanol sample together with the chemical shift data of Van Geet [11].

The lineshape analysis of the *AB* spin system corresponding to the diastereoisotopic methylene protons of the *N*-benzyl group was carried out by comparison with simulated spectra produced by the program DNMR 3H [12].

The temperature dependence of the resonance frequency differences  $\Delta\nu_{AB}$  is displayed on Tables 3 & 4. In regions where exchange broadening prevented direct measurement of  $\Delta\nu_{AB}$  these parameters were obtained by least square extrapolation from lower temperature values. The coupling constants  $J_{AB}$  were found to be temperature independent. The rate constant  $k$  for the exchange process and the spin-spin relaxation time  $T_2$  were adjusted to produce the best visual fit. The latter values did not differ significantly from those obtained from the low temperature limiting spectra

$$(T_2 = \frac{1}{\pi \omega_{1/2}}).$$

Activation parameters for the *AB* exchange process were obtained by a least square analysis of the rate constants as a function of temperature using the Eyring equation [13].

#### SCF — MO Calculations

Molecular orbital calculations of the activation enthalpy,  $\Delta H^\ddagger$  for the *N*-inversion of 3 and 4, were carried out using the MNDO [14] method with full geometry optimisation and the *ab initio* method (basis set STO-3G) [15], at the optimised MNDO geometry (STO-3G // MNDO).

Activation enthalpies for 3 and 4 were obtained by difference between the transition state (*N* planar) and the ground state (optimized geometry) enthalpies of formation (MNDO) or absolute energies (STO-3G // MNDO).

Activation entropies were obtained from the difference between the calculated molar entropy of the ground state and the planar

transition state, using the method described previously, [16] and the calculated MNDO normal vibrational frequencies [17].

To reduce the computation time, the benzyl groups of 1 and 2 were modelled by methyl groups.

Received, 2nd August 1985

## ACKNOWLEDGEMENTS

We thank Junta Nacional de Investigação Científica, Gulbenkian Foundation and NATO for partial financial support.

Calculations using Gaussian 76, MNDO and DNMR 3H were carried out on the CDC 760 Computer at the University of London Computer Centre and the CDC Cyber 174 and 170-855 computers at Imperial College Computer Center.

## REFERENCES

- [1] F.G. RIDELL, *Tetrahedron*, **37** 849 (1981).
- [2] W.D. EMMONS, *J. Amer. Chem. Soc.*, **79**, 5739 (1957).
- [3] J. LEE and K.G. ORRELL, *Trans. Faraday Soc.*, **61**, 2342 (1965).
- [4] a) F.G. RIDELL, J.M. LEHN and J. WAGNER, *J.C.S., Chem. Comm.*, 1403 (1968).  
b) D.L. GRIFFITH and B.L. OLSON, *J.C.S., Chem. Comm.*, 1682 (1968).  
c) M. RABAN, F.B. JONES, E.H. CARLSON, E. BANUCCI and N.A. LEBEL, *J. Org. Chem.*, **35**, 1496 (1970).
- [5] D.L. GRIFFITH, B.L. OLSON and J.D. ROBERTS, *J. Amer. Chem. Soc.*, **93**, 1648 (1971).
- [6] For example compare data from ref. 5 and M. RABAN and G.W.J. KENNEDY, *Tetrahedron Letters*, 1295 (1969).
- [7] T.B. POSNER, D.A. COUCH, and C.D. HALL, *J.C.S., Perkin 2*, 450 (1978).
- [8] M. IWAMURA, M. KATOH and H. IWAMURA, *Org. Magn. Reson.*, **14**, 392 (1980).
- [9] O.L. BRADY, F.P. DUNN and R.F. GOLDSTEIN, *J. Chem. Soc.*, 2390 (1926).
- [10] O. EXNER, *Coll. Czech. Chem. Comm.*, **20**, 202 (1955).
- [11] A.L. VAN GEET, *Anal. Chem.*, **40**, 2227 (1968).
- [12] G. STEVENSON and G. BINSCH, Quantum Chemistry Program Exchange, Program No. 458, Indiana State University, Indiana, U.S.A..
- [13] Cf. G. Binsch in «Dynamic Nuclear Magnetic Resonance Spectroscopy», Eds. L.M. Jacman and F.A. Cotton, Academic Press, London, 1975, Chapter 3, p. 70.
- [14] M.J.S. DEWAR and W. THIEL, *J. Amer. Chem. Soc.*, **99**, 4908 (1977); M.J.S. Dewar and M.L. McKee, *ibid.*, **99**, 5841 (1977); M.J.S. Dewar and H.S. Rzepa, *ibid.*, **100**, 58, 777 (1978); M.J.S. Dewar, M.L. McKee and H.S. Rzepa, *ibid.*, **100**, 3607 (1978); L.P. Davies, R.M. Guidry, J.R. Williams, M.J.S. Dewar and H.S. Rzepa, *J. Comput. Chem.*, **2**, 433 (1981); M.J.S. Dewar and H.S. Rzepa, *ibid.*, **4**, 158 (1983); M.J.S. Dewar and M.L. McKee, *ibid.*, **4**, 82 (1983).
- [15] *Ab initio* calculations were carried out using the Gaussian 76 program system; J.S. Binkley, R.A. Whiteside, P.C. Hariharan, R. Seeger, J.A. Pople, W.J. Hehre and M.D. Newton, Quantum Chemistry Program Exchange, **11**, 368 (1978).
- [16] M.J.S. Dewar and G.P. Ford, *J. Amer. Chem. Soc.*, **99**, 7822 (1977).
- [17] M.J.S. Dewar, G.P. Ford, M.L. McKee, H.S. Rzepa, W. Thiel and Y. Yamaguchi, *J. Mol. Structure*, **43**, 135 (1978).

## RESUMO

Da análise de  $^1\text{H}$  r.m.n. da N-benzil-N-metil-hidro-xilamina e seu anião, a não-equivalência magnética observada nos prótons benzílicos é racionalizada em termos de ser a inversão lenta do átomo de azoto o passo determinante da velocidade do processo dinâmico. Cálculos de orbitais moleculares (MNDO e *ab initio*) levados a cabo no composto modelo N,N-dimetil-hidroxilamina e respectivo anião emprestam suporte adicional a esta hipótese,



ABDOU O. ABDELHAMID  
NOSRAT M. ABED

Chemistry Department,  
Faculty of Science  
Cairo University,  
Giza, Egypt.



## SYNTHESIS OF PYRIDAZINE, PYRIDAZIN-3- ONE, 2-AMINO PYRROLE AND 2,5-DIAMINO-PYRIDINE DERIVATIVES FROM PROPANEDINITRILE

*Aromatic diazonium chlorides react with dicyanomethylene compounds 1 a-c and 12 to give the hydrazone derivatives, which are readily cyclized into pyridazine 4 and pyridazin-3-one 13 derivatives respectively. 2-Amino pyrrole 6 and dihydro pyridazin 3-one 14 derivatives are obtained by the reaction of 4 and 13 with zinc dust in presence of acetic acid. Also the reaction of acetoacetanilide with malononitrile in acetic and piperidine as a catalyst was studied. The structure of the compounds obtained have been assigned on the basis of elemental analysis and spectral data.*

## INTRODUCTION

Dicyanomethylene compounds **1**, readily obtained via the reaction of  $\beta$ -Keto anilide and  $\beta$ -Keto esters with malono-nitrile and ethylcyanoacetate [1-4], are versatile reagents and have been extensively utilised as intermediates in heterocyclic synthesis. [5-8] In this communication, we report the synthesis of pyridazine, amino pyrrole and diamino pyridine by the coupling of aromatic diazonium chlorides with dicyanomethylene compounds.

## RESULTS AND DISCUSSION

Dicyanomethylene compounds **1 a-c** couple with aromatic diazonium chlorides in a sodium acetate buffered solution or ethanol to yield the corresponding the hydrazone derivative **3**, which are readily cyclized into the pyridazine derivatives **4** in the reaction mixture (Scheme 1). The structure of the compound **4** was deduced from their elemental analyses and their spectra. Infrared spectrum of compound **4** contained bands of 3310, 2220, and 1670  $\text{cm}^{-1}$  due to the NH, CN, and CO groups respectively. Pmr spectrum in dimethyl sulfoxide- $\text{d}_6$  showed a multiplet at  $\delta$  7.0-7.8 (H, aromatic and NH) and a singlet at  $\delta$  2.4 (3H,  $\text{CH}_3$  Ppm. Spectra data and analytical analyses of compound **4 b-f** are summarised in Table 1,2.

Treatment of pyridazine derivatives **4** with Zinc dust in presence of acetic acid at 80°C gave amino pyrrole derivatives (Scheme 1). The structure of amino pyrrole **4** was established on the basis of analytical and spectroscopic data, for example, compound **6 c** exhibits 3420, 3320, 3220, 2210 and 1680  $\text{cm}^{-1}$  due to  $\text{NH}_2$ , CN and CO groups respectively. Its pmr spectrum showed 60.9 (t, 3H); 3.8 (s, 2H); 5.8 (s, 2H), and 7.3-7.8 (m, 10 H,) ppm. The signal at  $\delta$  5.8 ppm was disappeared upon shaking with  $\text{D}_2\text{O}$  and another signal appeared at  $\delta$  3.7 ppm.



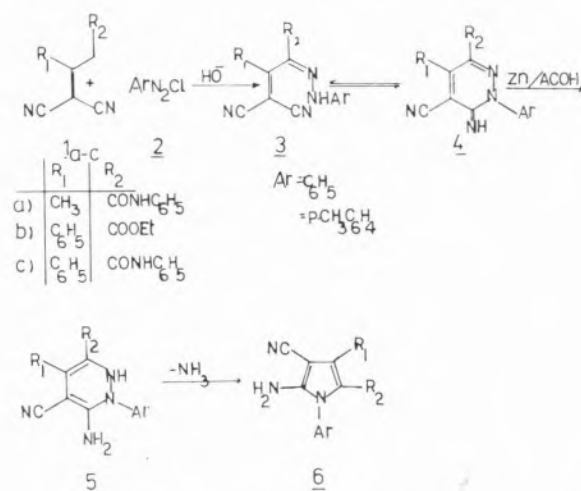
Table 2

IR Spectra (KBr). of some compound under study

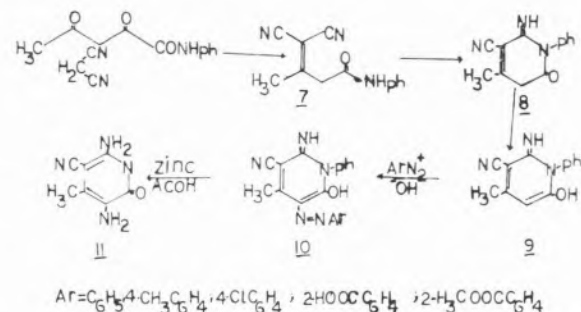
Compound No.	IR cm <sup>-1</sup>
4 b	3380 (NH); 3090 (CH); 2980 (CH <sub>3</sub> ), 2240 (CN), 1660 (Co); 1620 (C=N) and 1600 (C=C).
4 c	3290 (NH); 3020 (CH); 2980 (CH <sub>3</sub> ); 2220 (CN); 1710 (CO) and 1625 (C=N).
4 f	3450, 3320 (NH); 2200 (CN) and 1650 (Co).
6 b	3460, 3360, 3320 (NH <sub>2</sub> ); 2220 (CN); 1660 (Co) and 1630 (C=N).
6 c	3420, 3320, 3220 (NH <sub>2</sub> ); 2210 (CN); 1680 (Co); and 1620 (C=C).
6 e	3400, 3360, 3330 (NH <sub>2</sub> ); 2220 (CN), 1666 (CO), and 1600 (C=C).
10 b	3310 (NH); 220 (CN); and 1650 (CO) and 1590 (C=N).
11	3400, 3280, 3190 (NH <sub>2</sub> ); 2200 (CN) and 1650 (CO).
13 b	3320 (NH), 2220 (CN), and 1690, 1675 (Co).
14 b	2220 (CN); 1690 (CO); and 1620 (C=N) 3300 (NH); 2210 CN); and 1680 (CO).

The reaction of acetoacetanilide and malonitrile was mentioned before in non polar solvent [2,3], But, in this report, the reaction was carried in acetic acid. The compound, was isolated gave analytical data consistent with the formula C<sub>13</sub>N<sub>11</sub>N<sub>3</sub>O. Its infrared spectrum reveals bands at 3280 (NH), 2210 (NC), 1670 (CO) and 1620 (C=C) cm<sup>-1</sup>. Also pmr, showed signals at δ 2.3 (S, 3H), 6.1 (S, 1H), and 7-7.7 (m, 6H) ppm. On the basis of these data, the product was assigned the structure **8**. Compound **8** couple with aromatic diazonium chlorides in a sodium acetate buffered solution to yield the corresponding the azo derivatives **10**, which reduced by zinc dust in acetic acid to give diamino

pyridene derivative **11**. (Scheme 2) Infrared of **11** showed bands at 3460, 3400, 3280 (NH<sub>2</sub>), and 2200 (CN) cm<sup>-1</sup>. Pmr of **11** exhibit sig-



nals at δ 2.2 (S, 3H), δ 3.3 (S, 4H), and δ 7-7.5 (m, 5H) ppm. The signal at δ 3.3 ppm disappeared upon shaking with D<sub>2</sub>O and δ 3.9 ppm appeared.



Also, acetocatanilide react with ethylcyanoacetate in acetic acid in presence of piperidine as a catalyst to give **12**, which coupled with aromatic diazonium chlorides in ethanolic sodium acetate solution to yield the corresponding pyridazine derivatives **13**. (Scheme 3). Compound **13** was converted to dihydropyridazin -3- one derivatives **14** by Zinc dust in acetic -acid. The structures **13** and **14** were elucidated by elemental analyses and spectral data (See exp.), Scheme 3.

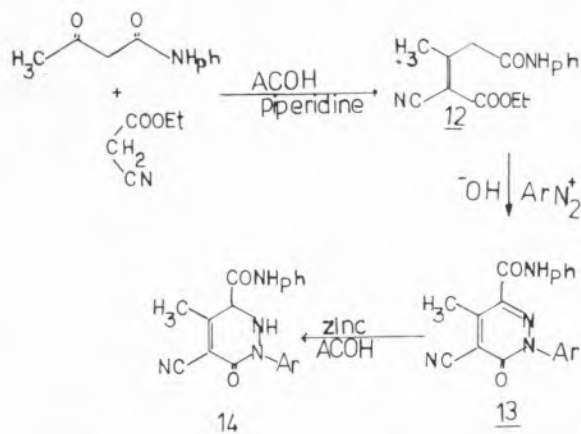
The results of the present work indicate the reaction of aromatic diazonium chlorides

Table I

Compound No.	R <sub>1</sub>	R <sub>2</sub>	Ar	M.P./°C	Molecular Formula	% C		% H		% N	
						Calcd (Found)	Calcd (Found)	Calcd (Found)	Calcd (Found)		
4 a	CH <sub>3</sub>	CONHC <sub>6</sub> H <sub>5</sub>	C <sub>6</sub> H <sub>5</sub>	160	C <sub>19</sub> H <sub>15</sub> N <sub>5</sub> O	69.28 (69.1)	4.59 (4.3)	21.26 (21.1)			
4 b	CH <sub>3</sub>	CONHC <sub>6</sub> H <sub>5</sub>	P-CH <sub>3</sub> C <sub>6</sub> H <sub>4</sub>	180	C <sub>20</sub> H <sub>17</sub> N <sub>5</sub> O	69.96 (69.7)	4.99 (5.0)	20.39 (19.9)			
4 c	C <sub>6</sub> H <sub>5</sub>	COOC <sub>2</sub> H <sub>5</sub>	C <sub>6</sub> H <sub>5</sub>	193	C <sub>20</sub> H <sub>16</sub> N <sub>4</sub> O <sub>2</sub>	69.75 (69.4)	4.68 (4.8)	16.27 (16.4)			
4 d	C <sub>6</sub> H <sub>5</sub>	COOC <sub>2</sub> H <sub>5</sub>	P-ClC <sub>6</sub> H <sub>4</sub>	50 s	C <sub>20</sub> H <sub>15</sub> N <sub>4</sub> ClO <sub>2</sub>	63.41 (63.1)	3.99 (4.0)	14.79 (14.9)			
4 e	C <sub>6</sub> H <sub>5</sub>	CONHC <sub>6</sub> H <sub>5</sub>	C <sub>6</sub> H <sub>5</sub>	155	C <sub>24</sub> H <sub>17</sub> N <sub>5</sub> O	73.64 (73.3)	4.37 (4.3)	17.89 (17.9)			
4 f	C <sub>6</sub> H <sub>5</sub>	CONHC <sub>6</sub> H <sub>5</sub>	P-CH <sub>3</sub> C <sub>6</sub> H <sub>4</sub>	230	C <sub>23</sub> H <sub>19</sub> N <sub>5</sub> O	74.05 (73.9)	4.72 (4.8)	17.27 (16.8)			
5 a	CH <sub>3</sub>	CONHC <sub>6</sub> H <sub>5</sub>	C <sub>6</sub> H <sub>5</sub>	265	C <sub>19</sub> H <sub>16</sub> N <sub>4</sub> O	72.13 (71.8)	5.09 (4.8)	17.70 (17.9)			
6 b	CH <sub>3</sub>	CONHC <sub>6</sub> H <sub>5</sub>	P-CH <sub>3</sub> C <sub>6</sub> H <sub>4</sub>	270	C <sub>20</sub> H <sub>18</sub> N <sub>4</sub> O	72.70 (72.6)	5.49 (5.5)	16.95 (17.2)			
6 c	C <sub>6</sub> H <sub>5</sub>	COOC <sub>2</sub> H <sub>5</sub>	C <sub>6</sub> H <sub>5</sub>	194	C <sub>20</sub> H <sub>17</sub> N <sub>5</sub> O <sub>2</sub>	72.49 (72.6)	5.17 (5.2)	12.68 (12.8)			
6 d	C <sub>6</sub> H <sub>5</sub>	CONHC <sub>6</sub> H <sub>5</sub>	C <sub>6</sub> H <sub>5</sub>	262	C <sub>24</sub> H <sub>18</sub> N <sub>4</sub> O	76.17 (75.9)	4.79 (4.9)	14.80 (15.0)			
6 e	C <sub>6</sub> H <sub>5</sub>	CONHC <sub>6</sub> H <sub>5</sub>	P-CH <sub>3</sub> C <sub>6</sub> H <sub>4</sub>	270	C <sub>23</sub> H <sub>20</sub> N <sub>4</sub> O	76.51 (76.3)	5.14 (4.9)	14.27 (14.4)			
10 a	—	—	C <sub>6</sub> H <sub>5</sub>	212	C <sub>19</sub> H <sub>15</sub> N <sub>5</sub> O	69.28 (69.2)	4.59 (4.6)	21.26 (21.5)			
10 b	—	—	P-CH <sub>3</sub> C <sub>6</sub> H <sub>4</sub>	265	C <sub>20</sub> H <sub>17</sub> N <sub>5</sub> O	69.95 (70.1)	4.99 (5.3)	20.39 (20.7)			
10 c	—	—	P-ClC <sub>6</sub> H <sub>4</sub>	264	C <sub>19</sub> H <sub>14</sub> N <sub>5</sub> ClO	62.72 (62.4)	3.88 (3.8)	19.25 (18.9)			
10 d	—	—	O-HOCC <sub>6</sub> H <sub>4</sub>	264	C <sub>20</sub> H <sub>15</sub> N <sub>5</sub> O <sub>3</sub>	64.33 (64.1)	4.05 (3.9)	18.76 (19.1)			
10 f	—	—	O-H <sub>3</sub> COOC <sub>6</sub> H <sub>4</sub>	259	C <sub>21</sub> H <sub>17</sub> N <sub>5</sub> O <sub>3</sub>	65.11 (64.9)	4.42 (4.5)	18.08 (18.2)			
11	—	—	—	245	C <sub>13</sub> H <sub>12</sub> N <sub>4</sub> O	64.98 (64.7)	5.03 (5.1)	23.32 (23.1)			
13 a	—	—	C <sub>6</sub> H <sub>5</sub>	230	C <sub>19</sub> H <sub>14</sub> N <sub>4</sub> O <sub>2</sub>	69.08 (69.1)	4.27 (4.1)	16.96 (17.2)			
13 b	—	—	P-CH <sub>3</sub> C <sub>6</sub> H <sub>4</sub>	220	C <sub>20</sub> H <sub>16</sub> N <sub>4</sub> O <sub>2</sub>	69.76 (69.4)	4.68 (4.8)	16.26 (15.8)			
14 a	—	—	C <sub>6</sub> H <sub>5</sub>	220	C <sub>19</sub> H <sub>16</sub> N <sub>4</sub> O <sub>2</sub>	68.66 (68.4)	4.85 (5.0)	16.85 (17.1)			
14 b	—	—	P-CH <sub>3</sub> C <sub>6</sub> H <sub>4</sub>	185	C <sub>20</sub> H <sub>18</sub> N <sub>4</sub> O <sub>2</sub>	69.35 (69.0)	5.24 (5.3)	16.47 (16.7)			

S: Sublimation.

with dicyanomethylene compounds, provides the basis of a convenient procedure for the



synthesis of pyridazine and amino pyrrole derivatives.

## EXPERIMENTAL

Melting points were determined with an electrothermal melting point apparatus (GrallenKamp) and are uncorrected. The IR spectra were measured on a Pye—Unicam SP 1000 spectrophotometer. PMR spectra were recorded on a Variam EM-360 instrument at 60 MHz in dimethylsulfoxide— $d_6$  solution, with tetramethylsilane as the internal standard. Elemental microanalyses were carried out by the Microanalytical laboratory, University of Cairo, Giza, Egypt. Alkylidene malononitrile 1 *a-c* are obtained as previously prepared in literature [2,3].

**4-cyano-3-imino-5,6-disubstituted-3,4-dihydropyridazine 4.** A solution of ylidenenitrile (0.005 mol) in ethanol (50 cm<sup>3</sup>) was stirred for 5 min with sodium acetate (3 g) and chilled in an ice-salt bath to 0-5°C. To the resulting cold solution was added the desired diazonium salt (0.005 mol) solution. After the addition was completed, the reaction mixture was stirred for additional 1h. The crude solid obtained was collected, washed with water and recrystallized from suitable solvent. The dihydropyridazine 4 prepared are listed (Table 1 and 2).

**5-Amino-1-Aryl-4-cyano-2,3-disubstituted pyrrole 6.** To a suspension of compound 4 (5 mmol) in acetic acid (20 cm<sup>3</sup>) at 80°C, Zinc dust (2 g) was added portionwise for 20 min. The reaction mixture was filtered while hot. The filtrate was diluted with 100 cm<sup>3</sup> water, the crude solid was collected and crystallized to give the corresponding 6 (Table 1 and 2).

**2-Aryl-4-cyano-5-methyl-3-oxo-2,3-dihydro-pyridazin-6-phenylcarboxamide 13-A** solution of compound 12 (0.005 mol) in ethanol (50 cm<sup>3</sup>) was stirred for 5 min with sodium acetate (3 g) at 0-5°C. To the resulting cold solution was added arene diazonium chloride (0.005 mol) solution, the reaction mixture was stirred at 0°C for 30 min. The crude product was collected and crystallized from acetic acid. The 3-oxo-dihydropyridazine 13 prepared are listed (Table 1 and 2).

**2-Aryl-4-cyano-5-methyl-6-oxo-1,2,3,6-tetrahydropyridazine-3-phenylcarboxamide 14**—To a suspension of compound 13 (5 mmol) in acetic acid (20 cm<sup>3</sup>) at 80°C, Zinc dust (3 g) was added portionwise for 15-20 min. The reaction mixture was filtered while hot. The filtrate was diluted (70 cm<sup>3</sup>) of water. The solid was collected and crystalized from dilute acetic acid to give the corresponding 14 (Table 1 and 2).

**2-Imino-4-methyl-6-hydroxy-3-carbonitrile-N-phenyl-pyridine 9.** A mixture of 1.8 g (0.01 mol) acetoacetanilide, 0.7 g (0.01 mol) malonitrile, one drop of piperidine and 20 cm<sup>3</sup> acetic acid was heated under reflux for 3 h. Colorless plates, m. p. 217°C; C<sub>13</sub>H<sub>11</sub>N<sub>3</sub>O, Anal. Found (calcd.): C, 69.2 (69.19); H, 4.7 (4.91); N, 18.7 (18.62).

**4-Arylazo-2-Imino-4-methyl-6-hydroxy-3-carbonitrile-N-phenyl pyridine 10**—A solution of compound 9 (0.005 mol) in ethanol (50 cm<sup>3</sup>) was stirred for 5 min with sodium acetate (3 g) at 0°C. To the resulting cold solution was added arene diazo-

nium chloride (0.005 mol) solution, the reaction mixture was stirred at 0°C for 30 min. The crude product was collected and crystallized from acetic acid. The compounds **10** prepared are listed in Table 1 and 2.

*2,5-Diamino -1,6-dihydro -4-methyl -6-oxo -1-phenyl pyridine -3-carbonitrile II*- To a suspension of compound **10a** (5 mmole) in acetic acid (20 cm<sup>3</sup>) at 80°C, Zinc dust (2 g) was added portionwise. The reaction mixture was filtered while hot. The filtrate was diluted with water. The crude solid was collected and crystallized from acetic acid to give the corresponding **II**. When the reaction was repeated for **10 b** and **10 c**, the compound **II** was obtained (m.p., mixed m.p. and spectral data).

(Received, 21st August 1985)

#### REFERENCES

- [1] T.R. KASTURI, V.K. SHARMA, A. SRINIVASAN, *Tetrahedron*, **29**, 4103 (1973).  
 [2] B. ZALESKA, B. SLUSARSKA, *Monatschef chem.*, **112**, 1187 (1981).

- [3] J.W. DUCKER, M.J. GUNTER, *Austr. J. Chem.*, **28**, 581 (1975).  
 [4] E.C. TAYLOR, K.S. HARTAKI, *J. Chem. Soc.*, 58, 2452 (1959).  
 [5] S.M. FAHMY, N.M. ABED, R.M. MOHAREB, M.H. ELNAGDI, *Synthesis*, 490 (1982).  
 [6] N.M. ABED, N.S. IBRAHIM, S.M. FAHMY, M.H. ELNAGDI, *Org. Prep. Pri*, **17**, 107 (1985).  
 [7] H.A.F. DABOUN, S.E. ABDOU, M.M. HUSSEIN, H. ELNAGDI, *Synthesis*, 503 (1982).  
 [8] K. GREWALS, U. HAIN, *Synthesis*, 62, (1984).  
 [9] BRIANT T. NEWBOLD «*The chemistry of hydrazo, azo and azoxy group*» Patai., ed, Johnwiely., New York N.Y., 1975, pag. 634 .

«*Síntese de derivados do propanodinitrilo e da piridazina, da 3-piridazinona, do 2-aminopirrole e da 2,5-diaminopiridina.*»

*Cloretos de arenodiazônio reagem com derivados do propanodinitrilo 1 a-c e 12 dando hidrazonas; estas são rapidamente ciclizadas dando os derivados 4 da piridazina e 13 da 3-piridazinona, respectivamente. Os derivados 6 do 2-aminopirrole e 14 da 1,6-di-hidro-3-piridazinona são obtidos por reação dos compostos 4 e 13 com zinco em ácido acético.*

*Estudou-se também a reação da acetoacetanilida com propanodinitrilo em ácido acético na presença de piperidina como catalisador.*

*A estrutura dos diferentes compostos foi estabelecida com base nas análises elementar e espectroscópica.*

MARIA MANUELA GONÇALVES MOTTA  
C. FERREIRA DE MIRANDA

Departamento de Química  
Universidade de Évora  
7000 Évora  
CECUL — Centro de Electroquímica  
e Cinética da Universidade de Lisboa.  
Faculdade de Ciências  
Lisboa



## ADSORPTION OF MOLYBDATE BY CLAY MINERALS I — KAOLINITE

*Adsorption of molybdate by kaolinite was investigated at 25°C in a 0.01 mol dm<sup>-3</sup> sodium chloride background medium at pH 3 to 8 and initial molybdenum concentrations ranging from 0.5 to 150 µgcm<sup>-3</sup>. Short term distribution equilibrium is attained in less than 10 hours and remains undisturbed for at least 48 hours. A maximum of adsorption is observed at pH = 3.8. The adsorption isotherm for pH = 4.6, the natural pH of kaolinite suspensions in 0.01 mol dm<sup>-3</sup> NaCl, fits well a Langmuir equation with a limiting value of 1.63 mg Mo/g kaolinite. For equilibrium Mo concentration in solution lower than 3 µg cm<sup>-3</sup>, i.e., the range normally found in the soil solution, the isotherm can be approached by a straight line and adsorption conveniently characterised by a distribution coefficient  $K_d = 160 \pm 4 \text{ cm}^3 \text{ g}^{-1}$ ; this is independent of the clay/solution ratio, Na,Cl-kaolinite shows a similar behaviour for the same low concentration range, but with higher adsorption.*

## 1 — INTRODUCTION

Clay minerals are potentially important in controlling the fixation and mobility of molybdenum in soils. Studies on the adsorption of molybdenum by the frequently occurring clay minerals, kaolinite, montmorillonite and illite are however scarce for kaolinite and lacking for the other two. Jones [1], in a comparative study of the adsorption of molybdenum by clay minerals and by iron and aluminium oxides, has investigated the adsorption of molybdate on kaolinite for a fixed initial molybdenum concentration and varying pH. Theng [2] has studied the adsorption isotherm of molybdate and its dependence on pH for a clay fraction of a Taita soil, reported to consist mainly of kaolinite and illite.

Adsorption isotherms provide a convenient means for describing adsorptive behaviour and have actually been used to predict the fertilizer requirements of soils [3]. They can yield (i), an equation which makes it possible to summarize adsorption by using a few numbers rather than by referring to a curve, and (ii), information about the nature of the adsorption process itself. However, since the isotherm is a macroscopic concept consistent with different mechanisms at the molecular level, such information must be supplemented with data concerning, e.g. rates of diffusion of exchangeable ions through the adsorbent, kinetics of the exchange reaction, and spectroscopy of the species at the adsorbent surface [4].

On the other hand, adsorption phenomena may present long term features differing from the short term behaviour, due to slow reaction between adsorbent and adsorbate. This has been observed and studied in particular in the case of the adsorption of phosphate by soils [5,6,7,8].

In the present work we investigate the short term adsorption of molybdate on kaolinite with the purpose of describing it with a minimal set of parameters; special attention is devoted to the range of molybdenum



concentrations usually found in the soil solution.

## 2 — EXPERIMENTAL

Light kaolin, (I) was obtained from BDH. X-ray diffraction analysis of this material showed besides the characteristic lines of kaolinite at 0.715 and 0.375 nm, weak lines at 1.0 and 0.496 nm indicating only a few per cent illite. Sedimentation analysis in hexametaphosphate medium yielded the following particle size distribution: 50-20  $\mu\text{m}$ , 5.9 %; 20-2  $\mu\text{m}$ , 0.8 %; 2-0.5  $\mu\text{m}$ , 65.0 %; < 0.5  $\mu\text{m}$ , 28.1 %. The specific BET ( $\text{N}_2$ ) area was 13  $\text{m}^2 \text{g}^{-1}$ . Na,Cl — kaolinite was prepared from (I) according to the method described by Posner and Quirk [9]. Otherwise, analytical grade reagents and deionized water were employed.

One gramme portions of kaolinite were placed in 250  $\text{cm}^3$  polythene bottles and vigorously shaken for one minute with adequate volumes of 0.01  $\text{mol dm}^{-3}$  sodium chloride. Aliquots of  $\text{Na}_2\text{MoO}_4 \cdot 2\text{H}_2\text{O}$  standard stock solutions were added to the suspensions. The bottles were shaken for 24 hours at 120 15 cm-strokes per minute in a waterbath at  $25.0 \pm 0.5^\circ\text{C}$ . 10  $\text{cm}^3$  samples were then taken for pH measurements and the bottles replaced upright, fully immersed, in the waterbath for a further half an hour period. Finally, the supernatants were first centrifuged and then filtered through a 0.4  $\mu\text{m}$  polycarbonate membrane filter. It was checked that no significant loss of molybdenum occurred during the filtration step.

For adsorption measurements at pH values other than the natural pH (4.6) of kaolinite suspensions in 0.01  $\text{mol dm}^{-3}$  sodium chloride, 0.01  $\text{mol dm}^{-3}$  HCl or NaOH were added to the suspensions in order to approximate the pH sought. A period of 24 hours was allowed for acid-base equilibration, and the final pH recorded prior to the addition of molybdate.

Molybdenum was determined in the filtrates by flameless atomic absorption at 313.3 nm

with a slit setting of 0.7 mm. The detection limit (1% absorption,  $A=0.004$ ) was 0.5  $\text{ng cm}^{-3}$  corresponding to 10  $\mu\text{g}$  molybdenum per fire, as 20  $\text{mm}^3$  injections were used. By suitable dilution of the samples their absorbances were kept within the range where linearity is observed and memory effects are negligible. Blanks corresponded to about 5 to 10 % of the measured absorbances. The average of three readings was taken for each solution; the variation coefficient of the mean was 2 %.

## 3 — RESULTS AND DISCUSSION

### a) Equilibration time

The influence of time of contact between solution and solid phase on the extent of adsorption was investigated for several initial molybdenum concentrations and for contact times from 0.5 to 48 hours. Figure 1 shows a typical equilibration curve: adsorption of molybdenum rises steeply to about 60 % of its final value in less than 1 hour, then continues with a decreasing rate and reaches a plateau in about 10 hours; the plateau extends up to 48 hours at least. Equilibration times of 24 hours are therefore adequate.

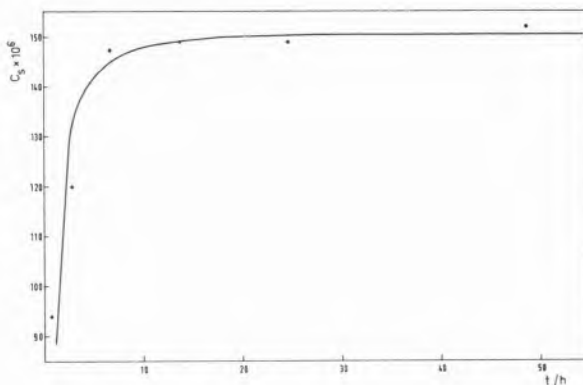


Fig 1

Effect of time of contact on the adsorption of molybdenum, 1 g kaolinite; 100  $\text{cm}^3$  0.01  $\text{mol dm}^{-3}$  NaCl;  $C_0(\text{Mo}) = 2.5 \mu\text{g cm}^3$ .

b) Clay/solution ratio

The influence of the clay/solution ratio on adsorption was investigated in the range 5-50 grams of kaolin per litre of solution and for an initial molybdenum concentration equal to  $2.5 \mu\text{g cm}^{-3}$ . This corresponded to  $0.3\text{-}1.7 \mu\text{g cm}^{-3}$  molybdenum in the aqueous phase at equilibrium.

From mass balance considerations the following relationship can be established

$$C_s = \frac{C_o}{\frac{m}{V} + \frac{1}{K_d}} \quad (1)$$

where  $C_o$  is the initial Mo concentration in solution in  $\mu\text{g cm}^{-3}$ ,  $C_s$  the equilibrium Mo concentration in the solid phase, also in  $\mu\text{g cm}^{-3}$ ,  $m$  is the mass of adsorbent (g) and  $V$  the volume ( $\text{cm}^3$ ) of solution,  $K_d = \frac{C_s}{C_e}$  is in general a function of  $C_e$ ; the equilibrium concentration in the liquid phase.

Equation (1) can be given the form

$$\frac{C_o}{C_s} = \frac{m}{V} + \frac{1}{K_d} \quad (2)$$

implying a linear dependence of  $\frac{C_o}{C_s}$  on  $\frac{m}{V}$  if  $K_d$  is constant. Figure 2 shows that this is indeed the case. The observed slope, 0.96, agrees with the theoretical value, 1, and the intercept yields  $K_d = 131 \text{ cm}^3 \text{ g}^{-1}$ . A better estimation of  $K_d$  because no extrapolation is involved, can be obtained by averaging the experimental  $C_s/C_e$  ratios, which yields  $K_d = 139 \pm 16 \text{ cm}^3 \text{ g}^{-1}$ .

Thus, for molybdenum equilibrium concentrations in solution up to  $1.7 \mu\text{g cm}^{-3}$  at least the adsorption equilibrium can be described by a distribution coefficient which does not

depend on the clay/solution ratio nor on molybdenum concentration.

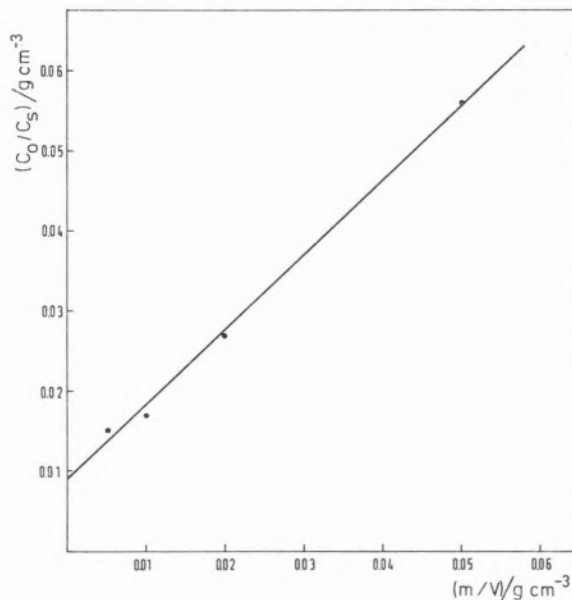


Fig. 2

Confirming that Mo adsorption does not depend on clay/solution ratio.

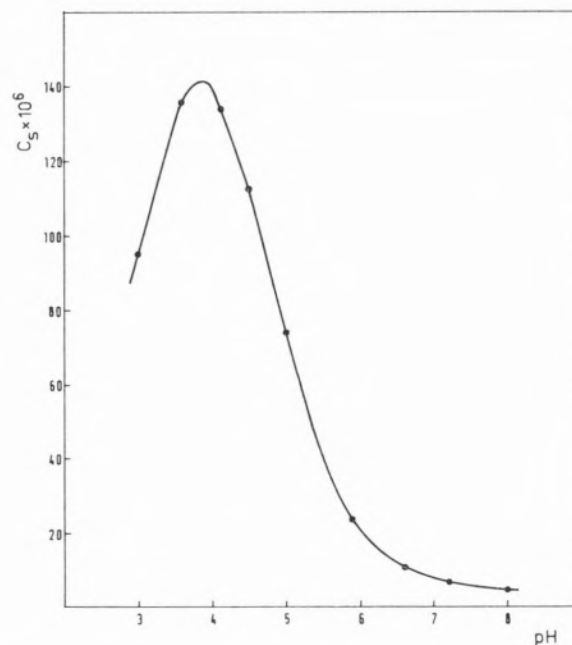


Fig. 3

Dependence of Mo adsorption pH. 10 g kaolin/dm<sup>3</sup>; C<sub>o</sub>(Mo) = 2 μg cm<sup>-3</sup>; 0.01 mol dm<sup>-3</sup> NaCl medium.

## c) pH

The dependence of molybdenum adsorption on pH is shown in figure 3. A maximum of adsorption is observed for  $\text{pH} = 3.8$ , *i.e.* near the  $\text{pK}$  of the  $\text{HMoO}_4^-$  ion [10] as required by the theory of Hingston et al. [11,12]. Essentially the same curves have been reported by Jones [1] for kaolinite under similar conditions ( $20 \text{ g clay/dm}^3$ ,  $C_0 = 2 \text{ } \mu\text{g cm}^{-3}$ ) and by Theng [2] for the clay fraction of a Taita soil containing mainly kaolinite and illite ( $2.5 \text{ g clay/dm}^3$ ,  $C_0 = 2.5 \text{ } \mu\text{g cm}^{-3}$ ,  $0.2 \text{ mol dm}^{-3} \text{ NaCl}$  medium).

## d) Pre-treatment of the adsorbent

Kaolinite in the Na,Cl homoionic form adsorbs more molybdenum than the untreated clay (Fig. 4), indicating that less accessible sites have been exposed by the pre-treatment of the adsorbent. The differences are significant enough to deserve further investigation.

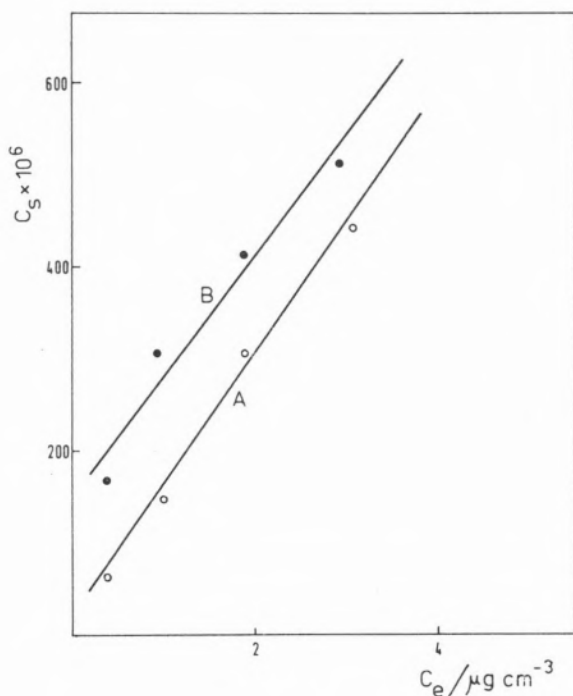


Fig. 4

Effect of the pre-treatment of kaolinite on the adsorption of molybdenum. A — untreated kaolinite; B — Na,Cl-kaolinite,  $10 \text{ g clay/dm}^3$ .

## e) Molybdenum concentration

Figure 5 shows the adsorption isotherm for equilibrium molybdenum concentrations in solution up to  $100 \text{ g cm}^{-3}$ , at  $\text{pH} 4.6$  and for a clay/solution ratio equal to  $10 \text{ g dm}^{-3}$ . The curve is of the L type (Giles classification [13]), indicating a moderately high affinity between molybdate and adsorbent.

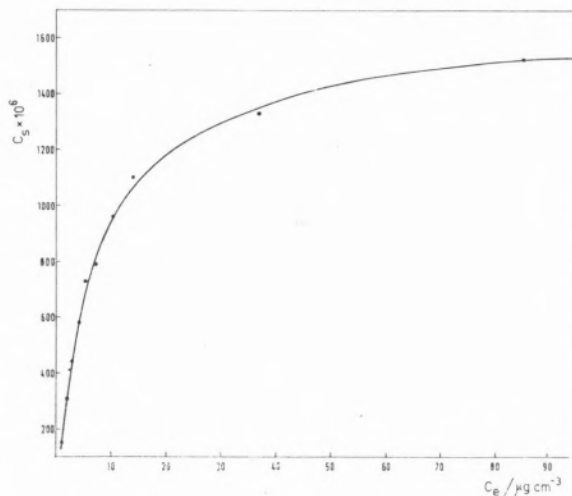


Fig. 5

Adsorption isotherm for molybdate on kaolinite at  $298 \text{ K}$  in  $0.01 \text{ mol dm}^{-3} \text{ NaCl}$  medium.

It conforms to the Langmuir equation, (Fig. 6):

$$\frac{C_e}{C_s} = 0.594 \times 10^{-3} C_e + 5.24 \times 10^{-3} \quad (4)$$

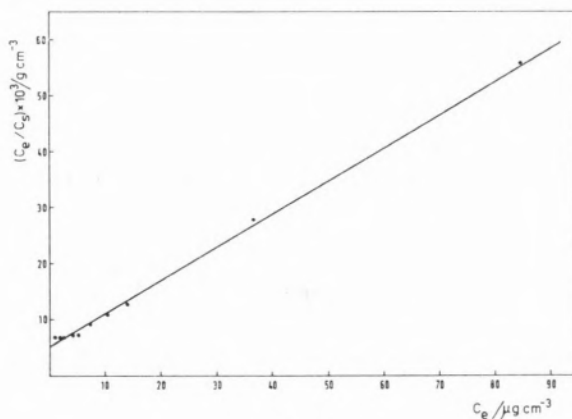


Fig. 6

Langmuir plot for the adsorption isotherm of fig 5.

For molybdenum equilibrium concentrations in solution lower than  $3 \mu\text{g cm}^{-3}$  the isotherm can be conveniently described by the straight line (Fig. 7)

$$C_s = 160C_e \quad (5)$$

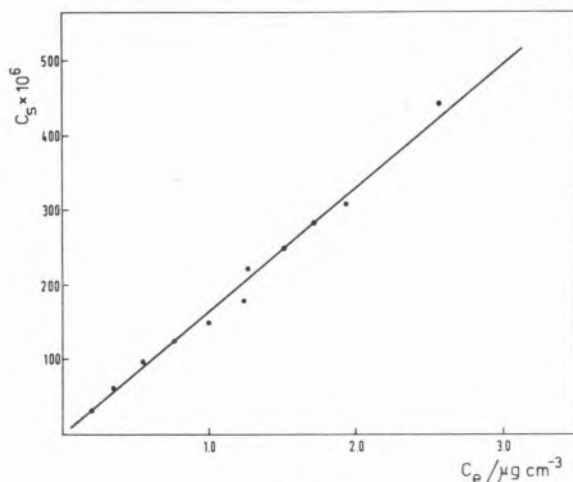


Fig. 7

Linear plot for adsorption isotherm of fig. 5 for  $C_e < 3 \mu\text{g cm}^{-3}$ .

and the adsorption equilibrium therefore characterized by a single parameter, the distribution coefficient  $K_d = 160 \pm 4 \text{ cm}^3 \text{ g}^{-1}$ . On the other hand, for  $C_e > 2 \mu\text{g cm}^{-3}$  a better Langmuir fit is given by the equation

$$\frac{C_e}{C_s} = 0.615 \times 10^{-3} C_e + 4.5 \times 10^{-3} \quad (6)$$

The differences between calculated and experimental  $C_s$  values amount to  $6 \pm 5 \%$  in the case of equation (5); for equation (6) the differences are  $3 \pm 2 \%$ , in better agreement with the variation coefficient for the experimental  $C_s$ ,  $2 \pm 1 \%$ .

Equation (6) indicates that saturation of the adsorbent by molybdate is achieved at  $1.63 \text{ mg Mo/g kaolinite}$ . Each molybdate ion may be attributed an individual area of  $0.3\text{--}0.4 \text{ nm}^2$ , considering the tetrahedral configuration of the ion and the O-O distance in sodium molybdate [14]. Thus, the total area

occupied by molybdate on saturated kaolinite amounts to  $3\text{--}4 \text{ m}^2$ ; this corresponds to about  $1/4$  of the total BET area of the adsorbent and may represent the area of the edge faces of the crystalites.

(Received, 19th April 1985; in revised form 24th September 1985)

## ACKNOWLEDGEMENTS

The authors wish to thank Prof. Manuela Brotas of the Faculdade de Ciências de Lisboa for the BET area determination, Dr. Vieira e Silva of the Instituto Nacional de Investigação Agronómica, Oeiras, for the granulometric and X-ray diffraction analyses, and Prof. Remy Freire, Director of the Instituto Nacional de Investigação das Pescas, Lisboa, for the kind permission to utilise the flameless atomic absorption equipment and other facilities which made this investigation possible.

## LITERATURE CITED

- [1] L.H.P. JONES, *J. Soil Sci.*, **8**, 313 (1957).
- [2] B.K.G. THENG, *N.Z.J.Sci.*, **14**, 1040 (1971).
- [3] D.J. GREENLAND, M.H.B. HAYES, (ed.), *The Chemistry of Soil Processes*, John Wiley & Sons, New York (1981), p. 232.
- [4] G. SPOSITO, *The Thermodynamics of Soil Solutions*, Oxford University Press, New York (1981), p. 151-2.
- [5] N.J. BARROW, *Soil Sci.*, **118**, 380 (1974).
- [6] N.J. BARROW, T.C. SHAW, *Soil Sci.*, **119**, 167 (1975).
- [7] N.J. BARROW, T.C. SHAW, *Soil Sci.*, **119**, 190 (1975).
- [8] N.J. BARROW, T.C. SHAW, *Soil Sci.*, **119**, 301 (1975).
- [9] A.M. POSNER, J.P. QUIRK, *Proc. Roy. Soc. A.*, **278**, 35 (1964).
- [10] A.E. MARTELL, R.M. SMITH, *Critical Stability Constants*, Plenum Press, New York (1982), p. 399.
- [11] F.J. HINGSTON, R.J. ATKINSON, A.M. POSNER, J.P. QUIRK, *Nature*, **275**, 1459 (1967).
- [12] F.J. HINGSTON, R.J. ATKINSON, A.M. POSNER, J.P. QUIRK, *Trans. 9th. Int. Cong. Soil Sci.*, **1**, 669 (1968).
- [13] G.H. GILES; D. SMITH, A. HUITSON, *J. Colloid Interface Sci.*, **47**, 755 (1974).
- [14] I. LINDQUIST, *Acta Chem. Scand.*, **4**, 1066 (1950).

**RESUMO**

Estudou-se a adsorção de molibdato por caulinite a 25°C em meio cloreto de sódio 0,01 molar, a pH entre 3 e 8 e para concentrações iniciais de molibdênio compreendidas entre 0,5 e 150  $\mu\text{g cm}^{-3}$ . O equilíbrio a curto termo é atingido em menos de 10 horas e permanece inalterado durante pelo menos 48 horas. A adsorção apresenta um máximo para pH = 3,8. A isotérmica de adsorção para pH = 4,6, que é o pH das suspensões de caulinite em NaCl 0,01 mol  $\text{dm}^{-3}$ , ajusta-se bem a uma equação de Langmuir com um

recobrimento igual a 1,63 mg Mo/g caulinite. Para concentrações de equilíbrio inferiores a 3  $\mu\text{g Mo/cm}^3$  ou seja da ordem das geralmente encontradas na solução do solo, a isotérmica confunde-se com uma recta e o equilíbrio pode vantajosamente ser caracterizado por um coeficiente de distribuição  $K_d = 160 \pm 4 \text{ cm}^3 \text{ g}^{-1}$  independente da razão massa de argila/volume de solução. Nesta mesma gama de concentrações a caulinite na forma homoiónica NaCl mostra um comportamento semelhante mas com valores mais altos para a adsorção.



ROSA A. LORENZO FERREIRA  
M.<sup>a</sup> DEL CARMEN CASAIS LAIÑO  
F. BERMEJO MARTINEZ

Department of Analytical Chemistry  
Faculty of Chemistry  
University of Santiago de Compostela  
Santiago de Compostela,  
Spain



---

## SPECTROPHOTOMETRIC DETERMINATION OF VANADIUM(IV) WITH ETHYLENEDIAMINE-N,N' DIPROPIONIC ACID (EDDPA)

*Complex formation between V(IV) and ethylenediamine-N,N' dipropionic acid was studied. The violet complex has absorption maxima at 545 nm in acid solution (pH 5.5). The effects of reagent increase, temperature and time were studied. The optimal interval for the application of Beer's law is between 140 to 350  $\mu\text{g}$  vanadium/ $\text{cm}^3$ . The nature of the complex in solution as well as the interferences, reproducibility and precision were investigated. This method is more sensible than others that use other chelating reagents analogous to EDTA as chromogenic reagents.*

## INTRODUCTION

Vanadium, in its pentavalent state in solution can be determined by a large number of spectrophotometric methods, but the methods that allow to determine vanadium (IV) are more rare. Some methods that determine V(IV) are:

The method that uses EDTA [2], is applicable to the determination of vanadium in concentration no smaller than 0.05 mg V/ $\text{cm}^3$  at 588 nm and pH range 4-7.

BERMEJO ET AL. [3] reviewed the absorption spectra of the V(IV) V(IV)-EDTA chelate solutions and found two absorption maxima at 588 and 770-775 nm. If the absorption is measured at 775 and pH range 2.5 to 3.5 the application range of the method is extended to 0.1-3.28 mg V/ $\text{cm}^3$ .

The chelate 1:1 V(IV)-PDTA [8] gives two absorption maxima at 580 and 780 nm and its absorption spectra remains unchanged in the pH interval 7-10. Beer's law is followed from 20 to 2400  $\mu\text{g}$  V/ $\text{cm}^3$  at both wavelengths.

AHMAD ET AL. (1) studied the complex that NTA forms with V(IV), such complex shows two maxima at 620 and 815 nm and the latter is the most intense. When they used an interval of pH 3.6 to 4.8, Beer's law is followed between 51 and 1623  $\mu\text{g}$  V/ $\text{cm}^3$ .

In this paper we report a new spectrophotometric method for the determination of vanadium. The violet complex EDDPA-V(IV) has an absorption maxima at 545 nm in acid solution (pH 5.5). The effects of reagent concentration, temperature and reaction time were studied. We have also investigated the nature of the complex in solution as well as the interferences, reproducibility and precision of the method.

## MATERIALS AND METHODS

### REAGENTS

*Standard vanadium (IV) solution.*—This solution was prepared from VOSO<sub>4</sub> 5H<sub>2</sub>O R.A..

The concentration was volumetrically determined with  $\text{KMnO}_4$  [4].

**EDDPA, 0,5 % solution.** — The solution was prepared by dissolving the appropriate amount of reagent in distilled water to 100  $\text{cm}^3$ .

**EDDPA, solution 0.02003 M.** — An aqueous solution was prepared by weighing 0.4080 g of ethylenediamine-N,N' dipropionic acid (Analytical Reagent grade. Dojindo Lab. Japan) and by dissolving it in distilled water to 100  $\text{cm}^3$ .

Sodium hydroxide solution 0.1 F.  
Hydrochloric acid solution 0.1 F.

#### APARATUS

Bausch & Lomb Model Spectronic 700 spectrophotometer. — The spectrophotometer was equipped with 10.00 mm cells.

Beckman Model Electromate pH meter. — The meter was equipped with glass and calomel electrodes (sensitivity  $\pm 0.02$  pH).

#### PROCEDURE

To a series of 25  $\text{cm}^3$  volumetric flasks transfer aliquots of standard vanadium (IV) solution, add 7  $\text{cm}^3$  of 0.5 % EDDPA solution, and the necessary drop of 0.1 F hydrochloric acid or sodium hydroxide solution to bring the pH approximately to 5.5 and dilute to the mark with distilled water. The absorbance measurements are carried out at 545 nm (or the scanning was made) using 10.00 mm cells and distilled water as a blank.

#### RESULTS AND DISCUSSION

##### Absorption spectra

In order to fix the optimum working wavelength, the spectral characteristics of the

vanadium (IV)-EDDPA system at various pH values were studied. Fig. 1 shows the results at pH 2.2; 5.5 and 9, from which the identity of the spectra at the given pH

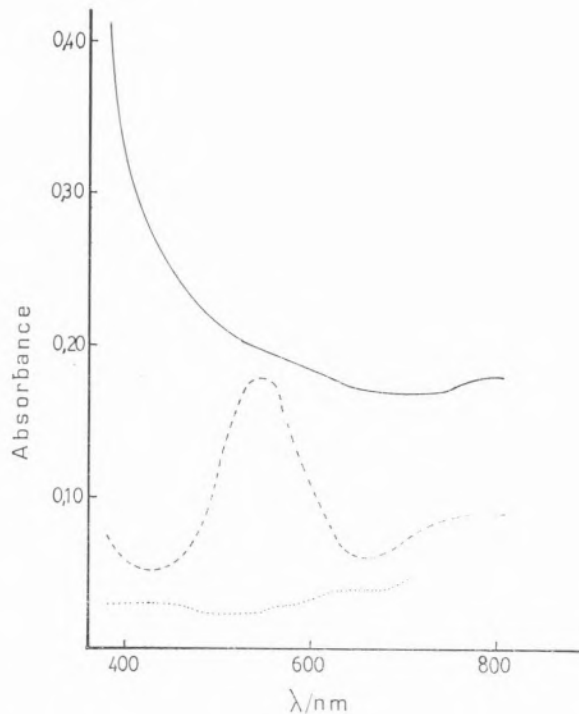


Figure 1

Absorption spectra of vanadium (IV) — EDDPA complex solutions at pH:

— 9.0  
- - - - 5.5  
..... 2.2

concentration of 118  $\mu\text{gV(IV)/cm}^3$

values is concluded, exhibiting a maximum at 545 nm and pH 5.5. In alkaline medium the complex is not stable.

##### Effect of the pH

The dependence of the absorbance with the pH was studied in the pH range 1.5-6.8 and is reproduced in Fig. 2. The complex shows maxima absorbance in the pH range 5-5.9. Establishing pH 5.5 as the working pH.

### Effect of reagent increase

Once the pH maximum was fixed, the effect of reagent increase was studied. It was found that 7 cm<sup>3</sup> of 0.5 % EDDPA solution was enough to form the complex, and further additions of the reagent did not appreciably affect the absorbance of the system.

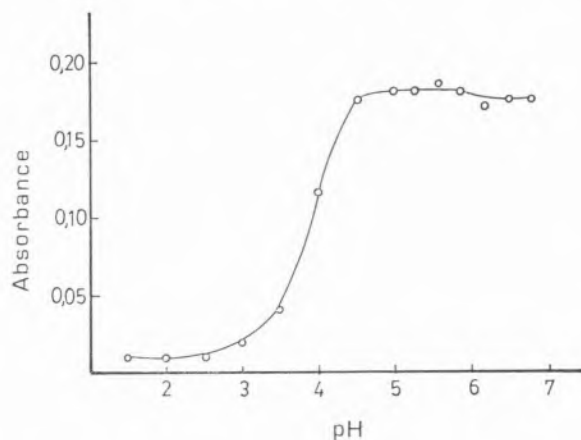


Figure 2

Effect of pH variations on the absorbance of the vanadium (IV)—EDDPA complex solutions. Vanadium (IV) concentration was of 118  $\mu\text{g}/\text{cm}^3$

### Time and temperature effects

The time and temperature effects on the stability of the vanadium (IV)-EDDPA system were also studied. Vanadium reacts instantly with EDDPA, the absorbance of the complex formed solution was unchanged for up to 24 hr and up to 80°C.

### Beer's law. Ringbom's interval and molar absorptivity

The relationship between the absorbed radiant energy and complex concentration was studied with the previously established conditions. Several standard solutions of the vanadium (IV)-EDDPA complex were prepared by taking aliquots of the standard solution of vanadium (IV), adding the reagent, adjusting the pH and diluting with

distilled water up to the mark. The absorbance of the solution was measured at 545 nm; the results are lineal on the calibration graph over the range 39-354  $\mu\text{g V}/\text{cm}^3$ . The molar absorptivity of the complex was calculated as 74.0  $\text{dm}^3 \cdot \text{mole}^{-1} \cdot \text{cm}^{-1}$  at 545 nm. The sensitivity according to SANDELL's expression (7) was 0.6884  $\mu\text{g} \cdot \text{cm}^{-2}$  and Ringbom's optimum interval is between 140 and 350  $\mu\text{g V}/\text{cm}^3$ .

### Reproducibility and precision

To carry out these studies nine series of solutions of different concentrations were prepared following the previously described procedure. The results obtained for concentrations of 39; 79; 118; 157; 197; 236; 276; 315 and 354  $\mu\text{g V}/\text{cm}^3$  are 0.0029; 0.0026; 0.0039; 0.0032; 0.0021; 0.0077; 0.0034; 0.0037 and 0.0053 of standard deviation, respectively.

The relative error on the mean value is ( $\sigma_m \cdot t / \bar{x} \cdot 100$ ) 2.95; 1.65; 1.53; 0.99; 0.52; 1.61; 0.61; 0.58 and 0.73 % at the same concentrations.

### Stoichiometry of the reaction

The stoichiometry of the complex was established by: JOB'S method of «continuous variations» [6], «molar ratio» of YOE and JONES [9] and «slope ratio» of HARVEY and MANNING [5]. The results are illustrated in figs. 3-5, from which it is inferred that the formation of the complex takes place in a vanadium (IV) to EDDPA ratio of 1:2.

### Effects of the others ions

The effect of neighbouring common ions upon the determination of vanadium (IV) was also studied. It was found that nitrite, oxalate, tungsten, phosphate, dichromate, bromate, molibdate and tartrate anions interfere. It was also found that the cations which interfere are: Mn(II), Pb(II), Al(III), Sn(II), Co(II), Fe(III) and Cu(II).

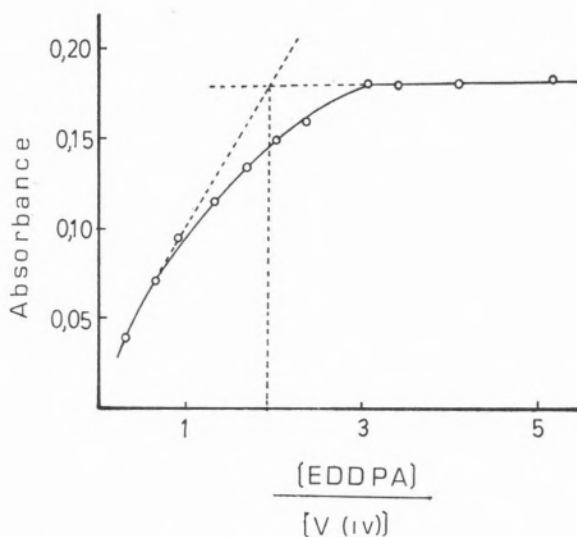


Figure 3

Application of the molar ratio method for determination of vanadium (IV)—EDDPA complex composition, pH = 5.5

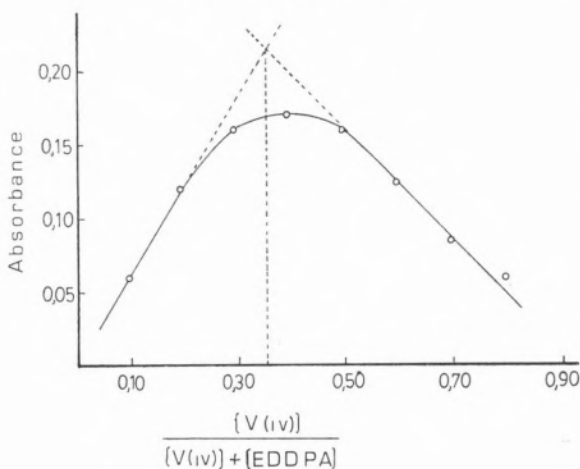


Figure 4

Application of the continuous variations for determination of vanadium (IV)—EDDPA complex composition, pH = 5.5

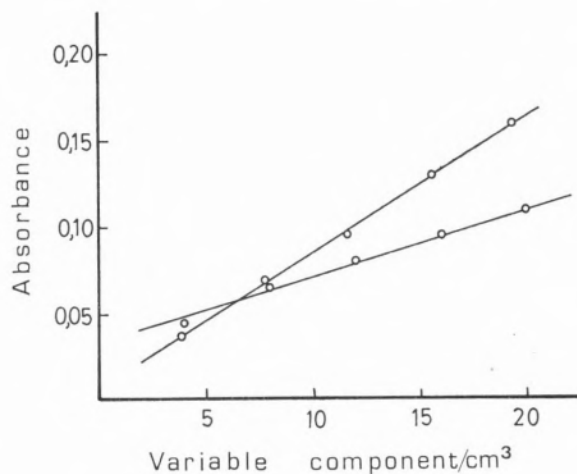


Figure 5

Application of the slope ratio method for determination of vanadium (IV)—EDDPA complex composition, pH = 5.5

#### Comparative study with other methods

With the purpose of meeting the importance of the present method, the values of the working wavelength, the range of Beer's law, pH and molar absorptivity of the different methods proposed for the determination of vanadium (IV) with chelate reagents analogous to EDTA, are summarized in the table.

#### CONCLUSIONS

The above investigation has led to the development of a new method for the determination of small amounts of vanadium using the vanadium (IV)-EDDPA chelate at pH 5.5 and measuring the absorbance at 545 nm.

Table

Characteristics of some chelates of vanadium(IV)

Chelate	pH	Absorption maxima(nm)	Range Beer's law( $\mu\text{g}/\text{cm}^3$ )	Molar Absorptivity	Ref.
V(IV) — EDTA	3.2	775	100-3280	22.2	[3]
V(IV) — PDTA	2-10	780	100-2400	25.0	[8]*
V(IV) — PDTA	2-10	580	100-2400	18.8	[8]*
V(IV) — NTA	3.6-4.8	815	51-1632	25.0	[1]
V(IV) — EDDPA	5.5	545	39-354	74.0	Proposed

\* Values calculated from the plots of the reference papers.

From the table it can be deduced that the proposed method is the most sensitive of all.

Received, 19th April 1985;  
in revised form, 25th September, 1985.

## REFERENCES

- [1] N. AHMAD, C. MUNIR, R. IQBAL, *Mikrochem. Journal* **23**, 56 (1978).
- [2] F. BERMEJO MARTINEZ, A. PRIETO BOUZA, *Inform. Quím. Anal.* **11**, 58 (1957).
- [3] F. BERMEJO MARTINEZ, MERCEDES MOLINA POCH, *Acta Cient. Compostelana*, **5**, 85 (1968).
- [4] C. DUVAL, «*Traité de Micro-Analyse Minerale*» Paris. Vol. II (1956).
- [5] A.E. HARVEY, D.L. MANNING, *J. Am. Chem. Soc.* **74**, 4744 (1952).
- [6] P. JOB, *Ann. Chim.*, **10**, 113 (1928).
- [7] A.B. SANDELL, «*Colorimetric Determination of Traces of Metals*»—Interscience. New York (1959).
- [8] S. VICENTE PEREZ, L. HERNANDEZ, J.M. PINILLA, *Inform. Quím. Anal.* **27**, 217 (1973).
- [9] H.J. YOE, A.L. JONES, *Anal. Chem.* **16**, 111 (1944).

## RESUMO

### Determinação espectrofotométrica de vanádio (IV) com ácido etilenodiamino-N,N'-dipropiônico (EDDPA)

Estudou-se a formação do complexo entre vanádio (IV) e o ácido etilenodiamino—N,N'—dipropiônico. O complexo, de cor violeta, tem um máximo de absorção a 545 nm, em meio ácido (pH=5.5). Estudaram-se os efeitos da temperatura, do tempo e do aumento da quantidade de reagente. O intervalo óptimo para aplicação da lei de Beer situa-se entre 140 e 350 µg vanádio/ml. Investigou-se a natureza do complexo em solução, bem como interferências, reprodutibilidade e a precisão. Este método é mais sensível do que outros em que se usam outros reagentes quelantes, análogos a EDTA, como reagentes cromogénicos.



ADELA BERMEJO BARRERA  
M.<sup>a</sup> CARMEN LUACES PAZOS  
F. BERMEJO MARTINEZ

Department of Analytical Chemistry  
Faculty of Chemistry  
University of Santiago de Compostela  
Santiago de Compostela,  
Spain



---

## SPECTROPHOTOMETRIC DETERMINATION OF PALLADIUM(II) WITH BUTYLENEDIAMINETETRA- METHYLENPHOSPHONIC ACID (BDTPMA) \*

*This article describes a spectrophotometric procedure for the determination of palladium (II). At pH 7.0 palladium(II) reacts with butylenediaminetetramethylenephosphonic acid (BDTPMA) to produce a complex with an absorption peak at 380 nm which over the range 1.68-28.54  $\mu\text{g Pd(II)}/\text{cm}^3$  conforms to Beer's law with a molar absorptivity of  $2.8 \times 10^4 \text{ dm}^3 \cdot \text{mol}^{-1} \cdot \text{cm}^{-1}$  and a sensitivity of 38  $\text{ng} \cdot \text{cm}^{-2}$ . Interferences, reproducibility and the stoichiometry of the complex were also determined.*

---

\* Part CXXIX of the series «Analytical applications of chelons».

## INTRODUCTION

A number of methods have been put forward for the spectrophotometric determination of palladium (II) after complexation with various ligands.

In a perchloric acid medium palladium (II) forms a 1:1 complex with EDTA which has absorption peaks at 390 nm at pH 2 and 337 between pH 2 and pH 10 [1]. The peak at 337 nm between pH 2 and pH 10 is also observed in the spectra of the 1:1:1 complexes formed with EDTA and halides in chloride or bromide media.

MACNEVIN and KRIEGE [2,3] have reported the spectrophotometric determination of palladium using a stable yellow 1:1 complex formed between EDTA and either palladium (II) or palladium (IV).

Over virtually the entire range of acidities palladium (II) forms complexes with NTA whose absorbance increases rapidly from pH 0 to pH 3, is constant in the pH range 3-11, and falls off at pH 11. In aqueous media 1:1 and 1:2 complexes are formed. Determinations carried out at 330 nm suffer interference by appreciable concentrations of other metals of the palladium group [4].

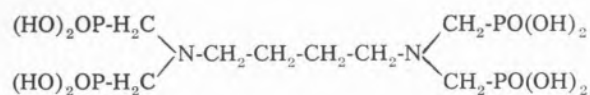
Spectrophotometric determination of palladium using the 340 nm absorption peak of the complex formed between palladium (II) and DCTA is interfered with ruthenium, iron and copper [5].

Palladium has also been determined spectrophotometrically at 300 or 410 nm using the 1:2 complex formed with *p*-aminophenylmercaptoacetic acid at pH 9.5 [6].

Microquantities of palladium can be measured spectrophotometrically in perchloric media using the very stable 1:2 complex formed with ethylenedithioacetic acid. No interference from other palladium group metals is observed.

This article describes a new method for the spectrophotometric determination of palladium (II) which uses its complex with buty-

lenediaminetetramethylenephosphonic acid (BDTMPA):



Other possible analytical applications of BDTMPA have already been investigated in our laboratory [8]. It was prepared using the method of MOEDRITZER and IRANI [13].

## MATERIALS AND METHODS

### REAGENTS

- *Standard palladium (II) solution* was prepared by dissolving 0.4795 g of PdCl<sub>2</sub> in 1 mol/dm<sup>3</sup> hydrochloric acid and diluting to 100 cm<sup>3</sup> with the same acid. The concentration of the resulting solution was measured by titration with EDTA was 0.04508 mol/dm<sup>3</sup>.
- *Standard BDTMPA solution* was prepared by dissolving 0.3812 g of recrystallized BDTMPA in dilute sodium hydroxide and diluting to 100 cm<sup>3</sup> with distilled water. Its concentration was 0.008212 mol/dm<sup>3</sup>.
- *BDTMPA solution, 0.1 %* was prepared by dissolving a suitable quantity of BDTMPA in dilute sodium hydroxide and making up with distilled water.
- *Hydrochloric acid, aqueous solutions 0.1 and 1.0 mol/dm<sup>3</sup>.*
- *Sodium hydroxide, aqueous solutions 0.1 and 1.0 mol/dm<sup>3</sup>.*

### APPARATUS

- *Bausch & Lomb, Spectronic 700 spectrophotometer, equipped with prismatic quartz cells with a 10 mm light path.*

— *Beckman Expandomatic pH-meter* equipped with a combined glass-calomel electrode sensitive to ± 0.02 pH units.

### PROCEDURE

Aliquots of the standard palladium (II) solution were introduced in 10 cm<sup>3</sup> volumetric flasks and 1 cm<sup>3</sup> of 0.1 % BDTMPA solution added together with enough drops of sodium hydroxide or hydrochloric acid as to achieve the acidity desired (the recommended working acidity is pH 7.0). After 40 min. in a boiling water bath, the solutions were left to cool and made up to the mark with distilled water. Spectrophotometric measurements were carried out at 380 nm using distilled water as reference.

## RESULTS AND DISCUSSION

### Absorption spectrum

In order to find an appropriate working wavelength absorption, spectra of the complex Pd(II)-BDTMPA were recorded at pH 2.0, pH 7.0 and pH 11.2. In view of the peak between 370 and 390 nm in the pH 7.0 spectrum shown in Figure 1, the wavelength of 380 nm was chosen. The pH 11.2 spectrum is similar to that of Figure 1, but the palladium(II) solution has greater background absorbance. At pH 2.0 the peak is very small, though located at the same wavelength.

### Effect of pH

The effect of pH on the absorbance of solutions of Pd(II)-BDTMPA was studied using a series of solutions prepared as above but with differing acidities. Absorbance was found to remain at a constant maximum over the range pH 3.5-10.5. The centre of this range, pH 7.0, was chosen as the working pH.

### Effect of the quantity of reagent

A study of the effect of the quantity of reagent at pH 7.0 showed that 1 cm<sup>3</sup> of 0.1 % BDTMPA solution was sufficient for forma-

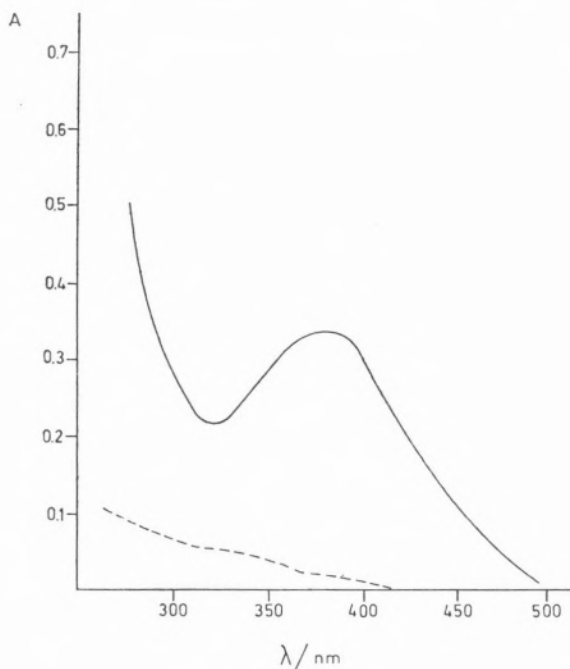


Fig. 1

Absorption spectra of the complex Pd(II)-BDTMPA (—) and of the cation Pd(II) (---) at pH 7.0, the concentration of Pd(II) being in each case 13.43 μg/cm<sup>3</sup>

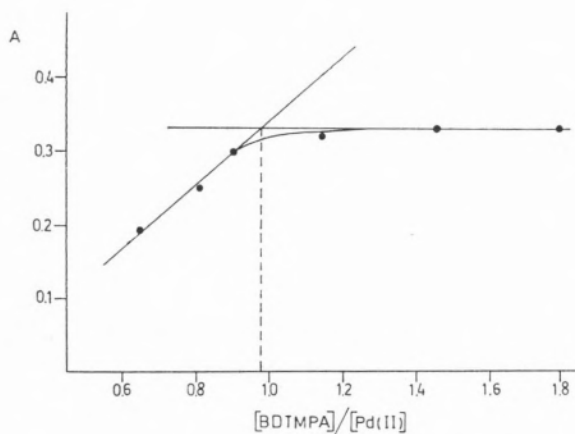


Fig. 2

Determination of the stoichiometry of the complex Pd(II)-BDTMPA by the «mole ratio» method

tion of the complex, and that excess reagent had no appreciable effect on absorbance at the working wavelength.

### Effects of temperature and time

The absorbance of solutions of Pd(II)-BDTMPA was found to increase with temperature up to 100°C. After 30 min in a boiling water bath the absorbance levelled off, no appreciable change being observed after longer periods of heating. A heating time of 40 min was established in order to stabilize the system. After 40 min. heating in a boiling water bath and subsequent cooling, no change in absorbance was observed until 5 hours later, when a slow decline began.

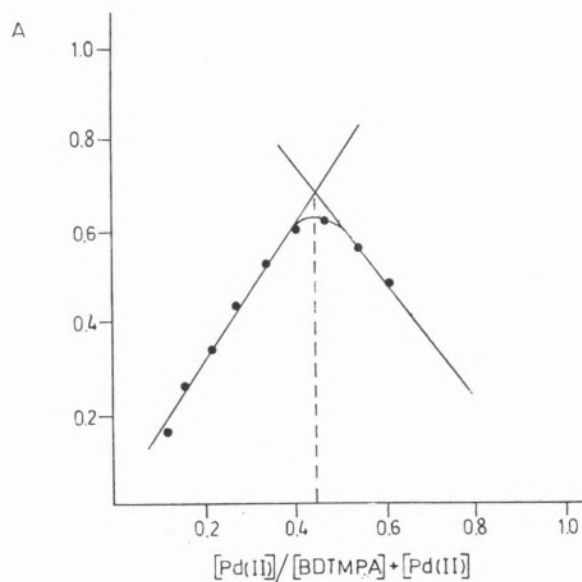


Fig. 3

Determination of the stoichiometry of the complex Pd(II)-BDTMPA by the «continuous variation» method

### Beer's Law, Ringbom's Interval and Molar Absorptivity

In order to verify that Beer's law was satisfied, a series of solutions were prepared as

above with concentration of palladium (II) in the range 1.68-28.54  $\mu\text{g}/\text{cm}^3$ . In the absence of interfering ions, the radiant energy absorbed was proportional to the concentration of palladium over the whole range. The molar absorptivity of the system was calculated as  $2.8 \times 10^4 \text{dm}^3 \cdot \text{mol}^{-1} \cdot \text{cm}^{-1}$  and its sensitivity as  $38 \text{ng} \cdot \text{cm}^{-2}$ . Ringbom's optimum interval was 8.40-28.54  $\mu\text{g Pd (II)}/\text{cm}^3$ , and the minimum photometric error 2.80 %.

#### Reproducibility and precision

The reproducibility and precision of the method were studied by carrying out nine determinations of each of four solutions with concentrations of 3.35, 10.07, 16.79 and 21.83  $\mu\text{g Pd (II)}/\text{cm}^3$ . The standard deviations of these observations were respectively 0.004, 0.005, 0.008 and 0.007; and their relative errors respect to the means 4.35, 1.48, 1.34 and 0.91 %.

#### Stoichiometry of the complex

The composition of the Pd (II)-BDTMPA complex was determined by three different procedures: the «mole ratio» of YOE and JONES [9], JOB's «continuous variations» method [10] and the «slope ratio» of HARVEY and MANNING [11].

In the «slope ratio» method, two series of solutions were prepared, in one of which all solutions contained the same concentration of BDTMPA ( $0.0002053 \text{mol} \cdot \text{dm}^{-3}$ ), but different concentrations of Pd (II), while in the other all solutions contained a concentration of  $0.0001578 \text{mol} \cdot \text{dm}^{-3}$  of Pd (II) but their BDTMPA contents differed.

The results obtained by using of the three methods were showed in Figures 2, 3 and 4 and imply that the metal-ligand ratio of the Pd (II)-BDTMPA complex is 1:1. A value of  $7.1 \times 10^5$  was calculated for the stabi-

lity constant of the system from the mole ratio and continuous variation data [12].

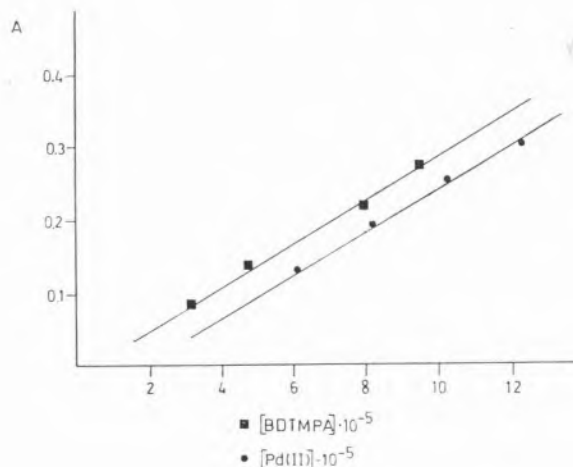


Fig. 4

Determination of the stoichiometry of the stoichiometry of the complex Pd(II)-BDTMPA by the «slope ratio» method

#### Effect of other ions

Investigation of the effect of other ions on the absorbance of Pd (II)-BDTMPA solutions showed that among anions there was no interference by chloride, chlorate, iodate, nitrate, nitrite, sulphate, sulphite, acetate, tartrate, oxalate, tungstate, carbonate or borate. Neither interference was observed when the quantity of palladium (II) was exceeded 60-fold by the quantity of bromide, 50-fold by the quantity of arsenate, 40-fold by the quantity of phosphate or 3-fold by the quantity of arsenite. Bromate, thio-sulphate, sulphide, cyanide, ferrocyanide and chromate were found to interfere when present in concentrations of the same order as that of the metal.

All cations studied interfered to some extent. A calcium/palladium ratio of 40 was found to be tolerable, as were quantities of zirconium, iron (III) and chromium (III) equal to the quantity of palladium, but vanadium, cobalt, nickel, manganese, beryllium, zinc, strontium, caesium, thorium, copper, alumi-

Table I

Characteristics of chelometric methods used for the determination of palladium(II)

Chelate	pH	Absorption maxima(nm)	Beer's law interval(ppm)	Molar Absorptivity (dm <sup>3</sup> .mol <sup>-1</sup> .cm <sup>-1</sup> )	Medium	Ref.
Pd(II)-EDTA	5-9	337	5-200	1.26×10 <sup>3</sup>	aqueous	[2]
Pd(II)-EDTA	1.6-2.0	377	5-200	0.60×10 <sup>3</sup>	aqueous	[2]
Pd(II)-NTA	7.0	330	20-200	—	chloride	[4]
Pd(II)-DCTA	—	340	10-80	1.05×10 <sup>3</sup>	aqueous	[5]
Pd(II)-p-APMAA	9.5	300	1.1-16.2	6.60×10 <sup>3</sup>	aqueous	[6]
Pd(II)-BDTMPA	7.0	380	1.68-28.54	2.84×10 <sup>3</sup>	aqueous	proposed

mium, mercury, magnesium, uranium, cadmium and ammonium all interfered whatever their concentration.

#### Comparison with other chelometric methods

Table I compares the main characteristics of the various chelometric methods that have been put forward for the spectrophotometric determination of palladium in the range 300-400 nm. It may be noted that the molar absorptivity of the complex with BDTMPA is more than double that of any of the other complexes except Pd(II)-p-APMAA which obeys Beer's law over a much narrower range of concentrations.

Received, 20th August 1985;  
in revised form, 30th September 1985.

#### REFERENCES

- [1] A.A. BIRYKOV, N.G. SHUNKOVA, *Zh. Anal. Khim.*, **21** (6) 702 (1966).
- [2] W.H. MACNEVIN, O.H. KRIEGE, *Anal. Chem.*, **26**, 1768 (1954).
- [3] W.H. MACNEVIN, O.H. KRIEGE, *J. Amer. Chem. Soc.*, **77**, 6149 (1955).
- [4] P. DESIDERI, F. PANTANI, *Talanta*, **8**, 235 (1961).
- [5] N.H. EZERKAYA, T.P. SOLOVYKHI L.P. BOCHKOVA, N.A. SUBOCHKHIM, *Zh. Anal. Khim.* **35** (1) 81 (1980).

- [6] E. FERNANDEZ GOMEZ, F. BERMEJO-MARTINEZ, J.A. RODRIGUEZ-VAZQUEZ, *Acta Química Compostelana*, **4** (1) 32 (1980).
- [7] A. NAPOLI *Ann. Chim. (Rome)*, **69** (7-8) 399 (1979).
- [8] A. BERMEJO-BARRERA, M.<sup>a</sup> C. LUACES-PAZOS, F. BERMEJO-MARTINEZ, *Acta Química Compostelana*, **VII** (4) 108 (1983).
- [9] J.H. YOE, A.C. JONES, *Ind. Eng. Chem. Anal. Ed.*, **16**, 111 (1944).
- [10] P. JOB, *Ann. Chim.*, **9**, 113 (1928); **11**, 97 (1953).
- [11] A.J. HARVEY, S.L. MANNING, *J. Amer. Chem. Soc.*, **72**, 4188 (1950); **74**, 4744 (1952).
- [12] A. BERMEJO-BARRERA, F. BERMEJO-MARTINEZ, «Los cálculos numéricos en la Química Analítica» 4.<sup>a</sup> Ed. ANQUE, Madrid 1981, pág. 323-326.
- [13] K. MOEDRITZER, R.R. IRANI, *J. Org. Chem.*, **31**, 1603 (1966).

#### RESUMO

#### Determinação espectrofotométrica de paládio (II) com ácido butilenodiaminotetrametileno-fosfórico (BDTMPA)

Descreve-se um método espectrofotométrico para o doseamento de paládio (II). A pH=7,0, o paládio (II) reage com o ácido butilenodiaminotetrametileno-fosfórico (BDTMPA), dando um complexo, com um máximo de absorção a 380 nm, absorvidade molar de  $2,8 \times 10^3 \text{ dm}^3 \text{ mol}^{-1} \text{ cm}^{-1}$ , sensibilidade de  $38 \text{ ng.cm}^{-2}$ , e que satisfaz à lei de Beer no intervalo 1,68-28,54  $\mu\text{g}$  de Pd(II)/cm<sup>2</sup>. Determinaram-se, também, interferências, reprodutibilidade e a estequiometria do complexo.





---

## ON THE VALIDITY OF LINEAR FREE ENERGY RELATIONSHIPS IN CHEMICAL KINETICS

S. J. FORMOSINHO  
Departamento de Química,  
Universidade de Coimbra  
3049 Coimbra Codex

Linear free energy relationships (LFER) have been used extensively in chemical kinetics (1). However such correlations, which have a strong empirical basis, should be contained in any theoretical model which relates activation energy and molecular structure. We have recently developed such a model (2, 3) which is quite general, because it encompasses, as particular cases, the well known BEBO and Marcus theories. Thus it is useful to investigate under what conditions LFER are valid. For a reaction  $A + BC \rightarrow AB + C$  the free energy of activation can be given by

$$\Delta G^\ddagger = (\Delta G^0 + \frac{1}{2} fd^2) / 2fd^2 \quad (1)$$

under the assumption that the bonds BC and AB have a harmonic behaviour with an average force constant  $f$ ;  $\Delta G^0$  is the reaction free energy and  $d$  is the sum of the bond distensions from reactant and product to the transition state. This parameter depends on the sum of the equilibrium bond lengths of BC and AB,  $l = l_{AB} + l_{BC}$ ,

$$d = \eta l \quad (2)$$

where the reduced bond distension  $\eta$  is

$$\eta = \frac{a' \ln 2}{n^\ddagger} + \frac{a'}{2\lambda^2} (\Delta G^0)^2 \quad (3)$$

$n^\ddagger$  is the bond order of the bonds in the transition state  $ABC^\ddagger$ ,  $a'$  is a constant ( $a' = 0.156$ ) and  $\lambda$  is the so called «mixing entropy», which has the dimensions of energy (2, 3).

LFER (1) can be conveniently expressed by

$$\Delta G_X^\ddagger - \Delta G_R^\ddagger = -2.3 RT \rho \sigma_X \quad (4)$$

where  $\Delta G_R^\ddagger$  is the activation free energy of a reaction considered as reference,  $\Delta G_X^\ddagger$  refers to the presence of a substituent (or different medium) and  $\rho$  and  $\sigma_X$  are parameters. The constant  $\rho$  is a function of the reaction ( $\rho = 1$  for the ionization of  $ArCO_2H$

at 25°C), and  $\sigma_X$  is a function of the substituent

$$\sigma_X = \log \frac{K_X}{K_R} \quad (5)$$

where  $K$  are the equilibrium constants of the reactions under consideration, which have free energies  $\Delta G_X^0$  and  $\Delta G_R^0$ . Consequently

$$\sigma_X = - \frac{(\Delta G_X^0 - \Delta G_R^0)}{2.3 RT} \quad (6)$$

Let us assume that the presence of a substituent  $X$  causes a change in the reaction free energy. Considering that we can neglect the contribution for the energy barrier of all bonds except the bond-breaking bond-forming ones, or that such effect can be expressed in terms of an overall force constant, it is reasonable to assume that changes in  $\Delta G^0$  are caused by changes in the potential energies of the reactive bonds, i. e., by changes in  $f$  and/or  $l$ . Consequently we can consider that

$$(a' ln2)^2 (f_X l_X^2 - f_R l_R^2) = \alpha (\Delta G_X^0 - \Delta G_R^0) \quad (7)$$

where  $\alpha$  is a constant of proportionality. With eq. (7) and under the assumption that the bond orders at the transition state are the same for the two reactions,  $n_X^\ddagger = n_R^\ddagger = n^\ddagger$ , then we can write

$$\Delta G_X^\ddagger - \Delta G_R^\ddagger = (\Delta G_X^0 - \Delta G_R^0) \frac{(2n^{\ddagger 2} + \alpha)^2}{8 \alpha n^{\ddagger 2}} \quad (8)$$

by neglecting the quadratic dependence of  $\eta$  on  $\Delta G^0$ , i. e.,  $|\Delta G^0| \ll \lambda$ . By comparison of eqs. (8) and (4) and (6) we conclude that

$$\rho = \frac{(2n^{\ddagger 2} + \alpha)^2}{8 \alpha n^{\ddagger 2}} \quad (9)$$

which shows that  $\rho$  is proportional to the bond order at the transition state.

For the reaction of ionization of benzoic acid which has  $n^\ddagger = 0.84$  (5), is  $\alpha = 1.41$ . With this same  $\alpha$  value and for the expected range of

$n^\ddagger$  values we have  $\rho = 1.294$  ( $n^\ddagger = 0.5$  and  $\rho = 1.031$  ( $n^\ddagger = 1$ )). The parameter  $\alpha$  should vary with the nature of the reaction and even negative values can be found, namely for strong exoenergetic reactions. For example with  $\alpha = -10$ ,  $\rho = -4.5$  ( $n^\ddagger = 0.5$ ), and  $\rho = 5.5$  with  $\alpha = 10$  which more than covers the experimental range of the  $\rho$  values (1). Substituent effects can cause change in free energies typically of  $15 \text{ kJ mol}^{-1}$ . With typical values for the ionization of benzoic acid,  $f_R = 4 \times 10^3 \text{ kJ mol}^{-1}$  and  $l = 2 \text{ \AA}$  (4), eq. (7) reveal that changes in  $|\Delta G_X^0 - \Delta G_R^0| = 15 \text{ kJ mol}^{-1}$  correspond to changes in  $f l^2$  of ca. 10 % with  $\alpha = 1.4$ . This is a reasonable change in force constants and/or equilibrium bond lengths for substituent effects. For other reactions even higher  $f_R$  and  $l_R$  values can be found, and for the set of values  $f = 6 \times 10^3 \text{ kJ mol}^{-1} \text{ \AA}^{-2}$   $l = 4 \text{ \AA}$  the estimated variation in  $f l^2$  with  $\alpha = \pm 10$  is only 14 %.

We can now discuss briefly under what conditions LFER cannot be verified:

- a — The force constants of the reactive bonds are not equal. This condition however is not restrictive of LFER as long as conditions of eqs. (7) can be verified by the force constant of the reactant and product.
- b — Eq. (7) is not valid. This condition is associated with the additivity rules, which are quite general molecular properties. However this topic can be addressed to the recent work of Murdoch (5).
- c — It is not possible to neglect the linear dependence of  $\eta$  on  $(\Delta G^0)^2$ . Such a dependence is proportional to the mixing entropy, which has been found to be also related with  $\Delta S^\ddagger$  (3). Since the effect of substituents or media on  $\Delta S$  may be different from the one on  $\Delta G$ , this condition may cause a breakdown of LFER. However this may cause some scatter in the linear relationships, but it is not expected to cause a strong failure of LFER.

d — The bond order at the transition state is not the same for all reactions. This causes the breakdown of LFER. An example will illustrate this point. We have shown that the bond order at the transition state varies continuously from  $n^\ddagger = 1/2$  for  $S_N^2$  to  $n^\ddagger = 1$  or even higher values for  $S_N^1$  mechanisms (3). In fact,  $\log(k_X/k_R)$  versus  $\sigma_X$  for the reactions of substituted benzyl chloride with triethylamine and benzyl bromides with pyridine, (supposedly typical nucleophilic substitutions), are strongly curved (6). Changes in the bond order  $n^\ddagger$  are caused by siphoning of electron density mainly from nonbonding and antibonding orbitals into bonding orbitals in the transition state (2, 3).

(Received, 25th September 1985)

#### ABSTRACT

*An intersecting-state-model which relates activation energy and molecular and thermodynamic parameters is used to investigate the validity of LFER in chemical*

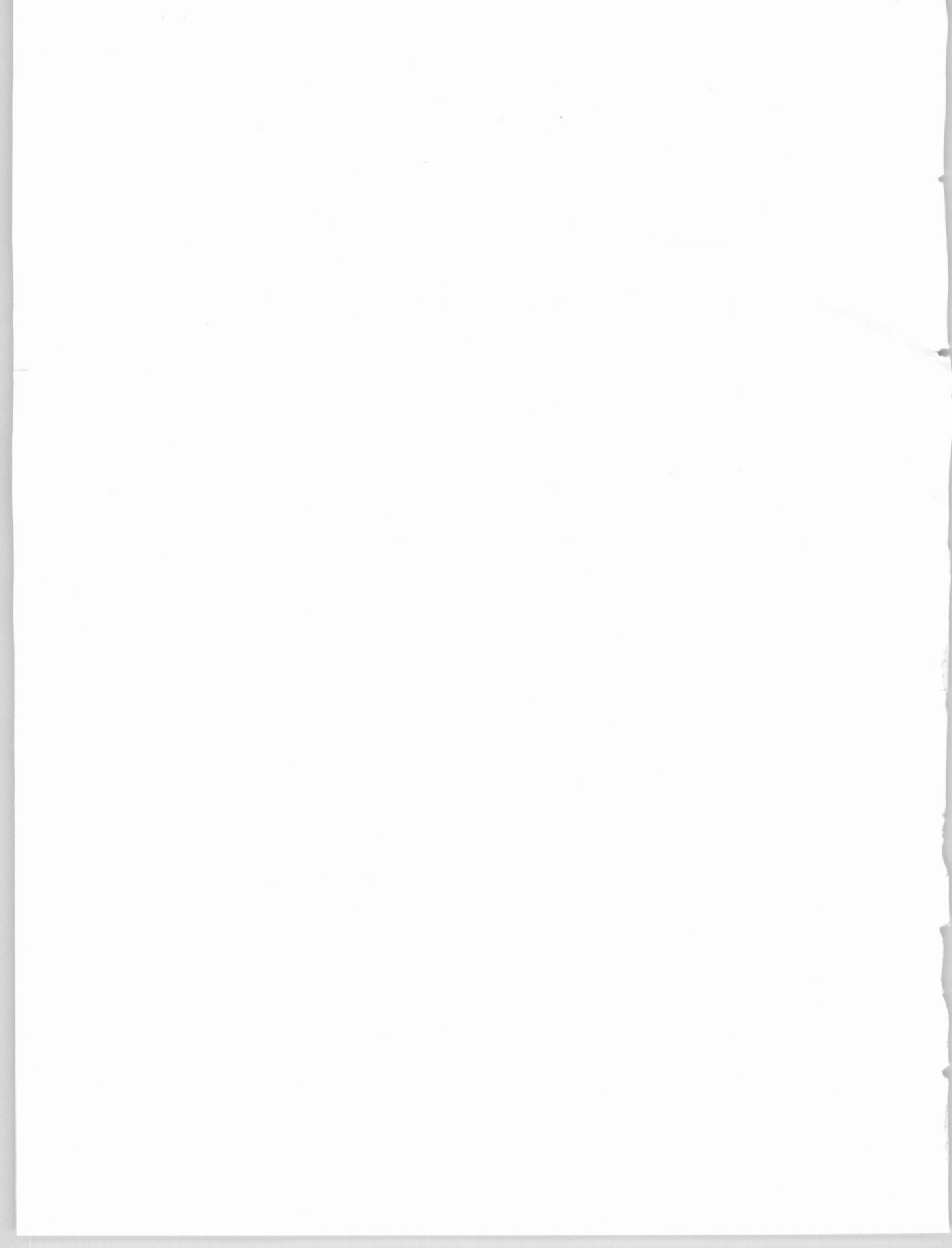
*kinetics. It is shown that such relationships should be verified as long as substituents or media do not alter the bond order of the transition states.*

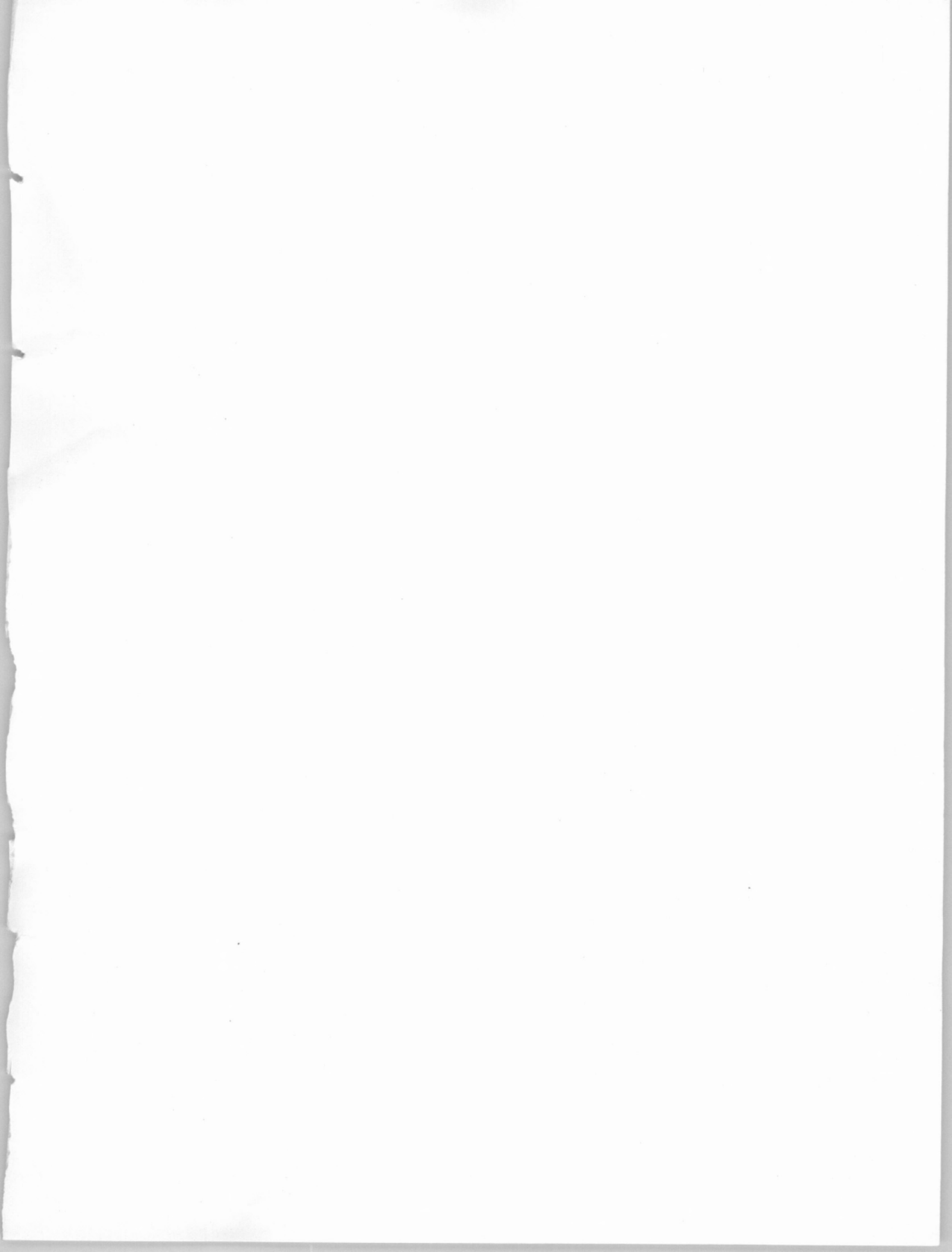
#### SUMÁRIO

*Através de um modelo de intersecção de estados que permite estimar energias de activação em função de parâmetros moleculares e termodinâmicos, mostra-se que a linearidade de relações de energia livre em cinética é verificada desde que a ordem de ligação do estado de transição seja independente da natureza de substituintes e solventes.*

#### REFERENCES

- [1] L. P. HAMMETT, «Physical Organic Chemistry», McGraw-Hill, New York, 1940, pp. 194-199; P. R. WELLS, «Linear Free Energy Relationships», Acad. Press, New York, 1968.
- [2] A. J. C. VARANDAS and S. J. FORMOSINHO, *J. Chem. Soc., Faraday Trans. 2*, **82**, 953 (1986).
- [3] S. J. FORMOSINHO, *Rev. Port. Quím.*, **27**, 427 (1985).
- [4] S. J. FORMOSINHO, *J. Chem. Soc. Perkin Trans. 2*, in press.
- [5] J. R. MURDOCH, *J. Am. Chem. Soc.*, **105**, 2260, 2667 (1983).
- [6] J. E. LEFFER and E. GRUNWALD, «Rates and Equilibria of Organic Reactions», John Wiley, New York, 1963, p. 190.









## INSTRUCTIONS FOR AUTHORS

1. The **Revista Portuguesa de Química** accepts for publication original papers, research notes and review articles.
2. All manuscripts will be sent to referees for assessment.
3. Manuscripts should be written either in Portuguese or English.
4. Three complete copies of the manuscript should be submitted to one of the Editors. The manuscript should be typed on only one side of the paper with double spacing throughout the text, tables, figure legends, footnotes, and list of references, and with a margin of not less than 4 cm on the left-hand side of each page. The title page should carry the title of the paper, the authors' names, the name and address of the laboratory where the work was done, the name and address of the person to whom proofs should be sent, and a short resuming title for printing at the head of each right-and printed page. An abstract, both in Portuguese and English, in not more than about 300 words should be included; it should be typed on a separate page. A list of figure legends, beginning on a new page, should be included. Finally, a list of references in numerical sequence, also beginning on a new page, should be included. References should be given in the *current* style of *Chemical Abstracts*, particular care being taken always to give authors' initials.  
Research notes should be brief, no more than five typed pages, and need no abstract.
5. Authors are strongly advised to adhere to international conventions in the choice of symbols, units and notation.  
A few non-SI units are acceptable without definition; these include Å, cm<sup>-1</sup>, eV and u (unified atomic mass unit). Atomic units are also acceptable provided they are stated explicitly as in the IUPAC recommendations (*Pure and Applied Chemistry*, 1978, **50**, 75). In general, however, non-SI units should be avoided, but in the rare cases where this is particularly inconvenient the non-SI units should be defined once in each paper.  
When numerical values of a physical quantity are tabulated, the expression placed at the head of the column should be a pure number. For example, a table of entropies could have as a heading S/(JK<sup>-1</sup> mol<sup>-1</sup>). Similarly, the axis labels for graphs should also be pure numbers, such as the quotient of the symbols for the physical quantity and the symbol for the unit used. Manuscripts which do not conform to these conventions will be edited appropriately and in some cases may be returned to the authors for editing, after they have been accepted.
6. There are no page charges for the journal. Offprints may be ordered from the editors at the proof stage.

